Fluorescent Dissolved Organic Matter in Natural Waters

Khan M. G. Mostofa, Cong-qiang Liu, Takahito Yoshioka, Davide Vione, Yunlin Zhang and Hiroshi Sakugawa

1 Introduction

Dissolved organic matter (DOM), of allochthonous and autochthonous origin, is a heterogeneous mixture of organic compounds, with molecular weights ranging from less than 100 to over 300,000 Da in natural waters (Hayase and Tsubota 1985; Thurman 1985; Ma and Ali 2009; Mostofa et al. 2009a). The DOM components are involved into key biogeochemical processes such as global carbon cycle, nutrient dynamics, photosynthesis, biological activity and finally as energy sources in the aquatic environments (Mostofa et al. 2009a, b; Hedges 1992). Among the

K. M. G. Mostofa (✉) · C. Q. Liu
State Key Laboratory of Environmental Geochemistry, Institute of Geochemistry, Chinese Academy of Sciences, Guiyang 550002, People's Republic of China
e-mail: mostofa@vip.gyig.ac.cn

T. Yoshioka
Field Science Education and Research Center, Kyoto University, Kitashirakawa Oiwake-cho, Sakyo-ku, Kyoto 606-8502, Japan

D. Vione
Dipartimento Chimica Analitica, University of Torino, I-10125 Turin, Italy

Centro Interdipartimentale NatRisk, I-10095 Grugliasco, (TO), Italy

Y. Zhang
Taihu Lake Laboratory Ecosystem Research Station, State Key Laboratory of Lake Science and Environment, Nanjing Institute of Geography and Limnology, Chinese Academy of Sciences, 73 East Beijing Road, Nanjing 210008, People's Republic of China

H. Sakugawa
Department of Environmental Dynamics and Management, Graduate School of Biosphere Science, Hiroshima University, 1-7-1, Kagamiyama, Higashi-Hiroshima 739-8521, Japan

K. M. G. Mostofa et al. (eds.), *Photobiogeochemistry of Organic Matter*, Environmental Science and Engineering, DOI: 10.1007/978-3-642-32223-5_6,

DOM components, only a limited fraction of organic compounds show fluorescence properties. These compounds are termed the fluorescent DOM (FDOM). In the pioneering works conducted by Kalle (1949, 1963) and Duursma (1974), the fluorescence of terrestrial humic substances served as a tracer of soil organic matter in freshwater and seawater environments. The fluorescence of humic substances has then been used to distinguish the mixing of river water with seawater as well as their sources (Otto 1967; Zimmerman and Rommets 1974; Dorsch and Bidleman 1982; Willey 1984; Hayase et al. 1987).

A number of excitation–emission (Ex/Em) maxima are detected for humic substances depending on their sources and nature (either fulvic acid or humic acid) in soil and natural waters (Christman and Ghassemi 1966; Ghassemi and Christman 1968; Levesque 1972; Almgren et al. 1975; Brun and Milburn 1977; Gosh and Schnitzer 1980; Momzikoff et al. 1992). The effects of the molecular weight of fulvic and humic acids (<10,000 to >300,000 Da) on fluorescence properties have been examined in earlier studies, particularly in lignin sulfonates (Christman and Minear 1967), soil fulvic and humic acids (Levesque 1972; McCreary and Snoeyink 1980), natural waters (Hall and Lee 1974; Stewart and Wetzel 1980; Visser 1984) and sediment pore waters (Hayase and Tsubota 1985, 1983). The results suggest that the Ex/Em wavelength maxima for humic acid are often present at longer wavelengths than those of fulvic acid. The position of these maxima is independent of the molecular weight, whilst smaller molecules in terrestrial fulvic and humic acids typically exhibit higher fluorescence intensity than the larger ones. It is also suggested that the fluorophores in humic acid are aromatic compounds with higher molecular weight compared to those in fulvic acid (Hayase and Tsubota 1985). The fluorescence quantum yields of commercial, soil and aquatic humic substances excited at 350 nm have been determined by Zepp and Scholtzhauer (1981). Linear correlations are observed between pH and the fluorescence intensity at the Ex/Em peaks of fulvic and humic acids in natural waters and in microbial cultures (Visser 1984). The fluorescence characteristics are different between coastal marine sedimentary humic and fulvic acids (Hayase and Tsubota 1985). The vertical distribution of humic-like fluorescent substances has been examined in marine waters (Hayase et al. 1987, 1988; Chen and Bada 1989, 1990, 1992; Hayase and Shinozuka 1995). The fluorescence intensity of humic-like substances is correlated with phosphate and nitrate in the deeper marine waters, suggesting that the production of humic-like substances and nutrients (phosphate and nitrate) results from the decomposition of settling particles in the water column (Hayase and Shinozuka 1995). Senesi (1990a) summarized the fluorescence properties of fulvic acid-like components in freshwater and seawater. All of these studies are two-dimensional and do not distinguish well the fluorescence excitation–emission (Ex/Em) peak positions that can be used for the characterization of the fluorophores of humic substances.

Coble et al. (1990) have firstly applied the three-dimensional fluorescence (excitation–emission matrix) spectroscopy (EEMS) to marine FDOM to distinguish between the humic-like and protein-like fluorescence peaks in seawater. Coble (1996) summarized the various fluorescence peaks that can be distinguished in river, lake and marine FDOM. They identified the Ex/Em wavelengths for humic-like

peaks at Ex/Em = 260/380–460 nm (Peak A) and 350/420–480 nm (Peak C), marine humic-like (recently called photobleached fulvic-like) at 312/380–420 nm (Peak M) and two protein-like peaks, i.e., tryptophan-like (275/340 nm; Peak T) and tyrosine-like (275/310 nm; Peak B) peaks. Since then a number of studies have identified humic-like and protein-like substances in natural waters (Mopper and Schultz 1993; de Souza-Sierra et al. 1994; Determann et al. 1994; 1996; Mayer et al. 1999; Parlanti et al. 2000; Yamashita and Tanoue 2003a). Mostofa et al. (2005a) have characterized the fluorescent whitening agents (FWAs) or components of household detergents (DAS1 and DSBP) in terms of their fluorescence characteristics at Ex/Em = 330–350/430–449 nm (Peak W) in sewerage-impacted rivers.

To find out more useful information in EEM spectra, Principal Component Analysis (PCA), a multivariate data analysis method, has been applied to the study of EEMs in marine science. PCA is a more comprehensive data analysis method than the traditional 'peak picking' techniques (Persson and Wedborg 2001). However, the two-way PCA models are insufficient for the modeling of the essentially three-way character of EEMs (Bro 1997). Recently, parallel factor analysis (PARAFAC), a statistical modeling approach, has been successfully applied to decompose EEMs of complex mixtures in aqueous solution into their individual fluorescent components (Bro 1997, 1998, 1999; Ross et al. 1991; Jiji et al. 1999; Baunsgaard et al. 2000; 2001; da Silva et al. 2002; Stedmon et al. 2003). The combination of EEM and PARAFAC is widely applied to isolate and distinguish the fluorescent components in terrestrial soil, pore waters and natural waters (Fulton et al. 2004; Cory and McKnight 2005; Hall et al. 2005; Stedmon and Markager 2005a, 2005b; Ohno and Bro 2006; Muller-Karger et al. 2005; Stedmon et al. 2007a, 2007b; Mostofa et al. 2010).

FDOM components can undergo photoinduced decomposition by natural sunlight in surface waters or in laboratory conditions. Photoinduced decomposition has been observed for FDOM in rivers (Mostofa et al. 2005a, 2007a, 2010; Gao and Zepp 1998; White et al. 2003; Patel-Sorrentino et al. 2004; Brooks et al. 2007), lakes (Ma and Green 2004; Garcia et al. 2005; Winter et al. 2007; Mostofa KMG et al., unpublished data), estuaries (Skoog et al. 1996; Moran et al. 2000; Osburn et al. 2009), wetlands (Brooks et al. 2007; Waiser and Robarts 2004), marine waters (Stedmon et al. 2007a, 2007b; Skoog et al. 1996; Ferrari et al. 1996a; Kieber et al. 1997; Miller et al. 2002; Lepane et al. 2003; Bertilsson et al. 2004; Boehme et al. 2004; del Vecchio and Blough 2004; Zanardi-Lamardo et al. 2004; Abboudi et al. 2008), extracted or standard fulvic acid and humic acid (Mostofa et al. 2005a; Winter et al. 2007; Lepane et al. 2003; Fukushima et al. 2001; del Vecchio and Blough 2002; Uyguner and Bekbolet 2005; Mostofa and Sakugawa 2009), and fluorescent whitening agents, standard or dissolved in natural waters (Mostofa et al. 2005a, 2010; Poiger et al. 1999). FDOM components are also decomposed microbiologically, in deep natural waters or upon dark incubation under laboratory conditions. A similar behavior has been observed for extracted or standard fulvic and humic acids (Mostofa et al. 2010, 2007a; Garcia et al. 2005; Moran et al. 2000; Lepane et al. 2003; Abboudi et al. 2008). Photochemistry is highly susceptible to degrade flurophores at both peak C- and A-regions, whilst microbial degradation is more susceptible to decompose flurophores

at peak A- and T_{UV}-regions. The latter fluorescent compounds are occasionally unable to undergo photoinduced decomposition, particularly the fluorophores at the T_{UV}-region (Mostofa et al. 2010).

A review by Leenheer and Croué (2003) includes the comparison between the fluorescence properties of various fluorophores within natural organic matter (NOM). Another review by Hudson et al. (2007) focuses on the effect of metal ions on DOM fluorescence and photodegradation, and on the application of DOM fluorescence in natural waters. A recent review by Coble (2007) covers the topic of marine optical biogeochemistry and discusses the chemical properties and the sinks of chromophoric or colored dissolved organic matter (CDOM), as well as its fluorescence characteristics. Another review covers the application of fluorescence to the identification and monitoring of sewerage-derived DOM and to the impact of treatment processes on fluorescence. It provides useful information on how fluorescence could be a potential tool for recycled water systems (Henderson et al. 2009). Finally, another review summarizes the fluorescence properties of various organic components. From field observations in natural waters and the use of standards, it can be derived that all the fluorescent components in DOM can be grouped in four regions: peak C-region (280–400/380–550 nm), peak A-region (220–280/380–550 nm), peak T-region (260–285/290–380 nm), and peak T_{UV}-region (215–260/280–380 nm) (Mostofa et al. 2009a).

This chapter will provide a general overview on the fluorophores, on the fluorescence properties of key organic substances in combination with their molecular characteristics, and on PARAFAC modeling to identify the fluorescent components. This paper will deal with the identification of autochthonous DOM, and in particular of autochthonous fulvic acids of algal or phytoplankton origin. It will be discussed how these autochthonous fluorescent components differ from allochthonous fulvic and humic acids. This review will extensively discuss the key factors that significantly affect the fluorescence properties of FDOM. It will also address the photoinduced and microbial FDOM degradation as well as the mechanisms, the controlling factors and their significance to understand the biogeochemical FDOM activity in freshwater and marine environments. Finally, a comparison will be provided of the relative importance of studying FDOM versus CDOM absorbance, as well as how fluorophores in FDOM differ from chromophores in CDOM.

2 Principle of Fluorescence (Excitation–Emission Matrix) Spectroscopy

Fluorescence (excitation–emission matrix, EEM) spectroscopy (EEMS) gives a three-dimensional image of an aqueous solution that is measured for the fluorescence intensity of the fluorophores as a function of the excitation and emission wavelengths. EEM spectra are a combination of multiple emission spectra at a range of excitations. EEMS finds wide applications due to its precise, quick and relatively simple characterization of DOM fractions in natural waters. The

principles of fluorescence spectroscopy have been summarized in earlier studies (Senesi 1990a; Hudson et al. 2007; Guilbault 1990; Grabowski et al. 2003; Oheim et al. 2006). An organic molecule has a series of closely spaced energy levels, and one of its electrons can be excited from a lower to a higher level upon absorption of a discrete quantum of light that is equal in energy to the difference between the two energy states (Fig. 1) (Senesi 1990a). Fluorescence can be simply defined as the emission of a photon at a longer wavelength (lower energy, $h\upsilon_F$) that occurs when the electron returns to the ground state. Radiation absorption occurs at a timescale of approximately 10^{-15} s, emission of fluorescence photons on a timescale of about 10^{-8} s, and internal conversion typically on a time scale of about 10^{-12} s or less (Fig. 1). Fluorescence is basically the reverse of absorption (Senesi 1990a).

When a fluorophore or fluorescent molecule absorbs a photon with a frequency υ, which corresponds to a photon energy $h\upsilon_{ex}$ (h = Planck's constant), its fluorescence emission can simply be depicted by the wave function ψ as below (Eqs. 2.1, 2.2):

$$\text{Excitation (absorption)}: \psi_0 + h\upsilon_{ex} \rightarrow \psi_e \tag{2.1}$$

$$\text{Fluorescence (emission)}: \psi_e \rightarrow \psi_0 + h\upsilon_F + \text{heat} \tag{2.2}$$

where ψ_0 is termed the ground state of the fluorophore and ψ_e is its first electronically excited state. The fluorescence emission energy, $h\upsilon_F$, varies depending on the return of the photon to the ground state level (ψ_0). A fluorophore in its excited state, ψ_1, can lose its energy by internal conversion such as 'non-radiative relaxation', where the excitation energy is dissipated as heat (vibrational relaxation) to the solvent.

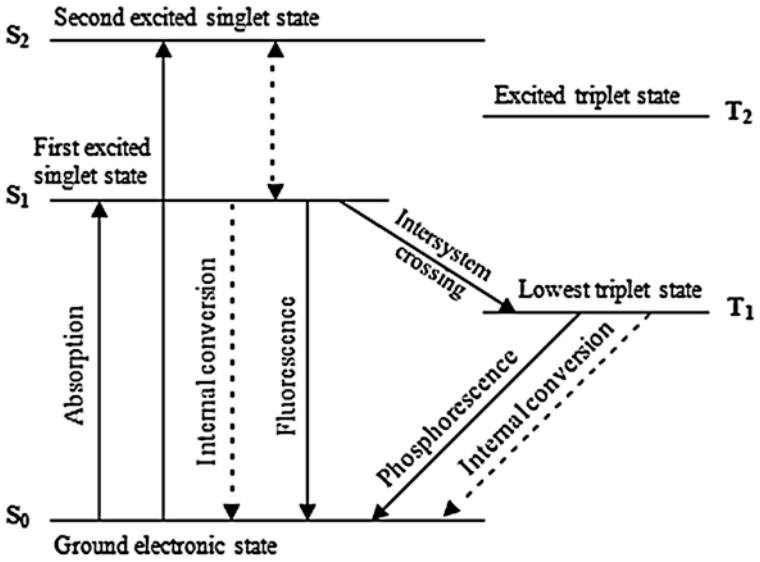

Fig. 1 Schematic energy level diagram for a diatomic molecule illustrating principal excited-state processes. *Data source* Senesi (1990a)

The key processes that compete with fluorescence emission from the lowest excited singlet to the ground state are internal conversion, intersystem crossing and photodegradation (Fig. 1) (Senesi 1990a). The internal conversion depends on several factors such as increasing solvation, increasing temperature and molecular flexibility. Such factors increase the interaction of a molecule with its medium and accelerate the rate of internal conversion by collisional deactivation. Intersystem crossing involves the transition from the lowest vibrational level of an excited singlet state to an upper vibrational level of a triplet state, or vice versa. A change of spin occurs in intersystem crossing, but its rate is usually slower compared to that of internal conversion. Photodegradation causes a decrease in fluorescence intensity, and its effect might be higher for light-sensitive organic substances. The probability of a photodegradation process depends primarily on the energy difference between the ground state and the first excited singlet, i.e. it increases when the energy content of the excited state is increased.

The fluorescence quantum yield (or efficiency) (Φ_f) is defined as the ratio of the number of emitted fluorescence photons to the number of photons absorbed (Senesi 1990a).

$$\Phi_f = \frac{\text{number of photons as fluorescence}}{\text{number of photons absorbed}}$$

The fluorescence efficiency determines the effectiveness with which the absorbed energy is re-emitted. It depends on several factors such as the molecular structure of the fluorescent molecule and its absorption nature, the non-radiative processes, the temperature and the wavelength used for excitation (Senesi 1990a; Wehry 1973).

The probability of finding a molecule in the excited state at a time t after the excitation source is turned off can be expressed as $\exp(-t/\tau)$ where τ is the fluorescence lifetime (Senesi 1990a). The fluorescence lifetime of a molecule is defined as the mean lifetime of the excited state before photon emission. The fluorescence intensity (F) typically follows a first-order kinetics and can be written as follows (Senesi 1990a):

$$F(t) = F_0 \exp(-t/\tau) \tag{2.3}$$

where $F(t)$ is the fluorescence intensity at the time t, F_0 the initial maximum intensity with the excitation source on, i.e. during excitation, t is the time elapsed after the excitation source is turned off, and τ is the fluorescence lifetime or the decay rate of fluorescence.

Fluorescence lifetimes or decay rates (τ) depend on the overall rates at which the excited state is deactivated with both radiative and non-radiative processes. It is ${\tau_{tot}}^{-1} = {\tau_{rad}}^{-1} + {\tau_{nrad}}^{-1}$. Fluorescence lifetimes for commonly used fluorescent molecules are typically of the order of nanoseconds. The intrinsic or natural lifetime (τ_0) corresponds to an absolute quantum efficiency (Φ_0) equal to 1. It happens when fluorescence is the only mechanism by which the excited

state returns to the ground state. When non-radiative processes are deactivating the excited state, the measured lifetime (τ) can be expressed as (Eq. 2.4) (Senesi 1990a):

$$\tau = \Phi_0 \tau_0 \tag{2.4}$$

where $\Phi < \Phi_0$ is the fluorescence quantum efficiency. Fluorescence intensity (F) is proportional to the number of excited states which, in turn, depends on the concentration of the absorbing molecules in solution. According to a basic equation, F can be expressed as follows (Senesi 1990a):

$$F = \Phi I_0 \left[1 - \exp\left(-\varepsilon bc\right)\right] \tag{2.5}$$

where Φ is the quantum efficiency, I_0 is the intensity of the incident radiation that is directly proportional to the fluorescence intensity (F), ε is the (neperian) molar absorptivity of the molecule at the excitation wavelength (higher ε values produce higher fluorescence intensities), b is the path length of the cell and c is the molar concentration of the molecule.

For very diluted solutions, where εbc is sufficiently small, Eq. 2.5 can be expressed as follows (Senesi 1990a):

$$F = \Phi I_0 \varepsilon bc \tag{2.6}$$

Equation 2.6 predicts a linear relationship between fluorescence intensity and concentration of the molecule when εbc is small. If the concentration of the molecule and, as a consequence, εbc increases, a non-linear relationship is followed by Eq. (2.5). Small εbc values indicate that the fluorescence intensity of the molecule is essentially homogeneous throughout the sample. On the other hand, larger εbc values result in a fluorescence intensity of the molecule that is no longer homogeneous within the cell, but is increasingly localized at its front surface (Senesi 1990a).

2.1 Fluorophores in the Fluorescent Molecule and their Controlling Factors

A fluorophore is defined as a part of an organic molecule, with or without electron-donating heteroatoms such as N, O, and S, or as a functional group of a highly unsaturated aliphatic molecule with a structure that can hold up an excited electron, or having extensive π-electron systems, which exhibits fluoresce with significant efficiency (Mostofa et al. 2009a). The major fluorophores in various fluorescent organic molecules in natural waters are composed of Schiff-base derivatives (–N=C–C=C–N–), –COOH, $–COOCH_3$, –OH, $–OCH_3$, –CH=O, –C=O, $–NH_2$, –NH–, –CH=CH–COOH, $–OCH_3$, $–CH_2–(NH_2)CH–COOH$, S-, O- or N-containing aromatic compounds (Mostofa et al. 2009a; Senesi 1990a; Leenheer and Croué 2003; Malcolm 1985; Corin et al. 1996; Peña-Méndez et al. 2005; Seitzinger et al. 2005; Zhang et al. 2005).

According to the basic principle of fluorescence, the elements O, N, S, and P as well as their related functional groups (C–O, C=C, φ–O, COOH, and C=O) in fulvic acid can show fluorescence properties. Each of the functional groups in fulvic acid is referred to as fluorophore. All fluorophores in a mother molecule can exhibit fluorescence properties and any change in the molecule can have an effect on the overall fluorescence properties (Senesi 1990a). Fluorophores present in allochthonous fulvic acid (or allochthonous humic acid or autochthonous fulvic acid) either at peak C-region (Ex/Em = 280–400/380–550 nm) or A-region (Ex/Em = 215–280/380–550 nm) in EEM spectra can be denoted as fluorochrome. The molecular structure of fulvic acid is not yet known because of the complicated chemical composition and relatively large molecular size. However, fulvic and humic acids of vascular plant origin have allowed a partial identification of their molecular structure as benzene-containing carboxyl, methoxylate and phenolic groups, carboxyl, alcoholic OH, carbohydrate OH, –C=C–, hydroxycoumarin-like structures, fluorophores containing Schiff-base derivatives, chromone, xanthone, quinoline ones, as well as functional groups containing O, N, S, and P atoms. Such functional groups include aromatic carbon (17–30 %) and aliphatic carbon (47–63 %) (Leenheer and Croué 2003; Malcolm 1985; Senesi 1990b; Steelink 2002). All of the cited functional groups can be considered as major fluorophores in fulvic and humic acids in natural waters. They can display two fluorescence peaks: peak C at longer wavelength (or peak C-region) and peak A at shorter ultraviolet (UV) wavelengths (or peak A-region) (Mostofa et al. 2009a, 2005a, 2010, 2007a; Senesi 1990a; Coble et al. 1990; Coble 1996, 2007; Mostofa KMG et al., unpublished data; Komaki and Yabe 1982; Schwede-Thomas et al. 2005; Nakajima 2006). The electronic transition of the lowest energy that involves a fluorophore in a molecule exhibits fluorescence (Ex/Em) with the highest intensity at peak C and A-regions. When a fluorophore is degraded by photolytic processes, another lowest energy fluorophore will subsequently produce the fluorescence peak in the respective regions. Therefore, a particular peak (e.g., peak C, peak A, peak T or T_{UV}) of a fluorescent molecule is the outcome of the contribution of all fluorophores present in the molecule itself.

The fluorescence properties of an organic molecule containing fluorophores depend on several inner (or internal) and external (local physical conditions in the fluorophore's microenvironment) factors associated with chemical structure (Mostofa et al. 2009a; Senesi 1990a, 1990b; Lakowicz 1999; Tadrous 2000; Wu et al. 2002, 2004a; Baker 2005). The inner or internal factors are: (i) the probability of absorbing a photon; (ii) the number of fluorophores or functional groups present in the molecule; and (iii) the quantum yield that measures the probability of radiative decay from the excited state; (iv) the extension of the π-electron system, which reduces the excitation energy and shifts the emission wavelengths toward higher values; (v) heteroatom substitution on aromatic compounds; (vi) electron withdrawing (meta-directing) functional groups in aromatic compounds, which reduce the fluorescence intensity; (vii) electron-donating (ortho–para directing) functional groups in aromatic compounds, which increase the fluorescence efficiency; (viii) functional groups such as carbonyl, hydroxide, alkoxide and amino ones, which shift fluorescence toward longer wavelengths; (ix) an increase

in structural rigidity that inhibits the internal conversion, thereby leading to an increase in fluorescence; (x) an increase in the solution redox potential, which enhances fluorescence; and (xi) the concentrations of solutes in aqueous media that would normally cause the fluorescence intensity to decrease when concentration is high.

External factors are: (xii) pH, considering that the fluorescence intensity markedly increases with increasing pH; (xiii) exposure of the fluorophores to an heat source, where increasing temperature causes fluorescence quenching; (xiv) complexation of metal ions with florophores of an organic molecule which can change the fluorescence intensity of that flurophore either enhanced or quenched compared to the original fluorescent DOM (see also chapter "Complexation of Dissolved Organic Matter with Trace Metal ions in Natural Waters") (Wu et al. 2004a, 2004b, 2004c; Smith and Kramer 1999; Ohno et al. 2007; Fu et al. 2007; Zhang et al. 2010; Manciulea et al. 2009; Mounier et al. 2011); (xv) inter- and intramolecular fluorescence quenching of the florophores in organic substance in the presence of other organic components (Marmé et al. 2003; Sun et al. 2012); (xvi) any changes in the molecule upon photoinduced or microbial degradation processes can alter its fluorescence properties, such as peak position and fluorescence intensity (Mostofa et al. 2009a; Senesi 1990a; Wu et al. 2004a). Light exposure can induce in a substantial decrease in the loss of fluorophore binding sites and the stability constant (Wu et al. 2004a; Kulovaara et al. 1995; Bertilsson and Tranvik 2000); and (xvii) any changes in the molecule upon microbial degradation processes can alter its fluorescence properties, such as peak position and fluorescence intensity (Mostofa et al. 2009a, 2007a, 2005b; Senesi 1990a; Moran et al. 2000).

2.2 Fluorescent Dissolved Organic Matter (FDOM) and its Characterization Using EEM Spectroscopy

Fluorescent dissolved organic matter (FDOM) is operationally defined as the dissolved organic matter (DOM) fraction that shows significant fluorescence efficiency or intensity at a particular excitation–emission wavelength (Mostofa et al. 2009a). The FDOM species that are commonly detected in aqueous solution are summarized in Table 1 (Senesi 1990a; Coble et al. 1990, 1998; Coble 1996, 2007; Mayer et al. 1999; Parlanti et al. 2000; Yamashita and Tanoue 2003a; Mostofa et al. 2005a, 2010; Mostofa KMG et al., unpublished data; Mostofa and Sakugawa 2009; Komaki and Yabe 1982; Schwede-Thomas et al. 2005; Nakajima 2006; Baker 2005; Zhang et al. 2010; Sugiyama et al. 2005; Liu and Fang 2002; Provenzano et al. 2004; Lu and Allen 2002; Moberg et al. 2001; Determann et al. 1998; Matthews et al. 1996; Baker and Curry 2004). They are humic substances (fulvic and humic acids) of vascular plant origin, marine humic-like compounds, autochthonous fulvic acids of algal origin, derived from photoinduced and microbial assimilation of lake algae, aromatic amino acids (tryptophan, tyrosine and phenylalanine), proteins, diaminostilbene-type (DAS1) and distyryl biphenyl (DSBP) fluorescent whitening agents (FWAs), other components of household detergents, and chlorophyll (Table 1).

Table 1 Fluorescence excitation/emission (Ex/Em) wavelengths of standard substances and the subsequent characteristic peaks of the reference components in natural waters

Samples	Fluorescence properties			Peak A-region	Peak T-region	Peak T_{UV}-region	References
Standard substances/Component type	Peak C-region						
	Peak C	Peak M_p	Peak W				
	Ex/Em (nm)						
Standard Suwannee River Fulvic Acid dissolved in Milli-Q waters (n = 5)[b]	330/462	–	–	250/462	–	–	Mostofa et al. (2005a), Mostofa KMG et al., (unpublished data)
Standard Suwannee River Fulvic Acid dissolved in Milli-Q waters (n = 5)[b]	–	–	–	230/441	–	–	Mostofa et al. (2005a), Mostofa KMG et al., (unpublished data)
Standard Suwannee River Fulvic Acid dissolved in Milli-Q waters	325/442	–	–	255/450	–	–	Nakajima (2006)
Standard Suwannee River Fulvic Acid dissolved in sea waters	345/452	–	–	255/451	–	–	Nakajima (2006)
Fulvic acids (IHSS standard, n = 5)	333 ± 4/452 ± 12	–	–	–	–	–	Baker (2005)
Suwannee River Fulvic Acid	325/450	–	–	260/460	–	–	Coble et al. (1990)
Fulvic acid, extracted from River	–	300–310/420–430	–	260–270/430–440	–	–	(Schwede-Thomas et al. (2005)
Fulvic acid, extracted from Lake	–	305/448	–	240/440	–	–	Mostofa KMG et al., (unpublished data)
Suwannee River and Pine Barrens (pH: 3–6)	330–340/451–467	–	–	240–260/427–468	–	–	Schwede-Thomas et al. (2005)
Fulvic acid (SJF)	–	310/419	–	–	–	–	Coble (1996), (2007)

(contniued)

Table 1 (contniued)

Samples	Fluorescence properties			Peak A-region	Peak T-region	Peak T_{UV}-region	References
Standard substances/Component type	Peak C-region						
	Peak C	Peak M_p	Peak W				
	Ex/Em (nm)						
Soil fulvic acid (Standard)	–	320/440	–	270–280/430–440	–	–	Sugiyama et al. (2005)
Standard Suwannee River Humic Acid[b]	350/461	300/461	–	255/461	–	–	Mostofa et al. (2005a)
Standard Suwannee River Humic Acid[b]	–	–	–	265, 230/436	–	–	Mostofa et al. (2005a)
Standard Suwannee River Humic Acid (n = 3)	320–345/478–498	–	–	–	–	–	Baker (2005)
Humic acid (EEP2)	–	310/428	–	–	–	–	Coble (1996), (2007)
Humic acid (EEP2)	–	310/423	–	–	–	–	Coble (1996), (2007)
Humic acid, extracted from Lake	–	295/464	–	255/464	–	–	Mostofa KMG et al., (unpublished data)
Protein-like, detected in sewerage samples[a]	–	–	–	–	280/339–346	230/339–346	Mostofa et al. (2010)
Protein-like, extracted from EPS	–	–	–	–	280–285/340–350	225/340–350	Liu and Fang (2002)
Aromatic protein or soluble microbial by-products-like	–	–	–	–	270–280/320–350	220–230/340–350	Mayer et al. (1999)
Tryptophan standard dissolved in Milli-Q waters (n = 3)[b]	–	–	–	–	275–280/352–356	225/343–358	Mostofa et al. (2005a), (2010)
Tryptophan standard dissolved in Milli-Q waters	–	–	–	–	275/357	Peak[c]	Nakajima (2006)

(contniued)

Table 1 (contniued)

Samples	Fluorescence properties			Peak A-region	Peak T-region	Peak T_{UV}-region	References
Standard substances/Component type	Peak C-region						
	Peak C	Peak M_p	Peak W				
	Ex/Em (nm)						
Tryptophan standard dissolved in sea waters	–	–	–	–	275/355	Peak	Nakajima (2006)
Tryptophan standard (n = 5)	–	–	–	–	283 ± 3/351 ± 2	231 ± 3/353 ± 4	Baker (2005)
Tryptophan	–	–	–	–	280/357	227/351	Baker (2005)
Tryptophan[b]	–	–	–	–	280/342–346	Peak	Yamashita and Tanoue (2003a)[b]
Tryptophan-like, extracted from EPS	–	–	–	–	275–280/322–336	220–230/328–334	Zhang et al. (2010)
Tyrosine standard dissolved in Milli-Q waters	–	–	–	–	275/303	230/304	Nakajima (2006)
Tyrosine standard dissolved in sea waters	–	–	–	–	275/304	230/307	Nakajima (2006)
Tyrosine standard dissolved in Milli-Q waters	–	–	–	–	270/314	Peak	Mostofa and Sakugawa (2009)
Tyrosine[b]	–	–	–	–	270–275/300–302	Peak	Yamashita and Tanoue (2003a)[b]
Tyrosine-like	–	–	–	–	275/310	Peak	Coble (1996)
Tyrosine	–	–	–	–	275/303	Peak	Parlanti et al. (2000)
Tyrosine-like, protein-like	–	–	–	–	275/310	Peak	Provenzano et al. (2004)
Tyrosine-like, protein-like	–	–	–	–	265–280/293–313	Peak	Lu and Allen (2002)
Phenylalanine standard dissolved in Milli-Q waters[b]	–	–	–	–	255–265/284–285	Peak	Yamashita and Tanoue (2003a)[b]

(contniued)

Table 1 (contniued)

Samples	Fluorescence properties			Peak A-region	Peak T-region	Peak T_{UV}-region	References
Standard substances/Component type	Peak C-region						
	Peak C	Peak M_p	Peak W				
	Ex/Em (nm)						
Phenylalanine standard dissolved in Milli-Q waters	–	–	–	–	260/286	Peak	Nakajima (2006)
Phenylalanine standard dissolved in sea waters	–	–	–	–	260/284	Peak	Nakajima (2006)
Distyryl biphenyl (DSBP), FWAs dissolved in Milli-Q waters (n = 3)	–	–	350/436	235–265/435–445	–	–	Mostofa et al. (2010)
DSBP, FWAs dissolved in Milli-Q waters	–	–	350/433	245/431	–	–	Nakajima (2006)
DSBP, FWAs dissolved in sea waters	–	–	345/435	245/437	–	–	Nakajima (2006)
DSBP, FWAs (n = 2)	–	–	355/430–432	Peak	–	–	Komaki and Yabe (1982)
Diaminostilbene-type (DAS1), FWAs dissolved in Milli-Q waters (n = 4)	–	–	335–355/438–449	240–245/434–446	–	–	Mostofa et al. (2010)
DAS1, FWAs dissolved in Milli-Q waters	–	–	335/435	250/439	–	–	Nakajima (2006)
DAS1, FWAs (n = 2)	–	–	340–343/430–432	Peak	–	–	Komaki and Yabe (1982)
DAS1, FWAs dissolved in sea waters	–	–	345/436	250/433	–	–	Nakajima (2006)
Chlorophyll-like, pigment-like	398/660	–	–	–	–	–	Coble et al. (1998)
Chlorophyll *a*	431/670	–	–	–	–	–	Moberg et al. (2001)

(contniued)

Table 1 (contniued)

Samples	Fluorescence properties			Peak A-region	Peak T-region	Peak T_{UV}-region	References
Standard substances/Component type	Peak C-region						
	Peak C	Peak M_p	Peak W				
	Ex/Em (nm)						
Chlorophyll *b*	435/659	–	–	–	–	–	Moberg et al. (2001)
Algae or phytoplankton, resuspensions in Milli-Q waters, collected from lake waters[a]	–	–	–	–	280/346, 270/327	230/346, 230/327	Mostofa KMG et al., (unpublished data)
Algae or phytoplankton, resuspensions in River waters, collected from lake waters[a]	–	–	–	–	285/340, 270/336	230/336	Mostofa KMG et al., (unpublished data)
Algae and bacteria, collected from marine waters	–	–	–	–	280/340	230/340, 230/305	Determann et al. (1998)
Corals	310–390/430–490	–	–	–	280/320–350	–	Matthews et al. (1996)
1,4-Dichlorobenzene dissolved in Milli-Q waters	–	–	–	–	–	225/294–299	Mostofa KMG et al., (unpublished data)
Anthracene dissolved in Milli-Q waters	340/401–405	–	–	250/401–404	–	–	Mostofa KMG et al., (unpublished data)
Phenanthrene dissolved in Milli-Q waters	350/367, 348	–	–	–	290/349, 366	–	Mostofa KMG et al., (unpublished data)
Perylene dissolved in Milli-Q waters	–	–	–	–	250/366, 348	–	Mostofa KMG et al., (unpublished data)

(contniued)

Table 1 (contniued)

Samples	Fluorescence properties			Peak A-region	Peak T-region	Peak T_{UV}-region	References
Standard substances/Component type	Peak C-region						
	Peak C	Peak M_p	Peak W				
	Ex/Em (nm)						
Naphthalene in landfill leachate	–	–	–	–	–	220–230/ 340–370	Baker and Curry (2004)
Melanoidin	–	363/458	–	–	–	–	Coble (1996), (2007)
Phenol	–	–	–	–	270/297	–	Coble (1996), (2007)
Phenol dissolved in Milli-Q water	–	–	–	–	270/299	–	Nakajima (2006)
Phenol dissolved in sea water	–	–	–	–	270/298	–	Nakajima (2006)
4-Biphenyl carboxaldehyde	–	305/410	–	–	–	255/315	Mostofa et al. (2010)
o-Cresol	–	–	–	–	275/303	215/304	Mostofa et al. (2010)
p-Cresol	–	–	–	–	280/309	225/309	Mostofa et al. (2010)
p-Hydroxyphenyl acetic acid	–	–	–	–	280/305	230/304	Mostofa et al. (2010)
Benzoic acid dissolved in Milli-Q waters	–	–	–	–	280/311	–	Nakajima (2006)
Benzoic acid dissolved in sea waters	–	300/396	–	–	–	–	Nakajima (2006)
o-Hydroxy benzoic acid or salicylic acid	–	300/407	–	235/410	–	–	Coble (1996), (2007)
o-Hydroxy benzoic acid or salicylic acid	–	314/410	–	–	–	–	Senesi (1990a)
3-Hydroxybenzoic acid	–	314/423	–	–	–	–	Senesi (1990a)
p-Hydroxybenzoic acid dissolved in Milli-Q water	–	–	–	–	–	255/318	Nakajima (2006)

(contniued)

Table 1 (contniued)

Samples	Fluorescence properties			Peak A-region	Peak T-region	Peak T_{UV}-region	References
Standard substances/Component type	Peak C-region						
	Peak C	Peak M_p	Peak W				
	Ex/Em (nm)						
p-Hydroxybenzoic acid dissolved in sea water	–	–	–	–	280/388	–	Nakajima (2006)
Methyl salicylate	366/448	302/448	–	–	–	–	Senesi (1990a)
p-Hydroxy benzaldehyde dissolved in Milli-Q waters	–	325/365	–	–	–	235/353	Nakajima (2006)
p-Hydroxy benzaldehyde dissolved in sea waters	330/372	–	–	240/389	–	–	Nakajima (2006)
p-Hydroxy acetophenone dissolved in Milli-Q waters	–	310/347	–	–	–	225/353	Nakajima (2006)
p-Hydroxy acetophenone dissolved in sea waters	340/382	–	–	240/386	–	–	Nakajima (2006)
Protocatechuic acid (ionized)	340–370/455	–	–	–	–	–	Senesi (1990a)
3-Hydroxycinnamic acid	–	310/407	–	–	–	–	Senesi (1990a)
Caffeic acid	365/450	–	–	–	–	–	Senesi (1990a)
Ferulic acid	350/440	–	–	–	–	–	Senesi (1990a)
ß-Naphthols (ionized)	350/460	–	–	–	–	–	Senesi (1990a)
Xanthone	–	410/456	–	–	–	–	Senesi (1990a)
3-Hydroxyxanthone	343, 365/465	–	–	–	–	–	Senesi (1990a)
3-Hydroxy quinoline	350/450	–	–	–	–	–	Senesi (1990a)

M_p means fluorescence Ex/Em maxima of fulvic acid which is photobleached by photochemical processes or by any other natural processes

[a]Indicates the organic components identified using PARAFAC modeling on sample EEM data and river EEM data is deducted from samples in case of algae

[b]Ranges expresses the authentic standard at various concentrations (1–5 mg L^{-1}) and mechanical reproducibility

peak indicates the occurrence of a peak that do not indentify

EPS extracellular polymeric substances

Coble (1996) firstly designated the fluorescence Ex/Em wavelength peaks of humic-like substances (peak C, peak M, and peak A) as well as of protein-like, tryptophan-like and tyrosine-like ones (peak T and peak B). Parlanti et al. (2000) slightly modified the wavelength ranges and designated them with new letters (α, β and ά, and γ and δ, respectively). Chen et al. (2003) selected the wavelength boundaries at various regions (Region I, Region II, Region III, Region IV, and Region V) to define DOM in natural waters. To account for all the FDOM components of allochthonous, autochthonous and anthropogenic sources, it is desirable to generalize the peak positions by combining the peak regions (Chen et al. 2003) and specifying the letters as made by Coble (Coble 1996). All aquatic scientists have accepted Coble`s specification, and further speciation makes it more complicated. Overviewing and justifying the wavelength ranges of the fluorescence Ex/Em peaks of Coble (1996) and Parlanti et al. (2000) with those of the field observations, Mostofa et al. (2009a) summarize and then specify the fluorescence peaks of various FDOM components at four regions: peak C-region (280–400/380–550 nm), peak A-region (215–280/380–550 nm), peak T-region (260–285/290–380 nm), and peak T_{UV}-region (215–260/280–380 nm) (Table 1) (Mostofa et al. 2009a).

Peak C-region accounts for the broader excitation–emission wavelength ranges at Ex/Em = 280–400/380–550 nm, which include the humic substances (fulvic acid and humic acid) of terrestrial vascular plant origin (C-like and M-like), autochthonous fulvic acids (C-like and M-like) of algal or phytoplankton origin, photo-bleached allochthonous fulvic acid, fluorescent whitening agents (FWAs) such as DAS1 and DSBP as well as few standard organic substances (Tables 1, 2) (Coble et al. 1990, 1998; Coble 1996, 2007; Mopper and Schultz 1993; Parlanti et al. 2000; Yamashita and Tanoue 2003a; Mostofa et al. 2005a; Stedmon et al. 2003, 2007a, 2007b; Fulton et al. 2004; Mostofa et al. 2010, 2007a; 2005b; Mostofa KMG et al., unpublished data; Moran et al. 2000; Komaki and Yabe 1982; Schwede-Thomas et al. 2005; Baker 2005; Sugiyama et al. 2005; Moberg et al. 2001; Chen et al. 2003; Klapper et al. 2002; Komada et al. 2002; Nagao et al. 2003; Boyd and Osburn 2004; Burdige et al. 2004; Conmy et al. 2004; Fu et al. 2006, 2010; Mostofa et al. 2007b; Gao et al. 2010).

Peak A-region accounts for the shorter wavelength region at Ex/Em = 215–280/380–550 nm, and all FDOM components showing fluorescence at the peak C-region can display their secondary fluorescence peaks at the A-region (Tables 1, 2) (Mostofa et al. 2009a, 2005a, 2010, 2007b; Coble et al. 1990; Coble 1996; Mopper and Schultz 1993; Parlanti et al. 2000; Fulton et al. 2004; Komaki and Yabe 1982; Schwede-Thomas et al. 2005; Baker and Curry 2004; Chen et al. 2003; Klapper et al. 2002; Boyd and Osburn 2004; Burdige et al. 2004; Fu et al. 2006, 2010; Suzuki et al. 1997; Zhang et al. 2009a). Peak T-region accounts for the fluorescence peaks at Ex/Em = 260–285/290–380 nm, which includes the primary and secondary fluorescence peaks of various organic substances such as protein-like, aromatic amino acids (tryptophan-like, tyrosine-like and phenylalanine-like), phenol-like compounds, algae, corals, benzoic acid, *p*-hydroxy benzoic acid, perylene, phenanthrene, *o*-cresol and *p*-cresol (Table 1) (Mostofa et al.

Table 2 The fluorescent components identified using PARAFAC modeling on the sample's EEM and their characteristic peaks as excitation (Ex)–Emission (Em) maxima

Fluorescent components	Components identified and sources	Fluorescence properties								References
		Peak C-region				Peak A-region	Peak T-region	Peak T_{UV}-region		
		Peak C	Peak M_p	Peak M	Peak W			Major	Minor	
		EX/Em (nm)								
Allochthonous fulvic acids (*C-like, A-like, and M-like*)										
Suwannee River Fulvic Acid (C-like), standard, dissolved in Milli-Q waters (n = 5)	Component 1, allochthonous	330/462	–	–	–	250/462	–	–	–	Mostofa et al. (2005a)[c], Mostofa KMG et al., (unpublished data)
Fulvic acid (C-like), Yellow River, upstream waters, China	Component 1	335/449	–	–	–	250/449	–	–	–	Mostofa KMG et al., (unpublished data)
Fulvic acid (C-like), Yellow River, mainstream waters, China	Component 1	340/440	–	295/440	–	250/440	–	–	–	Mostofa KMG et al., (unpublished data)
Fulvic acid (C-like), Nanming River, China	Component 1	300–310/ 423–448	–	–	–	235–255/ 425–447	–	–	–	Mostofa et al. (2010)
Fulvic acid (C-like)?, urban sewerage samples[RU]	Component 5	380/467	–	–	–	260/467	–	–	–	Guo et al. (2010)
Fulvic acid (C-like)?, drinking water treatment plant[RU]	Component 3	330/420	–	–	–	<250/420	–	–	–	Baghoth et al. (2010)
Fulvic acid (C-like), The Second Song Hua Jiang River, North-East China	Component 1	325–340/ 449–458	–	–	–	255–260/ 449–458	–	–	–	Mostofa KMG et al., (unpublished data)
Fulvic acid (C-like), LiaoHe River, North-East China	Component 1	330/449	–	–	–	260/449	–	–	–	Mostofa KMG et al., (unpublished data)
Fulvic acid (C-like), Yellow River, China (12 days dark incubation)	Component 1	300/449	–	–	–	250/449	–	–	–	Mostofa KMG et al., (unpublished data)
Fulvic acid (C-like), streams, springs and thermokarsts, CPCRW, Alaska	Component 1[c], allochthonous	–		Peak′	–	Peak′	–	–	–	Balcarczyk et al. (2009)

(contniued)

Table 2 (contniued)

Fluorescent components	Components identified and sources	Fluorescence properties								References
		Peak C-region				Peak A-region	Peak T-region	Peak T_{UV}-region		
		Peak C	Peak M_p	Peak M	Peak W			Major	Minor	
		EX/Em (nm)								
Fulvic acid (C-like), Occoquan Watershed (Northern Virginia, US)[RU]	Component 1, allochthonous	350/456	–	–	–	240/456	–	–	–	Holbrook et al. (2006)
Fulvic acid (C-like), Nishi-Mataya and Higashi-Mataya upstreams, Japan	Component 1	330–335/460–463	–	–	–	250–255/460–463	–	–	–	Mostofa et al. (2005b)[c]
Fuvic Acid (C-like), Yasu River, Lake Biwa watershed, Japan	Component 1	–	310/464	–	–	250/464	–	–	–	Mostofa et al. (2005b)[c]
Fuvic Acid (C-like), 3 Rivers (Ane, Echi and Amano), Lake Biwa watershed, Japan	Component 1	330–335/455–462	–	–	–	255/455–462	–	–	–	Mostofa et al. (2005b)[c]
Fulvic acid (C-like), Lake Biwa, epilimnion (0–20 m), during summer period	Component 1, allochthonous	–	295–310/449–450	–	–	250–255/449–450	–	–	–	Mostofa et al. (2005b)[c]
Fuvic acid (C-like), Lake Biwa, epilimnion (0–20 m), during winter period	Component 1, allochthonous	–	310/443	–	–	255–260/443	–	–	–	Mostofa et al. (2005b)[c]
Fulvic Acid (C-like), Lake Biwa, hypolimnion (40–80 m), during summer period	Component 1, allochthonous	–	300–305/444–461	–	–	255–260/444–461	–	–	–	Mostofa et al. (2005b)[c]
Fulvic acid (C-like), Lake Biwa, epilimnion (40–80 m), during winter period	Component 1, allochthonous	–	305–310/450–464	–	–	255–260/450–464	–	–	–	Mostofa et al. (2005b)[c]
Fulvic acid (C-like)?, Urdaibai and Foz Estuaries, Iberian Peninsula	Component 1, allochthonous	305/439	–	–	–	260/439	–	–	–	Santín et al. (2009)

(contniued)

Table 2 (contniued)

Fluorescent components	Components identified and sources	Fluorescence properties								References
		Peak C-region				Peak A-region	Peak T-region	Peak T_{UV}-region		
		Peak C	Peak M_p	Peak M	Peak W			Major	Minor	
		EX/Em (nm)								
Fulvic acid (C-like)?, Horsens Estuary, Jutland Peninsula, Denmark[RU]	Component 2, allochthonous	385/504	–	–	–	250/504	–	–	–	Stedmon and Markager (2005b)
Fulvic acid (C-like)?, Estuary of Horsens Fjord, Denmark[RU]	Component 3, allochthonous	360/478	–	–	–	270/478	–	–	–	Stedmon et al. (2003)
Fulvic acid (C-like), coastal shelf, South Atlantic Bight	Component 1, allochthonous	Peak′	–	–	–	250/452	–	–	–	Kowalczuk et al. (2009)
Fulvic acid (C-like)?, Bay waters, Barataria Basin (Louisiana, USA)[RUc]	Allochthonous	410/520	–	–	–	250/520	–	–	–	Singh et al. (2010)
Fulvic acid (C-like), Bay waters, Barataria Basin (Louisiana, USA)[RUc]	Component 1, allochthonous	340/440	–	–	–	250/440	–	–	–	Singh et al. (2010)
Fulvic acid (C-like)?, ground water, fresh and Florida Bay waters, Florida coastal Everglades	Component 6, allochthonous	Peak′	–	–	–	Peak′	–	–	–	Chen et al. (2010)
Fulvic acid-like?, glacial ice samples, Antarctic and Arctic Ocean	Component 3, autochthonous	Peak′	–	–	–	<250/446	–	–	–	Dubnick et al. (2010)
Fulvic acid-like (C-like)?, water extractable from sugar maple leaves	Component 5	315/429	–	–	–	Peak′	–	–	–	Hunt et al. (2008)
Photobleached fulvic acid (C-like), Yellow River, China (3 h sunlight irradiation)	Component 1	–	300–305/449	–	–	250/449	–	–	–	Mostofa KMG et al., (unpublished data)

(contniued)

Table 2 (contniued)

Fluorescent components	Components identified and sources	Fluorescence properties								References
		Peak C-region				Peak A-region	Peak T-region	Peak T_{UV}-region		
		Peak C	Peak M_p	Peak M	Peak W			Major	Minor	
		EX/Em (nm)								
Photobleached fulvic acid (C-like), Seto Inland Sea, Japan	Component 2, allochthonous	–	320–325/449–454	–	–	255–260/449–454	–	–	–	Mostofa KMG et al., (unpublished data)
Photobleached fulvic acid (C-like)?, Liverpool Bay, Irish Sea	Component 1	–	320/422	–	–	<250/422	–	–	–	Yamashita et al. (2011)
Fulvic acid (C-like), plant biomass, animal manure, and soils	Components 3, allochthonous	315/447	–	–	–	~250/447	–	–	–	Ohno and Bro (2006)
Suwannee River Fulvic Acid (A-like), standard, dissolved in Milli-Q waters (n = 5)	Component 2, allochthonous	–	–	–	–	230/441	–	–	–	Mostofa et al. (2005a)[c], Mostofa KMG et al., (unpublished data)
Fulvic acid (A-like), streams, springs and thermokarsts, CPCRW, Alaska	Component 2[c], allochthonous	–	–	–	–	Peak′	–	–	–	Balcarczyk et al. (2009)
Fulvic acid (A-like), Nishi-Mataya and Higashi-Mataya upstreams, Japan	Component 2	–	–	290–295/414	–	225/414	–	–	–	Mostofa et al. (2005b)[c]
Fuvic Acid (A-like), 3 Rivers (Ane, Echi and Amano), Lake Biwa watershed, Japan	Component 2	–	–	285–290/442	–	225/442	–	–	–	Mostofa et al. (2005b)[c]
Fulvic acid (A-like), Lake Biwa, epilimnion (0–20 m), during summer period	Component 2, allochthonous	–	–	–	–	225/442	–	–	–	Mostofa et al. (2005b)[c]

(contniued)

Table 2 (contniued)

Fluorescent components	Components identified and sources	Fluorescence properties								References
		Peak C-region				Peak A-region	Peak T-region	Peak T_{UV}-region		
		Peak C	Peak M_p	Peak M	Peak W			Major	Minor	
		EX/Em (nm)								
Fuvic acid (A-like), Lake Biwa, epilimnion (0–20 m), during winter period	Component 2, allochthonous	–	–	–	–	225/432–439	–	–	–	Mostofa et al. (2005b)[c]
Fulvic Acid (A-like), Lake Biwa, hypolimnion (40–80 m), during summer period	Component 2, allochthonous	–	–	–	–	225/432–442	–	–	–	Mostofa et al. (2005b)[c]
Fulvic acid (A-like), Lake Biwa, epilimnion (40–80 m), during winter period	Component 2, allochthonous	–	–	–	–	225/433–434	–	–	–	Mostofa et al. (2005b)[c]
Fulvic acid (A-like)?, Horsens Estuary, Jutland Peninsula, Denmark[RU]	Component 1, allochthonous	–	–	–	–	250/448	–	–	–	Stedmon and Markager (2005b)
Fulvic acid (A-like)?, Estuary of Horsens Fjord, Denmark[RU]	Component 1, allochthonous	–	–	–	–	240/436	–	–	–	Stedmon et al. (2003)
Fulvic acid (A-like)?, Estuary of Horsens Fjord, Denmark[RU]	Component 2, allochthonous	–	–	–	–	240/416	–	–	–	Stedmon et al. (2003)
Fulvic acid (A-like)?, deep waters of the Okhotsk Sea and North Pacific Ocean	Component 3, allochthonous	–	–	–	–	<260/460–480?	–	–	–	Yamashita et al. (2010)
Fulvic acid (M-like), Yellow River, mainstream waters, China	Component 2	–	–	290/429	–	235/429	–	–	–	Mostofa KMG et al., (unpublished data)

(contniued)

Table 2 (contniued)

Fluorescent components	Components identified and sources	Fluorescence properties								References
		Peak C-region				Peak A-region	Peak T-region	Peak T_{UV}-region		
		Peak C	Peak M_p	Peak M	Peak W			Major	Minor	
		EX/Em (nm)								
Fulvic acid (M-like), The Second Song Hua Jiang River, North-East China	Component 2	–	–	300/392–411	–	230–235/392–411	–	–	–	Mostofa KMG et al., (unpublished data)
Fulvic acid (M-like), LiaoHe River, North-East China	Component 2	–	–	285/387	–	230/387	–	–	–	Mostofa KMG et al., (unpublished data)
Fulvic acid (M-like), mainstream of NenJiang River, North-East China	Component 2	–	–	290/417	–	235/417	–	–	–	Mostofa KMG et al., (unpublished data)
Fulvic acid (M-like), tributaries of NenJiang River, North-East China	Component 2	–	–	310/417	–	235/417	–	–	–	Mostofa KMG et al., (unpublished data)
Fulvic acid (M-like)?, drinking water treatment plant[RU]	Component 2	–	–	320/410	–	250/410	–	–	–	Baghoth et al. (2010)
Fulvic acid (M-like), Occoquan Watershed (Northern Virginia, US)[RU]	Component 2, allochthonous	–	–	305/396	–	240/396	–	–	–	Holbrook et al. (2006)
Fulvic acid (M-like)?, river and coastal waters	Component 1, allochthonous	–		305/428	–	<260/428	–	–	–	Yamashita and Jaffé (2008)
Fulvic acid (M-like)?, ground water, fresh and Florida Bay waters, Florida coastal Everglades	Component 3, allochthonous	–	–	Peak′	–	Peak′	–	–	–	Chen et al. (2010)
Fulvic acid (M-like)?, river, esturine and coastal marine waters	Component 5	–	–	Peak′?	–	240/414	–	–	–	Fellman et al. (2010)

(continued)

Table 2 (contniued)

Fluorescent components	Components identified and sources	Fluorescence properties								References
		Peak C-region				Peak A-region	Peak T-region	Peak T_{UV}-region		
		Peak C	Peak M_p	Peak M	Peak W			Major	Minor	
		EX/Em (nm)								
Fulvic acid (M-like)?, water extractable from sugar maple leaves	Component 1	–	–	312/417	–	240/417	–	–	–	Hunt et al. (2008)
Allochthonous humic acids (*C-like, A-like, and M-like*)										
Suwannee River Humic Acid (C-like), standard, dissolved in Milli-Q waters (n = 4)	Component 1, allochthonous	350/461	300/461	–	–	255/461	–	–	–	Mostofa et al. (2005a)
Humic acid (C-like), streams, springs and thermokarsts, CPCRW, Alaska	Component 4, allochthonous	Peak′	–	–	–	Peak′	–	–	–	Balcarczyk et al. (2009)
Humic acid (C-like)?, soil and stream waters, temperate rainforest watersheds	Allochthonous	330/460–480	–	–	–	<250/450–460	–	–	–	Fellman et al. (2009)
Humic acid (C-like)?, soil solution samples, forest and wetland soils, rainforest watersheds	Allochthonous	370/440	–	–	–	<250/440	–	–	–	Fellman et al. (2008)
Humic acid (C-like)?, ground water, fresh and Florida Bay waters, Florida coastal Everglades	Component 5	Peak′	–	–	–	Peak′	–	–	–	Chen et al. (2010)
Humic acid (C-like), river and coastal waters	Component 2, allochthonous	340, 405/>500	–	–	–	<260/>500	–	–	–	Yamashita and Jaffé (2008)
Humic acid (C-like)?, river, esturine and coastal marine waters	Component 2	330/456–480	–	–	–	Peak′?	–	–	–	Fellman et al. (2010)

(contniued)

Table 2 (contniued)

Fluorescent components	Components identified and sources	Fluorescence properties								References
		Peak C-region				Peak A-region	Peak T-region	Peak T_{UV}-region		
		Peak C	Peak M_p	Peak M	Peak W			Major	Minor	
		EX/Em (nm)								
Humic acid (C-like)?, river, esturine and coastal marine waters	Component 3	290/510	–	–	–	–	–	–	–	Fellman et al. (2010)
Humic acid (C-like), Urdaibai and Foz Estuaries, Iberian Peninsula	Component 2, allochthonous	385/>500	–	–	–	256/>500	–	–	–	Santín et al. (2009)
Humic acid (C-like)?, Liverpool Bay, Irish Sea	Component 3	300, 410/510	–	–	–	Peak′	–	–	–	Yamashita et al. (2011)
Humic acid (C-like), coastal shelf, South Atlantic Bight	Component 4, allochthonous	390/508	–	–	–	270/508	–	–	–	Kowalczuk et al. (2009)
Humic acid (C-like), north Pacific and Atlantic oceans (BWE7 model)	Component 3[c], allochthonous	370/490	–	–	–	260/490	–	–	–	Murphy et al. (2008)
Humic acid (C-like), north Pacific and Atlantic oceans (Kauai model)	Component 1 (P3), autochthonous	380/498	–	–	–	<260/498	–	–	–	Murphy et al. (2008)
Humic acid (C-like)?, water extractable from sugar maple leaves	Component 2	351/459	–	–	–	240/459	–	–	–	Hunt et al. (2008)
Humic acid (C-like)?, compost products solution	Component 2	350/450	–	–	–	250/450	–	–	–	Yu et al. (2010)
Humic acid (C-like)?, municipal leachate samples	Component 2	360/458	–	300/458	–	250/458	–	–	–	Wu et al. (2011)
Humic acid (C-like)?, drinking water treatment plant[RU]	Component 1	360/480	–	–	–	260/480	–	–	–	Baghoth et al. (2010)
Humic acid (C-like), plant biomass, animal manure, and soils	Component 1, allochthonous	350–360/ 460–480	–	–	–	Peak′	–	–	–	Ohno and Bro (2006)

(continued)

Table 2 (contniued)

Fluorescent components	Components identified and sources	Fluorescence properties								References
		Peak C-region				Peak A-region	Peak T-region	Peak T_{UV}-region		
		Peak C	Peak M_p	Peak M	Peak W			Major	Minor	
		EX/Em (nm)								
Suwannee River Humic Acid (A-like), standard, dissolved in Milli-Q waters (n = 4)	Component 2, allochthonous	–	–	–	–	265, 230/436	–	–	–	Mostofa et al. (2005a)[c]
Humic acid (A-like)?, soil and stream waters, temperate rainforest watersheds	Allochthonous	–	–	–	–	<250/400	–	–	–	Fellman et al. (2009)
Humic acid (A-like)?, soil and stream waters, temperate rainforest watersheds	Allochthonous	–	–	–	–	<250/400	–	–	–	Fellman et al. (2009)
Humic acid (A-like)?, ground water, fresh and Florida Bay waters, Florida coastal Everglades	Component 2, allochthonous	–	–	–	–	Peak′	–	–	–	Chen et al. (2010)
Humic acid (A-like)?, river, esturine and coastal marine waters	Component 1	–	–	–	–	<250/ 450–470	–	–	–	Fellman et al. (2010)
Humic acid (A-like)?, water extractable from sugar maple leaves	Component 3	–	–	–	–	240/483	–	–	–	Hunt et al. (2008)
Humic acid (A-like)?, municipal leachate samples	Component 4	–	–	–	–	220/432	–	–	–	Wu et al. (2011)
Humic acid (M-like)?, soil solution samples, forest and wetland soils, rainforest watersheds	Allochthonous	–	–	300/416	–	240/416	–	–	–	Fellman et al. (2008)

(contniued)

Table 2 (contniued)

Fluorescent components	Components identified and sources	Fluorescence properties								References
		Peak C-region				Peak A-region	Peak T-region	Peak T_{UV}-region		
		Peak C	Peak M_p	Peak M	Peak W			Major	Minor	
		EX/Em (nm)								
Humic acid (M-like)?, soil and stream waters, temperate rainforest watersheds	Allochthonous	–	–	295/414	–	<250/414	–	–	–	Fellman et al. (2009)
Humic acid (M-like)?, municipal leachate samples	Component 1	–	–	330/412	–	240/412	–	–	–	Wu et al. (2011)
Humic acid (M-like), plant biomass, animal manure, and soils	Components 2, allochthonous	–		290–300/465	–	>240/465	–	–	–	Ohno and Bro (2006)
Autochthonous fulvic acid (*C-like*): *biologically or photochemically produced* –										
Autochthonous fulvic acid (C-like), mainstream of NenJiang River, North-East China	Component 1	350/460	–	–	–	260/460	–	–	–	Mostofa KMG et al., (unpublished data)
Autochthonous fulvic acid (C-like), tributaries of NenJiang River, North-East China	Component 1	340/460	–	–	–	260/460	–	–	–	Mostofa KMG et al., (unpublished data)
Autochthonous fulvic acid (C-like), surface waters (0–25 m), Lake Hongfeng, China	Component 1, algae or phytoplankton	335–340/442–464	–	–	–	260/442–464	–	–	–	Fu et al. (2010)[c]
Autochthonous fulvic acid (C-like), algae origin, microbial assimilations in Milli-Q waters	Component 1, algae or phytoplankton	340/442	–	290/442	–	260/442	–	–	–	Mostofa KMG et al., (unpublished data)

(continued)

Table 2 (contniued)

Fluorescent components	Components identified and sources	Fluorescence properties								References
		Peak C-region				Peak A-region	Peak T-region	Peak T_{UV}-region		
		Peak C	Peak M_p	Peak M	Peak W			Major	Minor	
		EX/Em (nm)								
Autochthonous fulvic acid (C-like), algae origin, microbial assimilations in River waters	Component 1, algae or phytoplankton	340–455	–	295–300/430–448	–	260–265/436–448	–	–	–	Mostofa KMG et al., (unpublished data)
Autochthonous fulvic acid (C-like), algae origin, photo assimilations in Milli-Q waters	Component 1, algae or phytoplankton	340/448	–	–	–	260/448	–	–	–	Mostofa KMG et al., (unpublished data)
Autochthonous fulvic acid (C-like), algae origin, photo assimilations in River waters	Component 1, algae or phytoplankton	340/454	–	–	–	270/454	–	–	–	Mostofa KMG et al., (unpublished data)
Autochthonous fulvic acid (C-like), algae origin, under a 12:12 h light/dark cycle	Autochthonous	355/445	–	–	–	280/435	–	–	–	Zhao et al. (2009)
Autochthonous fulvic acid (C-like) or hydrophilic DOM, three phytoplankton: 12:12 h light/dark cycle	Autochthonous	340–350/420–440	–	–	–	260–280/425–445	–	–	–	Aoki et al. (2008)
Autochthonous fulvic acid (C-like) or hydrophobic acid, three phytoplankton: 12:12 h light/dark cycle	Autochthonous	330–350/435–440	–	–	–	250–290/430–455	–	–	–	Aoki et al. (2008)
Autochthonous fulvic acid (C-like), streams, springs and thermokarsts, CPCRW, Alaska	Component 6, algae	Peak′	–	–	–	Peak′	–	–	–	Balcarczyk et al. (2009)

(contniued)

Table 2 (contniued)

Fluorescent components	Components identified and sources	Fluorescence properties								References
		Peak C-region				Peak A-region	Peak T-region	Peak T_{UV}-region		
		Peak C	Peak M_p	Peak M	Peak W			Major	Minor	
		EX/Em (nm)								
Autochthonous fulvic acid (C-like)?, fresh and Florida Bay waters, Florida coastal Everglades	Component 1, autochthonous	Peak′	–	–	–	Peak′	–	–	–	Chen et al. (2010)
Autochthonous fulvic acid (C-like), Lake Taihu	Component 1, phytoplankton	365/453	–	–	–	270/453	–	–	–	Zhang et al. (2009a)
Autochthonous fulvic acid (C-like)?, Sepetiba Bay, Brazil	Component 1, phytoplankton	350/400–450	–	–	–	275/400–450	–	–	–	Luciani et al. (2008)
Autochthonous fulvic acid (C-like), Sea ice, Baltic Sea coastal regions[RU]	Component 1	Peak′	–	–	–	Peak′	–	–	–	Stedmon et al. (2007a)
Autochthonous fulvic acid (C-like), deep waters of the Okhotsk Sea and North Pacific Ocean	Component 1	370/466	–	–	–	<260/466	–	–	–	Yamashita et al. (2010)
Autochthonous fulvic acid (C-like)?, Southern Ocean	Component 3	340/420	–	–	–	260/420	–	–	–	Wedborg et al. (2007)
Autochthonous fulvic acid (C-like), north Pacific and Atlantic oceans (Kauai model)	Component 8 (P8)[c], autochthonous	355/434	–	–	–	260/434	–	–	–	Murphy et al. (2008)
Humic-like, marine waters	Algae or phytoplankton	330–350/420–480	–	–	–	250–260/420–480	–	–	–	Coble (1996), Parlanti et al. (2000)
Autochthonous fulvic acid (M-like): biologically produced										
Marine humic-like, marine waters	Algae or phytoplankton	–	–	310–320/380–420	–	Peak′	–	–	–	Coble (1996), Parlanti et al. (2000)

(continued)

Table 2 (contniued)

Fluorescent components	Components identified and sources	Fluorescence properties								References
		Peak C-region				Peak A-region	Peak T-region	Peak T_{UV}-region		
		Peak C	Peak M_p	Peak M	Peak W			Major	Minor	
		EX/Em (nm)								
Autochthonous fulvic acid (M-like), surface waters (0–25 m), Lake Hongfeng, China	Component 2, algae or phytoplankton	–	–	295–300/396–422	–	235–240/296–422	–	–	–	Fu et al. (2010)[c]
Autochthonous fulvic acid (M-like), microbial assimilations of lake algae in river waters	Component 2, algae or phytoplankton	–	–	300/405	–	240/405	–	–	–	Mostofa KMG et al., (unpublished data)
Autochthonous fulvic acid (M-like), Lake Taihue	Component 4, phytoplankton	–	–	315/372	–	–	–	–	–	Zhang et al. (2009a)
Autochthonous fulvic acid (M-like)?, Lake Taihue	Component 3, phytoplankton	–	–	330/412	–	255/412	–	–	–	Zhang et al. (2009a)
Autochthonous fulvic acid (M-like), Lake Taihue[c]	Component 1, algae or phytoplankton	–	–	322/407	–	Peak′	–	–	–	Wang et al. (2007)
Autochthonous fulvic acid (M-like) or hydrophilic DOM, three phytoplankton: 12:12 h light/dark cycle	Autochthonous	–	–	320/385	–	–	–	–	–	Aoki et al. (2008)
Autochthonous fulvic acid (M-like) or hydrophobic acid, three phytoplankton: 12:12 h light/dark cycle	Autochthonous	–	–	330/385	–	–	–	–	–	Aoki et al. (2008)
Autochthonous fulvic acid (M-like), microbial assimilations of marine algae in Milli-Q waters	Component 2, algae or phytoplankton	–	–	290/400–410	–	Peak′	–	–	–	Parlanti et al. (2000)

(contniued)

Table 2 (contniued)

Fluorescent components	Components identified and sources	Fluorescence properties								References
		Peak C-region				Peak A-region	Peak T-region	Peak T_{UV}-region		
		Peak C	Peak M_p	Peak M	Peak W			Major	Minor	
		EX/Em (nm)								
Autochthonous fulvic acid (M-like), microbial assimilations of marine algae in sea waters	Component 2, algae or phytoplankton	–	–	300–310/ 400–410	–	Peak′	–	–	–	Parlanti et al. (2000)
Autochthonous fulvic acid (M-like)?, streams, springs and thermokarsts, CPCRW, Alaska	Component 8, algae	–	–	Peak′	–	Peak′	–	–	–	Balcarczyk et al. (2009)
Autochthonous fulvic acid (M-like), microbially produced in mesocosm experiment[RU]	Component 3, algae or phytoplankton	–	–	295/398	–	Peak′	–	–	–	Stedmon and Markager (2005a)
Autochthonous fulvic acid (M-like)?, microbially produced in mesocosm experiment[RU]	Component 5, phytoplankton	–	–	345/434	–	Peak′	–	–	–	Stedmon and Markager (2005a)
Autochthonous fulvic acid (M-like), river and coastal waters	Component 4, autochthonous	–	–	305/378	–	<260/378	–	–	–	Yamashita and Jaffé (2008)
Autochthonous fuvic acid (M-like)?, Florida Bay waters, Florida coastal Everglades	Component 4	–	–	Peak′	–	Peak′	–	–	–	Chen et al. (2010)
Photobleached autochthonous fulvic acid (M-like)?, Liverpool Bay, Irish Sea	Component 4	–		295/358	–	<250/358	–	–	–	Yamashita et al. (2011)

(continued)

Table 2 (contniued)

Fluorescent components	Components identified and sources	Fluorescence properties								References
		Peak C-region				Peak A-region	Peak T-region	Peak T_{UV}-region		
		Peak C	Peak M_p	Peak M	Peak W			Major	Minor	
		EX/Em (nm)								
Autochthonous fulvic acid (M-like)?, Sepetiba Bay, Brazil	Component 3, phytoplankton	–	–	320/380–420	–	Peak′	–	–	–	Luciani et al. (2008)
Autochthonous fulvic acid (M-like)?, river, esturine and coastal marine waters	Component 4	–	–	Peak′?	–	240/384	–	–	–	Fellman et al. (2010)
Autochthonous fulvic acid (M-like), Urdaibai and Foz Estuaries, Iberian Peninsula	Component 3, autochthonous	–	–	320/388	–	Peak′	–	–	–	Santín et al. (2009)
Autochthonous fulvic acid (M-like), Horsens Estuary, Jutland Peninsula, Denmark[RU]	Component 6[c], autochthonous	–	–	320/400	–	250/400	–	–	–	Stedmon and Markager (2005b)
Autochthonous fulvic acid (M-like), Estuary of Horsens Fjord, Denmark[RUc]	Component 4[c], autochthonous	–	–	325/416	–	250/416	–	–	–	Stedmon et al. (2003)
Autochthonous fulvic acid (M-like)?, Horsens Estuary, Jutland Peninsula, Denmark[RU]	Component 5, allochthonous/agriculture		–	325/428	–	–	–	–	–	Stedmon and Markager (2005b)
Autochthonous fulvic acid (M-like), coastal waters, Isa Bay	Component 6, autochthonous	–	–	325/385	–	260/385	–	–	–	Yamashita et al. (2008)
Autochthonous fulvic acid (M-like), coastal shelf, South Atlantic Bight	Component 3, autochthonous	–	–	310/400	–	250/400	–	–	–	Kowalczuk et al. (2009)

(contniued)

Table 2 (contniued)

Fluorescent components	Components identified and sources	Fluorescence properties								References
		Peak C-region				Peak A-region	Peak T-region	Peak T_{UV}-region		
		Peak C	Peak M_p	Peak M	Peak W			Major	Minor	
		EX/Em (nm)								
Autochthonous fulvic acid (M-like), deep waters of the Okhotsk Sea and North Pacific Ocean	Component 2	–	–	325/385	–	<260/385	–	–	–	Yamashita et al. (2010)
Autochthonous fulvic acid (M-like), north Pacific and Atlantic oceans (BWE7 model)	Component 2, autochthonous	–	–	315/418	–	Peak′	–	–	–	Murphy et al. (2008)
Autochthonous fulvic acid (M-like), north Pacific and Atlantic oceans (Kauai model)	Component 1 (P1), autochthonous	–	–	310/414	–	260/414	–	–	–	Murphy et al. (2008)
Autochthonous fulvic acid (M-like?, drinking water treatment plant[RU]	Component 6	–	–	300/406	–	<250/406	–	–	–	Baghoth et al. (2010)
Autochthonous fulvic acid (M-like)?, compost products solution	Component 1	–	–	330/410	–	230/410	–	–	–	Yu et al. (2010)
Autochthonous fulvic acid (M-like), pore waters, four lakes, China	Component 2, algae or phytoplankton	–	–	300–310/396–416	–	225–240/396–416	–	–	–	Li et al., Characteristics of sediment pore water dissolved organic matter in four Chinese lakes using EEM spectroscopy and PARAFAC modeling, (unpublished data)

(continued)

Table 2 (contniued)

Fluorescent components	Components identified and sources	Fluorescence properties								References
		Peak C-region				Peak A-region	Peak T-region	Peak T_{UV}-region		
		Peak C	Peak M_p	Peak M	Peak W			Major	Minor	
		EX/Em (nm)								
Protein-like substance										
Protein-like, streams, springs and thermokarsts, CPCRW, Alaska	Component 5, autochthonous	–	–	–	–	–	Peak′	Peak′	–	Balcarczyk et al. (2009)
Protein-like, sewerage drainage samples, Nanming River, China	Component 1	–	–	–	–	–	280/339–346	230/338–351	–	Mostofa et al. (2010)
Protein-like, washing samples collected after washing cloths	Component 1	–	–	–	–	–	280/344	235/348	–	Mostofa et al. (2010)
Protein-like, hydrophilic DOM fraction, three phytoplankton: 12:12 h light/dark cycle	Autochthonous	–	–	–	–	–	270–290/335–375	Peak′	–	Aoki et al. (2008)
Protein-like, hydrophobic acid fraction, three phytoplankton: 12:12 h light/dark cycle	Autochthonous	–	–	–	–	–	270–290/250–365	Peak′	–	Aoki et al. (2008)
Protein-like?, ground water, fresh and Florida Bay waters, Florida coastal Everglades	Component 8	–	–	–	–	–	Peak′	–	–	Chen et al. (2010)
Protein-like, coastal shelf, South Atlantic Bight	Component 6, autochthonous	–	–	–	–	–	290/356	250/356	–	Kowalczuk et al. (2009)
Protein-like?, Baltic Sea	Component 4, autochthonous	–	–	–	–	–	Peak′	Peak′	–	Stedmon et al. (2007a)

(contniued)

Table 2 (contniued)

Fluorescent components	Components identified and sources	Fluorescence properties								References
		Peak C-region				Peak A-region	Peak T-region	Peak T_{UV}-region		
		Peak C	Peak M_p	Peak M	Peak W			Major	Minor	
		EX/Em (nm)								
Protein-like, north Pacific and Atlantic oceans (BWE7 model)	Component 6, autochthonous	–	–	–	–	–	280/328	Peak′	–	Murphy et al. (2008)
Protein-like, north Pacific and Atlantic oceans (BWE7 model)	Component 7, autochthonous	–	–	–	–	–	300/338	240/338	–	Murphy et al. (2008)
Protein-like?, glacial ice samples, Antarctic and Arctic Ocean	Component 5, autochthonous	–	–	–	–	–	275/320	–	–	Dubnick et al. (2010)
Aromatic amino acids										
Tryptophan-like, soil and stream waters, temperate rainforest watersheds	Allochthonous	–	–	–	–	–	280/330–340	Peak	–	Fellman et al. (2009)
Tryptophan-like, Yasu River, Lake Biwa watershed, Japan	Component 2, autochthonous	–	–	–	–	–	280/344	230/344	–	Mostofa et al. (2005a)
Tryptophan-like, Occoquan Watershed (Northern Virginia, US)	Component 3, autochthonous	–	–	–	–	–	280/340	230/340	–	Holbrook et al. (2006)
Tryptophan-like, soil solution samples, forest and wetland soils, rainforest watersheds	Allochthonous	–	–	–	–	–	280/330–340	Peak	–	Fellman et al. (2008)
Tryptophan-like, Nanming River, China	Anthropogenic sources	–	–	–	–	–	275–280/333–351	225–235/338–351	–	Mostofa et al. (2010)
Tryptophan-like, urban sewerage samples[RU]	Component 1	–	–	–	–	–	275/339	220/339	–	Guo et al. (2010)

(continued)

Table 2 (contniued)

Fluorescent components	Components identified and sources	Fluorescence properties								References
		Peak C-region				Peak A-region	Peak T-region	Peak T_{UV}-region		
		Peak C	Peak M_p	Peak M	Peak W			Major	Minor	
		EX/Em (nm)								
Tryptophan-like, drinking water treatment plant[RU]	Component 4, autochthonous	–	–	–	–	–	290/360	<250/360	–	Baghoth et al. (2010)
Tryptophan-like, municipal leachate samples	Component 3	–	–	–	–	–	280/340	230/340	–	Wu et al. (2011)
Tryptophan-like, Estuary of Horsens Fjord, Denmark[RU]	Component 5, autochthonous	–	–	–	–	–	280/368	240/368	–	Stedmon et al. (2003)
Tryptophan-like, microbially produced in mesocosm experiment[RU]	Component 6, algae- or phytoplankton	–	–	–	–	–	280/338	Peak′	–	Stedmon and Markager (2005a)
Tryptophan-like, Horsens Estuary, Jutland Peninsula, Denmark[RU]	Component 7, autochthonous	–	–	–	–	–	280/344	Peak′	–	Stedmon and Markager (2005b)
Tryptophan-like, river and coastal waters	Component 7, autochthonous	–	–	–	–	–	295/340	Peak′	–	Yamashita and Jaffé (2008)
Tryptophan-like, river, esturine and coastal marine waters	Component 7	–	–	–	–	–	280/330–340	Peak′	–	Fellman et al. (2010)
Tryptophan-like, Liverpool Bay, Irish Sea	Component 5, autochthonous	–	–	–	–	–	280/334	Peak′?	–	Yamashita et al. (2011)
Tryptophan-like, marine waters	Autochthonous	–	–	–	–	–	270–280/320–350	Peak	–	Coble (1996), Parlanti et al. (2000)
Tryptophan-like, glacial ice samples, Antarctic and Arctic Ocean	Component 2, autochthonous	–	–	–	–	–	280/348	<250/348	–	Dubnick et al. (2010)
Tryptophan-like, compost products solution	Component 3	–	–	–	–	–	280/340	220/340	–	Yu et al. (2010)
Tryptophan-like, plant biomass, animal manure, and soils	Components 4, allochthonous	–	–	–	–	–	270/354	Peak′	–	Ohno and Bro (2006)

(contniued)

Table 2 (contniued)

Fluorescent components	Components identified and sources	Fluorescence properties								References
		Peak C-region				Peak A-region	Peak T-region	Peak T_{UV}-region		
		Peak C	Peak M_p	Peak M	Peak W			Major	Minor	
		EX/Em (nm)								
Tyrosine-like, streams, springs and thermokarsts, CPCRW, Alaska	Component 9, autochthonous	–	–	–	–	–	Peak′	Peak′	–	Balcarczyk et al. (2009)
Tyrosine-like, soil and stream waters, temperate rainforest watersheds	Allochthonous	–	–	–	–	–	275/304–306	Peak	–	Fellman et al. (2009)
Tyrosine-like, soil solution samples, forest and wetland soils, rainforest watersheds	Allochthonous	–	–	–	–	–	275/304–306	Peak	–	Fellman et al. (2008)
Tyrosine-like, Urdaibai and Foz Estuaries, Iberian Peninsula	Component 4, autochthonous	–	–	–	–	–	275/304	Peak′	–	Santín et al. (2009)
Tyrosine-like, microbially produced in mesocosm experiment[RU]	Component 4	–	–	–	–	–	275/306	Peak′	–	Stedmon and Markager (2005a)
Tyrosine-like, Horsens Estuary, Jutland Peninsula, Denmark[RU]	Component 8, autochthonous	–	–	–	–	–	275/304	Peak′	–	Stedmon and Markager (2005b)
Tyrosine-like, ground water, Fresh and Florida Bay waters, Florida coastal Everglades	Component 7	–	–	–	–	–	Peak′	Peak′	–	Chen et al. (2010)
Tyrosine-like, river, esturine and coastal marine waters	Component 8	–	–	–	–	–	275/304–306	Peak′	–	Fellman et al. (2010)
Tyrosine-like, coastal waters	Component 8, autochthonous	–	–	–	–	–	275/324	Peak′	–	Yamashita and Jaffé (2008)
Tyrosine-like, Liverpool Bay, Irish Sea	Component 6, autochthonous	–	–	–	–	–	275/302	Peak′?	–	Yamashita et al. (2011)

(continued)

Table 2 (contniued)

Fluorescent components	Components identified and sources	Fluorescence properties								References
		Peak C-region				Peak A-region	Peak T-region	Peak T_{UV}-region		
		Peak C	Peak M_p	Peak M	Peak W			Major	Minor	
		EX/Em (nm)								
Tyrosine-like, coastal waters, Isa Bay	Component 7	–	–	–	–	–	270/299	Peak′	–	Yamashita et al. (2008)
Tyrosine-like, coastal shelf, South Atlantic Bight	Component 5, autochthonous	–	–	–	–	–	270/332	Peak′	–	Kowalczuk et al. (2009)
Tyrosine-like, deep waters of the Okhotsk Sea and North Pacific Ocean	Component 4	–	–	–	–	–	275/306	Peak′?	–	Yamashita et al. (2010)
Tyrosine-like, north Pacific and Atlantic oceans (BWE7 model)	Component 1, autochthonous	–	–	–	–	–	275/300	Peak′	–	Murphy et al. (2008)
Tyrosine-like, marine waters	Autochthonous	–	–	–	–	–	275/310	Peak′	–	Coble (1996)
Tyrosine-like, water extractable from sugar maple leaves	Component 4	–	–	–	–	–	270/310	Peak′	–	Hunt et al. (2008)
Tyrosine-like, drinking water treatment plant[RU]	Component 7	–	–	–	–	–	270/306	Peak′?	–	Baghoth et al. (2010)
Tyrosine-like: plant biomass, animal manure, and soils	Components 5, allochthonous	–	–	–	–	–	273/309	Peak′	–	Ohno and Bro (2006)
Phenylalanine	Autochthonous	–	–	–	–	–	255–265/ 284–285	–	–	Yamashita and Tanoue (2003a)[b]
Phenylalanine-like?, glacial ice samples, Antarctic and Arctic Ocean	Component 1	–	–	–	–	–	265/306	Peak′	–	Dubnick et al. (2010)
Detergent-like or fluorescent whitening agents (FWAs)-like										
Detergents dissolved in Milli-Q waters, Nafine Chem Ind Ltd, China	Component 1	–	–	–	345/430 –435	240/429–433	–	–	–	Mostofa et al. (2010), Mostofa KMG et al., (unpublished data)

(contniued)

Table 2 (contniued)

Fluorescent components	Components identified and sources	Fluorescence properties								References
		Peak C-region				Peak A-region	Peak T-region	Peak T_{UV}-region		
		Peak C	Peak M_p	Peak M	Peak W			Major	Minor	
		EX/Em (nm)								
Detergents dissolved in Milli-Q waters, Nafine Chem Ind Ltd, China	Component 2	–	–	–	–	–	–	–	225/287–289	Mostofa et al. (2010), Mostofa KMG et al., (unpublished data)
Detergents dissolved in Milli-Q waters, Nice Group Co Ltd, China	Component 1	–	–	–	345/430	240/427	–	–	–	Mostofa et al. (2010), Mostofa KMG et al., (unpublished data)
Detergents dissolved in Milli-Q waters, Nice Group Co Ltd, China	Component 2	–	–	–	–	–	–	–	225/287	Mostofa et al. (2010), Mostofa KMG et al., (unpublished data)
Detergent-like, detected in river water samples	Component 1	–	–	–	335–345/ 432–437	255/425–447	–	–	–	Mostofa et al. (2010), Mostofa KMG et al., (unpublished data)
Detergent-like, detected in river water samples	Component 2	–	–	–	–	–	–	–	225/289 –294	Mostofa et al. (2010), Mostofa KMG et al., (unpublished data)
Detergent-like, Izumi and Hinotsume, Kurose River, Japan	Component 1	–	–	–	350/437	250/437	–	–	–	Mostofa et al. (2005a)
Detergent-like, detected in sewerage samples	Component 1	–	–	–	335–345/ 432–437	240–250/ 425–443	–	–	–	Mostofa et al. (2010), Mostofa KMG et al., (unpublished data)

(continued)

Table 2 (contniued)

Fluorescent components	Components identified and sources	Fluorescence properties								References
		Peak C-region				Peak A-region	Peak T-region	Peak T_{UV}-region		
		Peak C	Peak M_p	Peak M	Peak W			Major	Minor	
		EX/Em (nm)								
Detergent-like?, urban sewerage samples[RU]	Component 4	–	–	–	340/422	230/422	–	–	–	Guo et al. (2010)
Detergent-like, detected in sewerage samples	Component 2	–	–	–	–	–	–	–	225–230/ 291–296	Mostofa et al. (2010), Mostofa KMG et al., (unpublished data)
Detergent-like?, drinking water treatment plant[RU]	Component 5	–	–	–	340/440	250/440	–	–	–	Baghoth et al. (2010)
Algae or phytoplankton										
Algae (green) or bacteria in Milli-Q or river water samples, collected from lake surface waters	Component 1	–	–	–	–	–	280–285/ 340–346	230/346	–	Mostofa KMG et al., (unpublished data)[a]
Algae (green) or bacteria in Milli-Q or river water samples, collected from lake surface waters	Component 2	–	–	–	–	–	270/327–336	230/327–336	–	Mostofa KMG et al., (unpublished data)[a]

RU indicates the Raman Unit (nm-1) calibration of fluorescence intensity of the samples studied whereas excitation and emission wavelength is much differed from standard quinine sulfate unit (QSU) calibration (Mostofa et al. 2005b)

Peak M_p means fluorescence Ex/Em maxima of fulvic acid which is photobleached by photochemical processes or by any other natural processes

Peak M indicates the allochthonous and autochthonous fulvic acid (M-like)

[a]Indicates river EEM data is deducted from sample before PARAFAC modeling on the matrix data

[b]Ranges expresses the authentic standard at various concentrations (1–5 mg L^{-1}) and mechanical reproducibility

[c]Indicates that the components are identified using the PARAFAC model on the original EEM of that published paper

Peak′ means the peak is at this region, but not specified in the paper; *UD* unpublished data

? indicates the values mentioned here are different than in the paper

2009a, 2005a, 2010, 2007b; Mopper and Schultz 1993; Yamashita and Tanoue 2003a; Komaki and Yabe 1982; Nakajima 2006; Baker 2005; Chen et al. 2003; Burdige et al. 2004; Fu et al. 2006). Peak T_{UV}-region depicts the shorter (UV) wavelength ranges at Ex/Em = 215–260/280–380 nm, which includes mostly the secondary fluorescence peaks of various fluorescent organic substances such as proteins, aromatic amino acids (tryptophan-like, tyrosine-like and phenylalanine-like), algae, detergent component, phenol-like compounds, naphthalene, *o*-cresol, *p*-cresol, *p*-hydroxy benzaldehyde, *p*-hydroxy acetophenone, 1,4-dichlorobenzene, and 4-biphenyl carboxaldehyde (Table 1) (Mostofa et al. 2009a, 2010; Mopper and Schultz 1993; Yamashita and Tanoue 2003a; Nakajima 2006; Baker 2005; Baker and Curry 2004; Chen et al. 2003; Burdige et al. 2004; Fu et al. 2006). Note that the fluorescence intensity expressed as QSU (quinine sulphate unit) is considered to identify the authentic or valid excitation–emission wavelength maxima. In contrast, the maxima of the calibrated fluorescence intensity obtained using the Raman Unit (RU: nm^{-1}) method can be significantly shifted, particularly at the peak C-region (Mostofa et al. 2005b). Such issues are discussed in details later, in the fluorescence intensity normalization section.

2.3 PARAFAC Modeling in FDOM Study

Parallel factor (PARAFAC) modeling is a three-way multivariate analysis that can be applied on an additive mixture of fluorescence signals obtained from excitation–emission matrix spectra. PARAFAC is capable of isolating and quantifying the individual fluorescence component signals in terms of fluorescence intensity of FDOM in natural waters or in mixtures.

From the PARAFAC model (Harshman 1970) it can be implied that for any fluorophore, the emission intensity at a specific wavelength j that corresponds to excitation at the wavelength k can be expressed as follows (Eq. 2.7):

$$x_{jk} = ab_j c_k \tag{2.7}$$

where x_{jk} is the intensity of the light at the emission wavelength j and excitation wavelength k, a is the concentration (in arbitrary units) of the analyte, b_j is the relative emission at the wavelength j, and c_k is the relative amount of light absorbed at the excitation wavelength k. For any number of analytes and samples, the PARAFAC model can be developed into a set of trilinear terms and a residual array as (Eq. 2.8) (Stedmon et al. 2003)

$$x_{ijk} = \sum_{f=1}^{F} a_{ij} b_{jf} c_{kf} + \varepsilon_{ijk},\ i = 1, \ldots, I;\ j = 1, \ldots, J;\ k = 1, \ldots, K \tag{2.8}$$

where x_{ijk} is the fluorescence intensity of the ith sample at the emission wavelength j and excitation wavelength k. a_{if} is directly proportional to the concentration (in arbitrary units) of the analyte f in sample i. b_{jf} is directly proportional to

the quantum efficiency of fluorescence of the analyte f at the emission wavelength j. Similarly, c_{kf} is linearly related to the specific absorption coefficient at excitation wavelength k. F is the number of components in the model and ε_{ijk} is the residual matrix that indicates the variability not accounted for by the model.

Three steps are followed before running EEM data in the PARAFAC model (Bro 1997; Stedmon et al. 2003). First, the Milli-Q water blank is subtracted from every sample. Second, all values of the Raleigh light scattering are properly eliminated from the data of sample's EEMs to avoid any effect on the component numbers. Third, non-negative constraints are applied in the PARAFAC modeling to avoid negative values of excitation, emission and concentration in any model component.

By applying bilinear models to the EEM data (Bro 1999), it is possible to judge the residuals of the fit. If systematic variation is left in, the residuals that indicate more components can be extracted. If a plot of the residual sum of squares versus the number of components sharply flattens out for a certain number of components, this indicates the true number of components. To calculate variance-like estimators, the degrees of freedom are expressed as follows (Eq. 2.9):

$$\text{Dof}\,(F) = IJK - F\,(I + J + K - 2) \tag{2.9}$$

for a trilinear PARAFAC model where I, J and K are the dimensions of the first, second and third mode, respectively, and F is the number of components in the model (Bro 1997). In the PARAFAC model, it is important to select the true number of components, ranging from 1 until the proper components are identified. The true number (Bro 1997) of components is determined on the basis of the residuals, the core consistency (that must be 100 %), the number of iterations (which should be near zero) and the findings of the EEM spectra for the respective samples, with reference to the various standard substances. The loadings of the emission and excitation wavelengths are often used to check the variability of the selected components (Stedmon et al. 2003). The three key ways of determining the true number of components are (Bro 1997): (i) Spilt-half experiments, (ii) judging residuals, and (iii) comparison with the external knowledge of the original EEM images and data being modeled. The other most important factors that one needs to know before PARAFAC modeling are: (i) Selection of the proper excitation–emission wavelength ranges for the measured samples. Such ranges significantly affect the shape and images of the isolated components, as well as the reproducibility of fluorescence intensity. Depending on the nature of FDOM components in natural waters, the most chosen wavelength ranges could be 220–400 nm for excitation and 280–550 nm for emission. (ii) Similar types of samples must be modeled individually. For example, individual modeling should be made of upstream rivers with merely natural sources of DOM, downstream rivers with a variety of DOM sources, and lake waters with both autochthonous and allochthonous sources of DOM. PARAFAC can identify the key fluorescent components in DOM, but it cannot isolate the minor ones that remain as a residue (Stedmon et al. 2003).

2.3.1 Characterization of FDOM Using EEM in Combination with PARAFAC

PARAFAC modeling, a three-way method with its origin in psychometrics (Harshman 1970; Caroll and Chang 1970), can be effectively applied to isolate the EEMs of either an aqueous mixture of organic components or of natural DOM into their individual fluorescence components (Bro 1997, 1998, 1999; Ross et al. 1991; Jiji et al. 1999; Baunsgaard et al. 2000, 2001; da Silva et al. 2002; Stedmon et al. 2003, 2007a, 2007b; Cory and McKnight 2005; Mostofa et al. 2010; Wedborg et al. 2007; Hiriart-Baer et al. 2008; Hunt et al. 2008; Luciani et al. 2008; Kowalczuk et al. 2009; Ohno et al. 2009; Zhao et al. 2009; Baghoth et al. 2010; Chen et al. 2010; Dubnick et al. 2010; Fellman et al. 2008, 2009, 2010; Guo et al. 2010; Singh et al. 2010; Yu et al. 2010; Wu et al. 2011; Yamashita et al. 2010, 2011). The EEMs often involve various types of overlapping peaks because of the natural DOM composition, which makes it difficult to identify the fluorescent component peaks and their intensities. PARAFAC, a statistical modeling approach, can isolate the fluorescent components from EEMs and then determine the concentration of the fluorescing compounds.

The EEM in combination with PARAFAC analysis has been applied to separate and identify the various DOM components and their concentrations in rivers and freshwaters (Mostofa et al. 2010; Chen et al. 2010; Fellman et al. 2009, 2010; Holbrook et al. 2006; Hua et al. 2007; Balcarczyk et al. 2009), lakes (Cory and McKnight 2005; Chin et al. 1994; Gron et al. 1996), wetlands (Fellman et al. 2008; Holbrook et al. 2006), estuaries (Stedmon et al. 2003; Hall et al. 2005; Stedmon and Markager 2005a, 2005b; Fellman et al. 2010; Santín et al. 2009), bays and marine waters (Luciani et al. 2008; Fellman et al. 2010; Singh et al. 2010; Yamashita et al. 2010, 2011, 2008; Murphy et al. 2008), lake sediment pore waters (Li et al., Characteristics of sediment pore water dissolved organic matter in four Chinese lakes using EEM spectroscopy and PARAFAC modeling, unpublished data), wastewaters (Baghoth et al. 2010; Guo et al. 2010; Wu et al. 2011), landfill leachate (Baker and Curry 2004; Lu et al. 2009) and soil (Ohno and Bro 2006; Fellman et al. 2008, 2009). PARAFAC is also adopted in a wide range of different applications, such as the identification of autochthonous fulvic acids of algal origin that can be distinguished from allochthonous fulvic acid (Mostofa et al. 2009b; Stedmon et al. 2007b; Mostofa KMG et al., unpublished data; Zhang et al. 2009a; Li et al., Characteristics of sediment pore water dissolved organic matter in four Chinese lakes using EEM spectroscopy and PARAFAC modeling, unpublished data). PARAFAC can also be used to trace photoinduced and microbial changes in DOM components and their intensities (Cory and McKnight 2005; Stedmon and Markager 2005a; Stedmon et al. 2007a; Mostofa et al. 2010), in water source categorization (Hua et al. 2007) and in correlation with water quality parameters (Hayase and Tsubota 1985), in the identification of changes in the fulvic acid redox state (Fulton et al. 2004; Cory and McKnight 2005), and finally in studying interactions between trace metals and DOM (Yamashita and Jaffé 2008).

The most common fluorescent DOM components isolated from DOM in natural waters using PARAFAC modeling are allochthonous fulvic acids and humic acids of vascular plant origin, autochthonous fulvic acids (termed C-like and M-like based on the component's peak positions) of algal (or phytoplankton) origin, aromatic amino acids (tryptophan, tyrosine and phenylalanine), FWAs (DAS1 and DSBP), green algae, chlorophyll *a* (Chl *a*) and chlorophyll *b* (Table 2) (Coble 1996; Parlanti et al. 2000; Yamashita and Tanoue 2003a; Mostofa et al. 2005a, Mostofa et al. 2005b, 2010; Stedmon et al. 2003, 2007a; Stedmon and Markager 2005a, 2005b; Ohno and Bro 2006; Mostofa KMG et al., unpublished data; Fu et al. 2010; Zhang et al. 2009a; Wedborg et al. 2007; Hunt et al. 2008; Luciani et al. 2008; Kowalczuk et al. 2009; Zhao et al. 2009; Baghoth et al. 2010; Chen et al. 2010; Dubnick et al. 2010; Fellman et al. 2008, 2009, 2010; Guo et al. 2010; Singh et al. 2010; Yu et al. 2010; Wu et al. 2011; Yamashita et al. 2010, 2011; Holbrook et al. 2006; Balcarczyk et al. 2009; Santín et al. 2009; Murphy et al. 2008; Yamashita et al. 2008; Li et al., Characteristics of sediment pore water dissolved organic matter in four Chinese lakes using EEM spectroscopy and PARAFAC modeling, unpublished data; Yamashita and Jaffé 2008; Aoki et al. 2008; Wang et al. 2007). These fluorescent components generally exhibit fluorescence at peak C-, peak A-, peak T- and T_{UV}-regions (Table 2). Their fluorescence properties are depicted in Sect. 2.5, as a function of the molecular structure of the respective components.

2.4 Fluorescence Intensity of a Molecule and its Normalization

A fluorescent molecule has one, two or several fluorescence peaks, and each peak can be denoted as fluorophore or fluorochrome. For example, fulvic acid has two fluorescence peaks in EEM spectra, namely peak C at longer wavelength and peak A in the shorter-wavelength UV region. The fluoresce intensity of fulvic acid is higher at peak A-region compared to the peak C-region (Mostofa et al. 2009a, 2005a, 2010; Coble 1996; Yamashita and Jaffé 2008). On the other hand, humic acid has several fluorescence peaks such as peak M, peak C and peak A. The peak A-region has usually the highest fluorescence intensity (Mostofa et al. 2009a, 2005a, 2010; Coble 1996; Yamashita and Jaffé 2008). Tryptophan amino acid has two fluorescence peaks: peak T at relatively longer wavelengths and peak T_{UV} in the shorter-wavelength UV region (Mostofa et al. 2009a, 2005a, 2010; Coble 1996; Yamashita and Jaffé 2008). The latter has usually the highest fluorescence intensity. The fluorophore or flurochrome at peak C or peak A of humic and fulvic acids are the result of the contribution of several fluorophores, because the macromolecular structures of these compounds generally include a number of functional groups (Mostofa et al. 2009a; Senesi 1990a; Malcolm 1985). Tryptophan amino acid has only one florophore at each peak position (T and T_{UV}) that can be denoted as single fluorophore.

The fluorescence intensity of a sample is normalized to monitor the stability of the light (or energy) emitted by the xenon lamp in the fluorometer, to compare

with former published results and is vital for theoretical and technical fluorescence measurement, which has been expressed by means of three methods in earlier studies. (i) The typically used standard quinine sulfate method is the fluorescence intensity normalized to that of aqueous solutions of quinine sulfate monohydrate (at ppm or ppb levels) in either 0.05–0.1 M or 0.1 N solution of sulfuric acid (H_2SO_4). However, aquatic scientists use different scaling units to express the fluorescence intensity, such as millifluorescence (mFI) (Dorsch and Bidleman 1982; Hayase et al. 1987), the fluorescence unit (flu) (Chen and Bada 1992), Raman-normalized quinine sulfate equivalents (QSE) (Coble et al. 1998; Kowalczuk et al. 2009), and the quinine sulfate unit (QSU) (Coble 1996; Mopper and Schultz 1993; Yamashita and Tanoue 2003a; Mostofa et al. 2005a; Nagao et al. 2003; Burdige et al. 2004; Zhang et al. 2009a, 2009b; Coble et al. 1993; Obernosterer and Herndl 2000). (ii) The arbitrary unit method is the direct fluorescence intensity that is primarily detected by the fluorescence spectrophotometer (Mayer et al. 1999; Cory and McKnight 2005; Fu et al. 2007, 2006; Baker and Curry 2004; Chen et al. 2003; Klapper et al. 2002; Yue et al. 2006). The Raman peak intensity of Milli-Q water at Ex/Em = 348 or 350 or 275/303 nm over the analysis period (or the QS solution as mentioned before) is used to monitor the stability of light emitted by the xenon lamp in the fluorometer. (iii) The Raman Unit (RU) method is the corrected fluorescence intensity, where the Raman signals are corrected by the baseline and integrated over the entire Raman peak for each excitation wavelength. Then, the fluorescence intensities are divided by the Raman area for the corresponding excitation wavelength to obtain a RU (nm^{-1}) (Determann et al. 1994, 1996; Stedmon et al. 2003; Fulton et al. 2004; Mostofa et al. 2005b; Matthews et al. 1996; Nieke et al. 1997; Hayakawa et al. 2003; Yoshioka et al. 2007; Huguet et al. 2009). The RU calibration processes are difficult at the shorter wavelength regions due to noise, whilst the fluorescence intensities at longer excitation wavelengths tend to be enhanced (Mostofa et al. 2005b). Because of RU calibration on fluorescence intensities over all the excitation wavelengths, it is possible to have artifacts that produce unusual fluorescent components that are not shown in the original EEM spectra.

For example, the results of PARAFAC modeling on QSU and RU EEM data of upstream (Nishi-Mataya) and lake waters (Lake Biwa) show the presence of fulvic acid-like substance (components 1 and 2) with two fluorescence peaks for component 1, at Ex/Em = 320/442 (peak C) and 255/442 nm (peak A) (Fig. 2a). There is no specific peak for component 2, which only has strong fluorescence intensity at Ex/Em = 225–230/428 nm (Fig. 2b) in QSU of upstream waters. Photobleached fulvic acid-like compounds have two fluorescence peaks at Ex/Em = 310/450 nm (peak C) and 250/450 nm (peak A) (component 1, Fig. 2e), while component 2 is associated to photobleached autochthonous fulvic acid-like material with a weak peak at Ex/Em = 280/442 nm (component 2, Fig. 2f) in QSU of lake water. On the other hand, in RU units the respective fluorescent components are composed of the two fluorescence peaks at Ex/Em = 370/474 nm (peak C) and 270/474 nm (peak A) for component 1 (Fig. 2c). Component 2 has a peak at Ex/Em = 330/427 nm (peak C) in upstream waters. In lake waters, the fluorescence peaks for component 1 are 350/461 nm and 260/461 nm (Fig. 2g), and the peaks for component 2 are

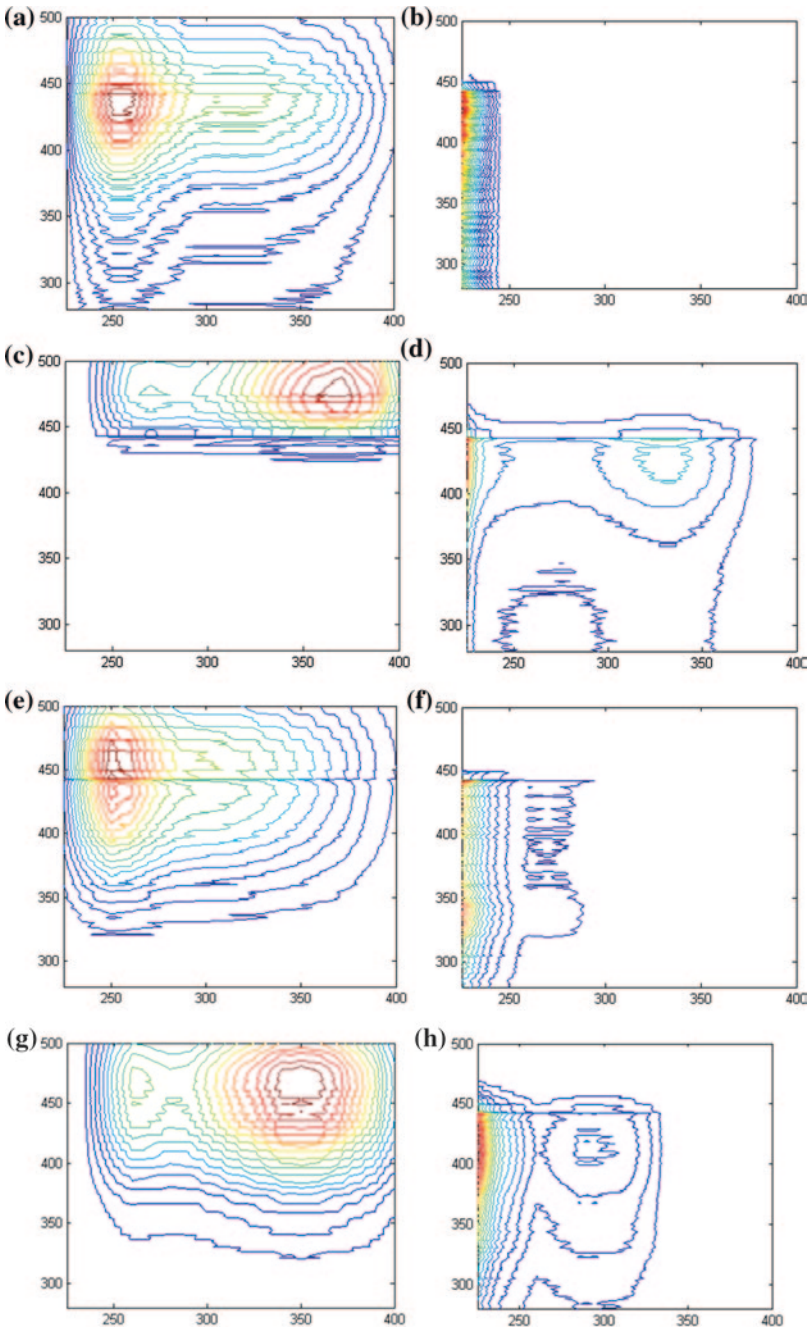

Fig. 2 Differences in the EEM images of fluorescent components identified using PARAFAC modeling on a.u. (or QSU) calibration (**a**, **b** Nishi-Mataya upstream and **e**, **f**: Lake Biwa surface waters) and Raman Unit calibration (**c**, **d** Nishi-Mataya upstream and **g**, **h**: Lake Biwa surface waters). PARAFAC analysis is conducted on earlier published and their respective a.u. *Data source* Mostofa et al. (2005b)

295/409 nm and 230/409 nm (Fig. 3h). The results show that the excitation–emission (Ex/Em) wavelengths of both peaks C and A in fulvic acid-like substances are shifted in the RU calibration compared to QSU. The fluorescence intensities of peak C in RU calibration are higher than in the peak A-region, which is entirely opposite to QSU calibration. The fulvic acid-like components in QSU of upstream waters (Fig. 2a, b) are characteristically similar to standard Suwannee River Fulvic Acid (Fig. 2a, b). The fulvic acid-like component (component 1) and autochthonous fulvic acid-like component (component 2) in QSU data of lake waters are similar to their respective photo-bleaching components, which have been detected in lake surface waters during the summer stratification period (Mostofa et al. 2005b). It can be noted that the PARAFAC modeling has been carried out on published data of monthly samples collected at Nishi-Mayata upstream (April, May, July, and August) and Lake Biwa surface waters (2.5, 10 and 20 m depth for April, July, August and September) (Mostofa et al. 2005b). The results indicate once more that both the excitation–emission wavelength peaks and their respective fluorescence intensities are significantly changed when using RU calibration. Therefore, it is strongly recommended that the calibration of the fluorescence intensity data of EEM spectra is carried out using either the QSU method or arbitrary units, avoiding the RU calibration method. It is also recommended that before measurement of the samples, Xe-light in the fluorescence spectrophotometer is corrected according to the instrument's guidelines using a Rhodamine B solution.

2.5 EEM Properties and Molecular Characteristics of Key FDOM Components Identified by PARAFAC

The molecular, chemical and EEM properties of the various FDOM components in natural waters are discussed below.

Allochthonous Fulvic Acids (C-like, A-like and M-like)

Standard Suwannee River Fulvic Acid (SRFA) is composed of two fluorescent components identified by PARAFAC modeling on its EEM. The first component is denoted as allochthonous fulvic acid (C-like), which includes two fluorescence peaks at Ex/Em = 295–410/439–520 nm (peak C-region) and at Ex/Em = 240–270/439–520 nm (peak A-region) (Figs. 2a, 3a; Table 2). The peak A of the allochthonous fulvic acid (C-like) often has higher fluorescence intensity (by ~1.30–3.0 times) compared to the peak C-region. Note that the Raman Unit (RU) calibration often returns longer excitation wavelengths, particularly at the peak C-region, compared to standard quinine sulfate (or other) calibration. The allochthonous fulvic acid (C-like) is identified at Ex/Em = 325–340/442–462 nm and 250–260/450–451 nm for standard SRFA dissolved in Milli-Q waters. The corresponding wavelengths are 345/452 and 255/451 nm for SRFA dissolved in seawater; 300–340/419–467 and 240–280/427–468 nm for fulvic acid extracted

from rivers and lakes; 300–340/423–464 and 235–260/425–464 nm for various upstream and rivers, but not in the water Raman Unit (RU: nm^{-1}) calibration (330–380/420–467 and 240–260/4420–467 nm, respectively); 295–310/443–464 and 250–260/443–464 nm in lakes; 305/439 and 260/439 nm in estuaries, which shifts to 360–385/478–504 and 250–270/478–504 nm in RU calibration; 320–325/422–454 and <250/422–454 nm in bay and marine waters (but one finds 340–410/440–520 and 250/440–520 nm upon RU calibration in bay waters from the Barataria Basin); 300–305/449 and 250/449 nm in irradiated river waters; 315/429 nm in water extracted from sugar maple leaves; 315/447 and ~250/447 nm in plant biomass, manure and soil (Tables 1, 2) (Stedmon et al. 2003; Stedmon and Markager 2005b; Ohno and Bro 2006; Mostofa et al. 2010; Mostofa KMG et al., unpublished data; Nakajima 2006; Hunt et al. 2008; Kowalczuk et al. 2009; Baghoth et al. 2010; Chen et al. 2010; Dubnick et al. 2010; Fellman et al. 2010; Guo et al. 2010; Singh et al. 2010; Yamashita et al. 2010, 2011; Balcarczyk et al. 2009; Santín et al. 2009). Note that longer excitation–emission maxima have been observed at the C-region for SRFA dissolved in sea water compared to Milli-Q water. This is presumably linked to the formation of complexes of trace elements in seawater with the functional groups (or flurophores) bound in SRFA. Complex formation can significantly enhance electron promotion at peak C from the ground to the excited state by longer wavelength energy. The lower excitation energy can shift the Ex/Em maxima to longer wavelengths. This will be explained in detail in the section that deals with the effect of salinity.

The second component is denoted as allochthonous fulvic acid (A-like) and is typically composed of a strong fluorescence shoulder (or peak) at Ex/Em = 225–250/413–448 nm (peak A-region) and of a minor peak at Ex/Em = 280–295/414–442 nm (peak C-region) (Fig. 3b). The allochthonous fulvic acid (A-like) is identified at 230/441 nm (peak A-region) in SRFA dissolved in Milli-Q waters; 225–230/414–442 nm (peak C-region) and 285–295/414–442 nm (minor peak at peak C-region) in upstream waters (Figs. 2b, 3b); 225/432–442 nm in lakes; 240–250/416–448 nm in estuaries, and <260/(not mentioned) nm in marine waters (Table 2) (Stedmon et al. 2003; Stedmon and Markager 2005b; Mostofa KMG et al., unpublished data; Yamashita et al. 2010; Balcarczyk et al. 2009).

The third component of allochthonous fulvic acid exhibits fluorescence excitation–emission maxima at Ex/Em = 285–310/387–429 nm (peak C-region) and Ex/Em = 230–260/387–429 nm (peak A-region). The fluorescence intensity at peak A-region is >1.50 times higher than at C-region (Fig. 3c; Table 2). The Ex/Em maxima of this component at peak C-region occur at relatively shorter wavelengths compared to those of the allochthonous fulvic acid (C-like). Therefore, the third component can be denoted as allochthonous fulvic acid (M-like). Allochthonous fulvic acid (M-like) has been detected at Ex/Em = 285–310/387–429 nm at peak C-region and 230–240/387–429 nm at peak A-region in the waters of the Yellow River and Heilongjiang (Amur) River watershed (China); 305/396 and 240/396 nm in Occoquan Watershed (USA); 305/428 and <240–260/414–428 nm in marine waters; 320/410 and 250/410 nm in drinking water treatment plants, and 312/417

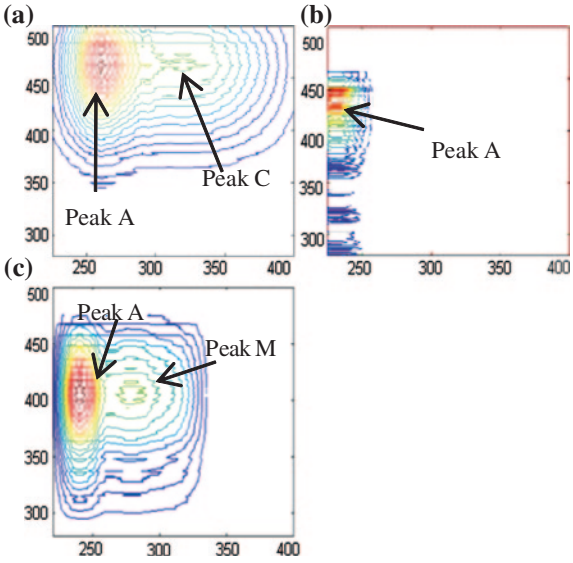

Fig. 3 The fluorescent components of allochthonous fulvic acid (C-like) (**a**) and allochthonous fulvic acid (A-like) (**b**) of standard Suwannee River Fulvic Acid's aqueous samples and of allochthonous fulvic acid (M-like) (**c**) of upstream waters (Yellow River, China) identified using PARAFAC modeling on their respective EEM spectra. Allochthonous fulvic acids (C-like and A-like) are similar to those of stream allocthonous fulvic acid (C-like and A-like) (Fig. 2a, b) of upstream water samples (Nishi-Mataya upstream). PARAFAC analysis is conducted on earlier published and their respective a.u. data (*Data source* Mostofa et al. 2005a; Mostofa KMG et al., unpublished data).

and 240/417 nm in water extracted from sugar maple leaves (Fig. 3c; Table 2) (Mostofa KMG et al., unpublished data; Hunt et al. 2008; Baghoth et al. 2010; Chen et al. 2010; Fellman et al. 2010; Holbrook et al. 2006; Yamashita and Jaffé 2008). The origin of this component is presumably located in the terrestrial soil ecosystem. Experimental results show that allochthonous fulvic acid (M-like) is entirely decomposed photolytically in the upstream waters and in the main channel waters of the Yellow River, because this component is minor (~5 %) compared to the major component (~89 %) of allochthonous fulvic acid (C-like) in the total Yellow River DOM (Mostofa KMG et al., unpublished data). On the other hand, the allochthonous fulvic acid (M-like) undergoes complete microbial degradation after 12 days of dark incubation in both upstream and main channel filtered waters of the Yellow River at room temperature. This indicates that the allochthonous fulvic acid (M-like) is both photolytically and microbially labile in natural waters.

The molecular structure of fulvic acid is not yet known because of the complicated chemical composition and relatively large molecular size. The molecular weight of fulvic acid is approximately 2310 Da (Chin et al. 1994); it is generally composed of relatively few aromatic groups, which yield 14–20 % of aromatic carbon compared to 30–51 % for humic acid (Malcolm 1985; Steelink 2002; Gron et al. 1996). The fluorophores associated with the low molecular weight fraction of

fulvic acid (<10 kDa) exhibit relatively high fluorescence intensity, which gradually decreases with an increase in molecular weight (Hayase and Tsubota 1985; Levesque 1972; Gosh and Schnitzer 1980; McCreary and Snoeyink 1980; Visser 1984). The fulvic acid fluorophores have relatively smaller functional groups and show higher fluorescence intensity at peak C- and A-regions compared to humic acids (Hayase and Tsubota 1985; Mostofa et al. 2009a, 2005a).

Photobleached Allochthonous Fulvic Acids

Photobleached fulvic acid generally arises from the degradation of fluorophores bound to the allochthonous fulvic acid (generally C-like), which thus results in the excitation–emission maxima of peak C having relatively shorter wavelengths compared to those of the initial fluorescence maxima (Fig. 3d, e). Photoinduced degradation causes decomposition of allochthonous fulvic acids (C-like, A-like and M-like) in natural waters (Fig. 3d, e) (Mostofa et al. 2005a; Mostofa et al. 2005b, 2010, 2007a; Moran et al. 2000). In field observations of the waters of Lake Biwa, the fluorescence excitation–emission maxima at the peak C-region are detected at

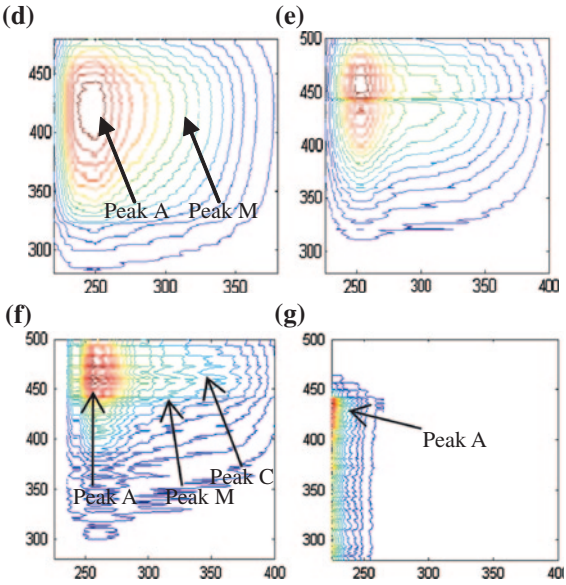

d, **e** The fluorescent components of standard Suwannee River Humic Acids in EEM data of its aqueous samples identified using PARAFAC modeling. PARAFAC analysis is conducted on earlier published and their respective a.u. data. *Data source* Mostofa et al. (2005a). **f**, **g** The fluorescent component of photobleached fulvic acids of irradiated river waters (3 h irradiation by midday sunlight, Nanming River, China) and lake surface waters during the summer stratification period (2.5–20 m, Lake Biwa, Japan) identified using PARAFAC modeling. *Data source* Mostofa et al. (2010, 2005b).

shorter wavelengths (Ex/Em = 295–310/443–450 nm) in surface waters (0–20 m) compared to the deep water layers (40–80 m) (Ex/Em = 300–310/444–464 nm). Furthermore, maxima are 320–325/422–454 nm in sea waters and 300–305/449 and 250/449 nm in irradiated river waters (Table 2) (Mostofa KMG et al., unpublished data; Mostofa et al. 2005b; Yamashita et al. 2011). The excitation–emission maxima of the fluorescence peak C are shifted in irradiated samples from longer to shorter wavelength regions, which gives a blue-shift of the peak position (Mostofa et al. 2005a, 2007a; Moran et al. 2000). Such blue-shift phenomenon is the photoinduced result of the mineralization of fluorophores that are present in the molecular structure of fulvic acids. Irradiation decomposes the allochthonous fulvic acid (A-like and M-like) entirely (Table 2) (Mostofa KMG et al., unpublished data). Photobleached fulvic acid is generally detected in the surface waters of rivers, lakes, estuaries and oceans (Table 2) (Brooks et al. 2007; Mostofa et al. 2007a, 2005b; Garcia et al. 2005; Skoog et al. 1996; Moran et al. 2000; Osburn et al. 2009; Lepane et al. 2003; Abboudi et al. 2008; Poiger et al. 1999; Zhang et al. 2009b).

Allochthonous Humic Acids (C-like, A-like and M-like)

The standard Suwannee River Humic Acid (SRHA) has three fluorescent components, namely allochthonous humic acid (C-like), humic acid (A-like) and humic acid (M-like). They can be identified using PARAFAC modeling of EEM spectra in a variety of waters (Fig. 3f, g; Table 2). The allochthonous humic acid (C-like) shows three fluorescence peaks, of which two are at Ex/Em = 285–340/460–480 nm (shorter wavelength) and at 350–405/480–508 nm (longer wavelength, peak C-region). The third peak is located at Ex/Em = 240–270/460–508 nm in the peak A-region (Fig. 3f; Table 2). Allochthonous humic acid (C-like) has been detected at Ex/Em = 320–350/461–498 and 300/461 nm (peak C-region) and at 255/461 nm (peak A-region) in standard SRFA dissolved in Milli-Q water; at 295–310/423–464 and 255/464 nm in extracted humic acid; at 330/456–480 and <250/450–460 nm in river and soil waters; at 385/>500 and 256/>500 nm in estuaries; at 300–340/>500–510, 290–405/>500–510 and <260–270/>508 nm in bay and marine waters; at 370–380/490–498 and <260/490–498 nm in the north Pacific and Atlantic ocean; at 360/458–480, 300/458 and 250–260/458–480 nm in drinking water treatment plants and municipal wastes; at 370/440 and <250/440 nm in soil; at 351/459 and 240/459 nm in water extracted from sugar maple leaves; finally, at 350–360/460–480 nm in plant biomass, manure and soil (Fig. 3f; Table 2) (Coble 1996; Mostofa et al. 2005a; Ohno and Bro 2006; Baker 2005; Hunt et al. 2008; Kowalczuk et al. 2009; Baghoth et al. 2010; Chen et al. 2010; Fellman et al. 2008, 2010; Guo et al. 2010; Yu et al. 2010; Wu et al. 2011; Yamashita et al. 2011; Balcarczyk et al. 2009; Santín et al. 2009; Murphy et al. 2008; Yamashita and Jaffé 2008).

The allochthonous humic acid (A-like) can exhibit a strong shoulder (not often a clear peak) at peak A-region in a wide range of emission wavelengths.

The C-region peak does not appear because of relatively strong fluorescence intensity at the peak A-region, which explains why this component can be denoted as humic acid (A-like) (Fig. 3g; Table 2). The allochthonous humic acid (A-like) has been identified at Ex/Em = ~ 230/436 nm, with a minor peak at 265/436 nm, in the peak A-region of SRHA dissolved in Milli-Q water; at <250/400 nm in stream waters; at <250/450–470 in estuaries and coastal marine waters; at 240/483 nm in water extracted from sugar maple leaves; and at 220/432 nm in municipal leachate samples (Fig. 3g; Table 2) (Mostofa et al. 2005a; Hunt et al. 2008; Chen et al. 2010; Fellman et al. 2009, 2010; Wu et al. 2011; Murphy et al. 2008). The EEM images and the fluorescence properties of allochthonous humic acid (A-like) are apparently similar to those of allochthonous fulvic acid (A-like). Another component of allochthonous humic acid (M-like) is presumably occurring in soil samples together with allochthonous humic acid (C-like). The allochthonous humic acid (M-like) is often detected at Ex/Em = 300/416 nm in the peak C-region and at 240/416 nm in the peak A-region in soil; at 295/414 and <250/414 nm in stream waters and soil; at 330/412 and 240/412 nm in municipal leachate samples; at 295–300/465 and >240/465 nm in plant biomass, manure and soil (Ohno and Bro 2006; Fellman et al. 2008, 2009; Wu et al. 2011).

The allochthonous humic acid (C-like) can show a fluorescence peak at longer Ex/Em wavelengths in the peak C-region, whereas allochthonous fulvic acid (C-like) often shows fluorescence at shorter Ex/Em wavelengths. Allochthonous humic acids (C-like, A-like and M-like) are not often detected in natural waters, particularly in waters with low DOC concentration. Allochthonous fulvic acid is generally more concentrated than humic acid in natural water, with a ratio of fulvic to humic acid that is typically 9:1. In some cases, especially for high-DOC waters, the ratio decreases to 4:1 or less (Malcolm 1985; Peuravuori and Pihlaja 1999). For this reason, allochthonous humic acids are not often observed. The molecular structure of humic acid is not yet defined due to its complex chemical composition. It is generally highly aromatic in nature, with 30–51 % of aromatic carbon compared to 14–20 % of aromatic carbon in fulvic acid (Malcolm 1985; Steelink 2002; Gron et al. 1996). The high aromaticity and the functional groups of humic acid are responsible for the appearance of several fluorescence peaks at peak C-regions and A-regions (Tables 1, 2). The fluorophores associated with the low molecular weight fraction of humic acid (<10 kDa) exhibit relatively high fluorescence intensity. Fluorescence sharply decreases in the molecular weight fractions of 100–300 kDa and further increases for humic acid fractions >300 kDa (Hayase and Tsubota 1985; Levesque 1972; Gosh and Schnitzer 1980; McCreary and Snoeyink 1980; Visser 1984). The fluorophores bound to humic acid are functional groups with relatively high molecular weight. They show fluorescence in the peak C-region as well as peak A-region (Hayase and Tsubota 1985; Mostofa et al. 2009a, 2005a; Kowalczuk et al. 2009; Santín et al. 2009; Yamashita and Jaffé 2008). Humic acid undergoes photoinduced decomposition by sunlight in natural waters.

Autochthonous Fulvic Acids (C-like and M-like)

Two fluorescent components can be autochthonously produced from algae or phytoplankton biomass under photorespiration or microbial respiration (or assimilation) in natural waters (Fig. 3h–l; Table 2) (Mostofa et al. 2009a, b; Coble 1996, 2007; Parlanti et al. 2000; Stedmon et al. 2007a; Zhang et al. 2009a; Balcarczyk et al. 2009; Murphy et al. 2008; Aoki et al. 2008). The first component can exhibit either two or three fluorescence peaks, at Ex/Em = 330–370/434–480 nm and 290–300/430–448 nm in the peak C-region as well as 250–270/434–480 nm in the peak A-region (Fig. 3h–j; Tables 1, 2). The EEM images of the first autochthonous fluorescent component are similar to those of the allochthonous fulvic acid (C-like). Therefore, this component can be denoted as autochthonous fulvic acid (C-like). The early stage of autochthonous fulvic acid (C-like) when it originates from algae can exhibit three fluorescence peaks, which are subsequently altered into two peaks (Mostofa KMG et al., unpublished data). The EEM spectra shows that the fluorescence intensity of autochthonous fulvic acid

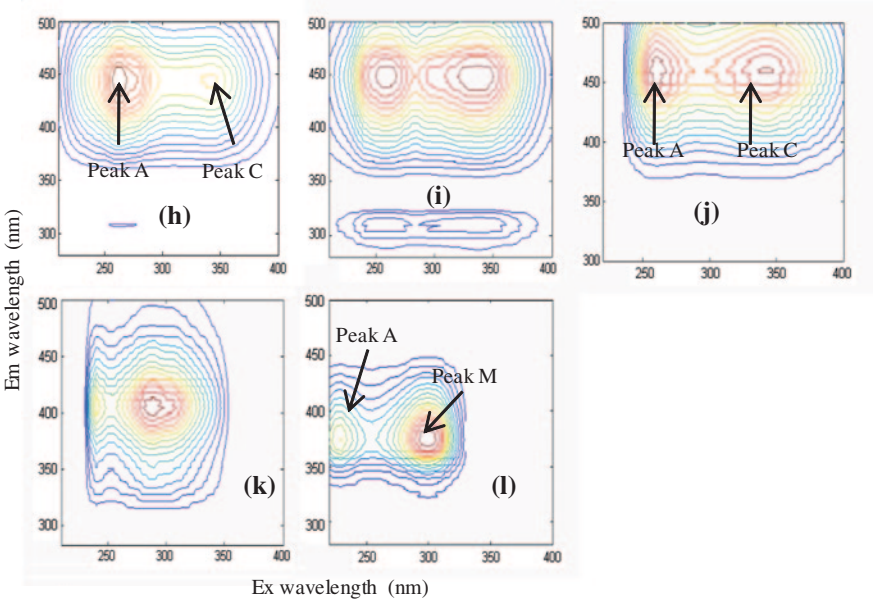

Fig. 3 Continued

The fluorescent components of autochthonous fulvic acid (C-like) under microbial respiration or assimilation of lake algae (**h**), autochthonous fulvic acid (C-like) under photorespiration or assimilation of lake algae (**i**) in natural waters, Tributary of NenJiang River, China (**j**) as well as autochthonous fulvic acid (M-like) in microbial respiration of lake algae (**k**) and in surface waters of Lake Hongfeng, China (**l**) identified using PARAFAC modeling on the EEM spectra of their respective samples. *Data source* Mostofa KMG et al., (unpublished data).

(C-like) at the peak C-region is relatively high, or similar to the intensity at the peak A-region (Fig. 3h–j; Table 2) (Mostofa et al. 2009b; Stedmon and Markager 2005a; Balcarczyk et al. 2009). In contrast, the fluorescence intensity of allochthonous fulvic acid (C-like) is higher at peak A-region than at peak C-region (Figs. 2a, 3a). The autochthonous fulvic acid (C-like) showed fluorescence peaks at Ex/Em = 340–350/460 nm in the peak C-region and at 260/460 nm in the peak A-region in mainstream and tributaries of NenJiang River, China; at 335–340/442–464 nm and 260/442–464 nm in surface waters of Lake Hongfeng, China; at ~360/~460 nm (peak A-region not mentioned) in streams; at 340–350/460, 340/448–454 and 260–270/448–454 nm upon photo-assimilation of algae in Milli-Q and river water; at 340/448–455, 290–300/430–448, and 260–448 nm upon microbial respiration (or assimilation) in Milli-Q and river water; at 365/453 and 270/453 nm upon microbial respiration (or assimilation) of phytoplankton in isotonic water (0.5 ‰ salinity); at 355/445 and 280/435 nm when originateng from algae under both light and dark incubation (12 h each); at 350/400–450 and 275/400–450 nm in bay waters (Brazil); at 370/466 and <260/466 nm in the deep waters of Okhotsk Sea and the North Pacific Ocean; at 340/420 and 260/420 nm in the Southern ocean; at 355/434 and 260/434 nm in north Pacific and Atlantic oceans; and at 330–350/420–480 and 250–260/420–480 nm in marine waters (Table 2) (Mostofa et al. 2009b; Coble 1996, 2007; Parlanti et al. 2000; Stedmon et al. 2007a; Zhang et al. 2009a; Wedborg et al. 2007; Luciani et al. 2008; Zhao et al. 2009; Chen et al. 2010; Yamashita et al. 2010; Balcarczyk et al. 2009; Murphy et al. 2008).

On the other hand, the second fluorescent component of algal or phytoplankton origin can exhibit one strong fluorescence peak in the peak C-region and one minor peak (not often shown) in the peak A-region. The peak in the C-region is located at shorter wavelengths compared to the first component of autochthonous fulvic acid (C-like) (Fig. 3k, l) (Mostofa et al. 2009b; Coble 1996, 2007; Parlanti et al. 2000; Stedmon et al. 2003, 2007a; Stedmon and Markager 2005a, 2005b; Zhang et al. 2009a; Balcarczyk et al. 2009; Murphy et al. 2008; Yamashita et al. 2008; Yamashita and Jaffé 2008; Wang et al. 2007). Considering the EEM images of the second fluorescent component, which are similar to those of allochthonous fulvic acid (M-like) (Fig. 3c) and of marine humic acid denoted as M (Coble 1996), such component can be denoted as autochthonous fulvic acid (M-like). The autochthonous fulvic acid (M-like) of algae or phytoplankton origin usually exhibits two fluorescence peaks at Ex/Em = 290–330/358–434 nm in the peak C-region and at 225–360/358–416 nm in the peak A-region (Table 2). The autochthonous fulvic acid (M-like) is often detected in several studies in field and experimental observations, at Ex/Em = 295–300/396–422 nm in the peak C-region and at 235–240/396–422 nm in the peak A-region in surface waters (0–25 m) of Lake Hongfeng, China; at 315/372 nm in the waters of Lake Taihu; at 322/407 nm in the waters of Lake Taihue; at 300/406 and 240/405 nm upon microbial respiration (or assimilation) of algae in river water; at 290–310/400–410 nm upon microbial assimilation of marine algae in Milli-Q water; at 295/398 nm upon microbial production in a mesocosm experiment; at 320–325/388–428 nm in estuaries;

at 305/378 and <260/378 nm in river and coastal waters; at 295–325/358–420 and 260/385 nm in bay waters; at 310/380–420 and 240–250/384–400 nm in the coastal waters of South Atlantic Bight; at 325/385 and <260/385 nm in the deep waters of the Okhotsk Sea and North Pacific Ocean; at 310–315/414–418 and 260/414 nm in the waters of the north Pacific and Atlantic oceans; at 310–320/380–420 nm in marine waters; at 300/406 and <250/410 nm in drinking water treatment plants; and at 330/410 and 230/410 nm in compost products solutions (Fig. 3k, l; Tables 1, 2) (Mostofa et al. 2009b; Coble 1996, 2007; Parlanti et al. 2000; Stedmon et al. 2003, 2007a; Stedmon and Markager 2005a, 2005b; Zhang et al. 2009a; Luciani et al. 2008; Baghoth et al. 2010; Chen et al. 2010; Fellman et al. 2010; Yu et al. 2010; Yamashita et al. 2010, 2011, 2008; Balcarczyk et al. 2009; Murphy et al. 2008; Li et al., Characteristics of sediment pore water dissolved organic matter in four Chinese lakes using EEM spectroscopy and PARAFAC modeling, unpublished data; Yamashita and Jaffé 2008; Wang et al. 2007). The autochthonous fulvic acid (M-like) shows much higher fluorescence intensity at peak C-region than at peak A-region (Fig. 3k, l). In contrast, allochthonous fulvic acid (M-like) shows more intense fluorescence (often twofold) at peak A-region than at peak C-region (Fig. 3c). The variation in the Ex/Em wavelengths of the peaks for autochthonous fulvic acid (C-like and M-like) can be caused by pH, ionic strength, the presence of the trace elements that form complexes with DOM, water origin (Milli-Q, river, lake and seawater) and solvents, content of DOM as well as presence and nature of its components, and finally instrumentation (Mostofa et al. 2009a; Senesi 1990a; Coble et al. 1990; Wu and Tanoue 2001a; Wu et al. 2005; Lochmuller and Saavedra 1986). The molecular weight of autochthonous fulvic acids has been determined as ~<1900 for those originating from photoinduced assimilation of algae under natural sunlight, and ~<1700 upon microbial assimilation of algae in Milli-Q water (Mostofa KMG et al., unpublished data). The functional groups of autochthonous fulvic acid (C-like and M-like) are entirely unknown, which could be the focus for future research challenges. Because of higher fluorescence intensity at the peak C-region compared to allochthonous fulvic and humic acids, autochthonous fulvic acids of algal origin are expected to be quite rich in fluorophores. Autochthonous fulvic acid (C-like) of microbial/algal origin is rapidly decomposed by natural sunlight. This might be an effect of high fluorescence intensity at the peak C-region, which may be linked to high reactivity in natural waters (Mostofa KMG et al., unpublished data). It has recently been found that algal-derived DOM is a more efficient photoinduced substrate than allochthonous DOM (Johannessen et al. 2007; Hulatt et al. 2009).

Protein-Like Component

The protein-like component shows two fluorescence peaks at Ex/Em = 280–300/328–356 nm (peak T) in the peak T-region and a peak at Ex/Em = 235–250/338–356 nm (peak T_{UV}) in the T_{UV}-region (Fig. 3m, n; Tables 1, 2). The EEM images of the protein-like component show that the fluorescence intensity at

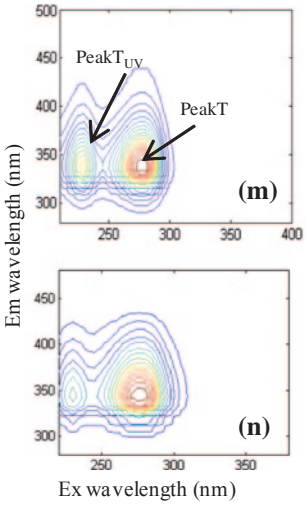

The fluorescent components of protein-like component of algae origin in aqueous samples (**m**), and in sewerage drainage waters (**n** Nanming River, China) identified using PARAFAC modeling on the EEM spectra of their respective samples. (*Data source* Mostofa et al. 2010; Mostofa KMG et al., unpublished data). The fluorescent components of standard tryptophan amino acid

the peak T-region is much higher than at the peak T_{UV}-region (Fig. 3m, n). The protein-like component has been identified at Ex/Em = 280/339–346 nm at the peak T-region and at 230–235/339–346 nm at the peak T_{UV}-region in sewerage waters and washing waters; at 280–285/340–350 and 225/340–350 nm in extracted protein from extracellular polymeric substances (EPS); at 270–280/320–350 and 225/343–358 nm in aromatic proteins or soluble microbial by-products; at 290/356 and 250/356 nm in coastal shelf waters; at 280–300/328–338 and 240/338 nm in north Pacific and Atlantic ocean; and at 275/320 nm in glacial ice samples from the Antarctic and Arctic ocean (Fig. 3m, n; Tables 1, 2) (Mayer et al. 1999; Mostofa et al. 2010; Liu and Fang 2002; Kowalczuk et al. 2009; Chen et al. 2010; Dubnick et al. 2010; Balcarczyk et al. 2009; Murphy et al. 2008). The protein-like component belongs to a molecular size range of >0.1 μm in natural waters (Wu and Tanoue 2001a).

Aromatic Amino Acids (Tryptophan, Tyrosine and Phenylalanine)

The tryptophan-like, tyrosine-like and phenylalanine-like components are often detected in natural waters (Tables 1, 2). The tryptophan-like component has two fluorescence peaks; the first one is located at Ex/Em = 275–285/321–360 nm in the longer wavelength region (peak T), the second one at Ex/Em = 225/340–360 nm in the shorter wavelength region (peak T_{uv}) (Fig. 3o, p; Tables 1, 2). Tryptophan-like component is has been detected at Ex/Em = 275–285/342–357 nm in tryptophan standard dissolved in Milli-Q water and at 275/355 when dissolved in seawater

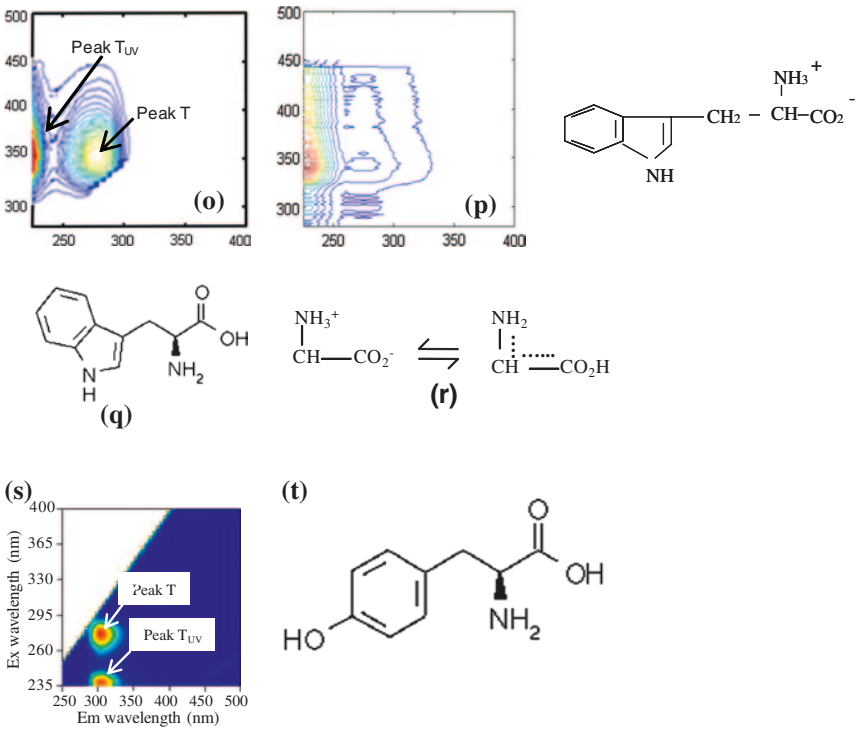

Fig. 3 Continued
(**o**) in EEM data of its aqueous samples and in river waters (Yasu River, Japan) identified using PARAFAC modeling. PARAFAC analysis is conducted on earlier published and their respective a.u. data (*Data source* Mostofa et al. 2005a, 2005b). The molecular structure of tryptophan (**q**) and its resonance configuration (**r**). The fluorescent EEM spectra of standard tyrosine amino acid (**s**) dissolved in Milli-Q waters (*Data source* Nakajima 2006).

(275/357 nm in Milli-Q water); at 275–280/322–336 and 220–230/328–334 nm in tryptophan extracted from EPS; at 275–285/330–351 and 225–235/338–351 nm in various freshwaters; at 275–290/339–360 and 230/340 nm in sewerage samples and drainking water treatment plants; at 280/338–368 and 240/368 nm in estuaries; at 280–295/330–340 nm in bay and coastal waters; at 270–280/320–350 nm in marine waters; at 280/348 and <250/348 nm in ice samples from the Antarctic and Arctic ocean; at 280/330–340 nm in soil; at 280/340 and 220/340 nm in compost products solutions; and at 270/354 nm in plant biomass, animal manure and soil (Coble 1996; Parlanti et al. 2000; Yamashita and Tanoue 2003a; Mostofa et al. 2005a, 2010; Stedmon et al. 2003; Stedmon and Markager 2005a, 2005b; Ohno and Bro 2006; Nakajima 2006; Baker 2005; Zhang et al. 2010; Provenzano et al. 2004; Lu and Allen 2002; Dubnick et al. 2010; Fellman et al. 2008, 2009, 2010; Guo et al. 2010; Yu et al. 2010; Wu et al. 2011; Yamashita et al. 2011; Holbrook et al. 2006;

Yamashita and Jaffé 2008). The molecular formula of tryptophan is $C_{11}H_{12}N_2O_2$ and its molecular weight is 204.23. The chemical structure of tryptophan, $C_8H_5(NH)–CH_2(NH_3^+)CHCOO^-$, is relatively simple (Fig. 3q). The fluorophore at peak T is probably linked to the functional group, $–CH_2–(NH_3^+)–CH–COO^-$, while the fluorophore at peak T_{uv} is probably connected to the $C_8H_5(NH)–$ group that contains the aromatic ring (Mostofa et al. 2009a). The resonance configuration of the functional group, $–CH_2–(NH_3^+)–CH–COO^-$ (Fig. 3r), may confirm the peak position of the T-region at longer wavelengths than the T_{UV}-region. The fluorescence intensity of tryptophan at peak T_{uv} is much stronger (two to threefold higher) than that of peak T. It might be a useful indicator to differentiate the tryptophan-like component from the protein-like component, which typically shows higher fluorescence at the peak T-region than at the peak T_{UV}-region (Fig. 3m, n). Tryptophan is derived microbially from algae, phytoplankton and bacteria in freshwater, marine and sediment pore waters (Chen and Bada 1989; Coble 1996; Yamashita and Tanoue 2003a; Mostofa et al. 2005b; Determann et al. 1998; Baek et al. 1988; Petersen 1989; Wu and Tanoue 2001b; Wu et al. 2001; Cammack et al. 2004). Its very intense fluorescence in aqueous solution could be connected to the functional group $–CH_2–(NH_3^+)–CH–COO^-$ (Fig. 3r). Tryptophan is decomposed both photolytically and microbially in natural waters (Mostofa et al. 2010, 2007a; Winter et al. 2007; Moran et al. 2000). The fluorescence Ex/Em wavelength maxima of tryptophan mostly depend on the polarity of the solvent and the type of the protein. The fluorescence of protein-bound tryptophan is in fact shifted to shorter wavelengths due to shielding from water (Lakowicz 1983; Wolfbeis 1985).

The tyrosine-like component can exhibit two fluorescence peaks at Ex/Em = 270–280/293–314 nm in the peak T-region and at 230/304–307 nm in the peak T_{UV}-region (Fig. 3s; Tables 1, 2). The tyrosine-like component has been detected at Ex/Em = 270–275/303–314 nm (peak T-region) and at 230/304 nm (peak T_{UV}-region) in a tyrosine standard dissolved in Milli-Q water, and at 275/304 and 230/307 nm when the standard was dissolved in seawater; at 265–280/293–313 nm in rivers and other freshwater systems; at 275/<300 nm in lakes; at 275/304–306 nm in estuaries; at 270–275/299–332 nm in sea water; at 275/304–306 in soil; at 270/310 nm in water extracted from sugar maple leaves; at 270/306 nm in drinking water treatment plants; and at 273/309 nm in plant biomass, animal manure and soil (Fig. 3s; Tables 1, 2) (Coble 1996; Parlanti et al. 2000; Yamashita and Tanoue 2003a; Mostofa and Sakugawa 2009; Nakajima 2006; Provenzano et al. 2004; Lu and Allen 2002; Zhang et al. 2009a; Hunt et al. 2008; Kowalczuk et al. 2009; Baghoth et al. 2010; Chen et al. 2010; Fellman et al. 2008, 2009, 2010; Yamashita et al. 2010, 2011; Murphy et al. 2008; Yamashita and Jaffé 2008). Tryptophan and tyrosine when present together in peptides (component 4) are detected from two peaks at Ex/Em = 275/306, 338 nm (T-region) during algal blooming periods, as derived from a mesocom experiment (Table 2) (Stedmon and Markager 2005a). Tyrosine is derived microbially from algal biomass in freshwater and marine environments (Coble 1996; Yamashita and Tanoue 2003a; Stedmon and Markager 2005a; Determann et al. 1998). Comparison of tyrosine and trytophan concentrations with their respective fluorescence intensities

in seawater samples as well as standard samples suggests that the fluorescence of tryptophan is approximately four times higher than that of tyrosine (Yamashita and Tanoue 2003a; Mostofa KMG and Sakugawa LH, unpublished data). The molecular formula of tyrosine is $C_9H_{11}NO_3$ and its molecular weight is 181.19. The different chemical structure of tyrosine compared to tryptophan (Fig. 3t) could account for its much lower fluorescence intensity (Yamashita and Tanoue 2003a; Mostofa KMG et al., unpublished data).

Phenylalanine shows two fluorescence peaks at Ex/Em = 255–265/284–286 nm (peak T-region) and at Ex/Em = ~ 220/284–286 nm (peak T_{UV}-region) in marine waters and in standards dissolved in Milli-Q or seawater (Fig. 3u; Tables 1, 2). The phenylalanine-like component has been identified at Ex/Em = 260/286 nm for a phenylalanine standard dissolved in Milli-Q water, and at 260/284 nm for a phenylalanine standard dissolved in sea water; at 255–265/284–285 nm in marine waters; and at 265/306 nm in ice samples from the Antarctic and Arctic Ocean (Yamashita and Tanoue 2003a; Nakajima 2006; Dubnick et al. 2010). The molecular formula of phenylalanine is $C_9H_{11}NO_2$ and its molecular weight is 165.19. The absence of the OH group in the benzene ring of phenylalanine (Fig. 3v) can account for the reduced fluorescence intensity when compared to tyrosine, and for the presence of fluorescence excitation–emission maxima at shorter wavelength regions than for tyrosine or tryptophan.

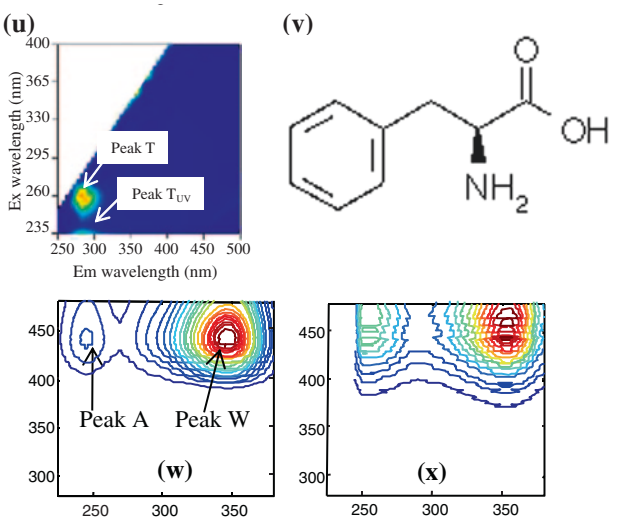

The molecular structure of tyrosine (**t**). **u**, **v** The fluorescent EEM spectra of standard phenylalanine amino acid (**u**) dissolved in Milli-Q waters (*Data source* Nakajima 2006). The molecular structure of phenylalanine (**v**). The fluorescent components of standard DSBP (**w**) in its aqueous samples and in downstream waters (**x** Kurose River, Japan) identified using PARAFAC modeling on their respective EEM data (*Data source* Mostofa and Sakugawa 2009).

Distyryl biphenyl

The aqueous solutions of distyryl biphenyl (DSBP) show two fluorescence peaks at Ex/Em = 350/436 nm (C-region) and at 235–265/435–445 nm (A-region) (Fig. 3w,x; Table 1). The EEM images and the fluorescence peaks of DSBP (Fig. 3w, x) are similar to those of autochthonous fulvic acid (C-like), showing strong fluorescence intensity at the peak C-region than at the peak A-region (Fig. 3h–j). The DSBP component (C-like) has been detected at Ex/Em = 350–355/430–436 nm in the peak C-region and at 235–265/431–446 nm in the peak A-region for a DSBP standard dissolved in Milli-Q water, and at 345/435 and 245/437 nm for DSBP dissolved in seawater (Table 1) (Mostofa et al. 2010; Komaki and Yabe 1982; Nakajima 2006). DSBP is one of the key components of fluorescent whitening agents in natural waters (Managaki and Takada 2005). DSBP is rapidly decomposed by natural sunlight, at a much faster rate compared to DAS1 in natural waters (Mostofa et al. 2005a; Poiger et al. 1999). The molecular structure of (DSBP), 4,4′-bis[(2-sulfostyryl) biphenyl, is shown in (Fig. 3y), with a molecular weight of 562 Da. The DSBP photoinduced decomposition is considered to be caused by an oxidative cleavage of the double bond, followed by the production of various aldehydes such as 2-sulfonic acid benzaldehyde, 4-aldehyde-4′-(2-sulfostyryl)biphenyl (4-benzaldehyde-2′-sulfonic acid-stilbene) and 4,4′-bisaldehyde biphenyl (Guglielmetti 1975; Kramer et al. 1996).

Diaminostilbene-type

The Diaminostilbene-type (DAS1) shows several fluorescence excitation–emission maxima at Ex/Em = 335–355/430–449 nm (peak C-region) and at 240–250/433–446 nm (peak A-region) in aqueous solution (Fig. 3z; Table 1). DAS1 fluorescence peaks have been identified at Ex/Em = 335–355/435–449 and 240–250/434–446 nm for standard DAS1 in Milli-Q water and at 345/436 and 250/433 nm for standard DAS1 dissolved in sea water; and at 340–343/430–432 nm for standard DAS1 in aqueous solutions (Fig. 3z) (Mostofa et al. 2010; Komaki and Yabe 1982; Nakajima 2006). DAS1 is rapidly decomposed by natural sunlight, although it undergoes relatively slower photodegradation compared to DSBP (Mostofa et al. 2005a; Poiger et al. 1999). The molecular structure of DAS1, 4,4′-bis[(4-anilino-6-morphilino-s-triazine-2-yl)amino] 2,2′-stilbenedisulfonate is shown in (Fig. 3a′). Itsphotodegradation yields alcohols, aldehydes and some unidentified products. It is reported that the degradation of DSBP decreases in the presence of DOM, but it is not hindered by DOM in natural waters (Kramer et al. 1996). Its molecular weight is 924 Da.

Detergents (Commercial or Household)

The household detergents are composed of two fluorescent components identified using PARAFAC modeling on the EEM spectra of the detergents solutions (Fig. 3b′, c′). The first component is denoted as detergent component (C-like),

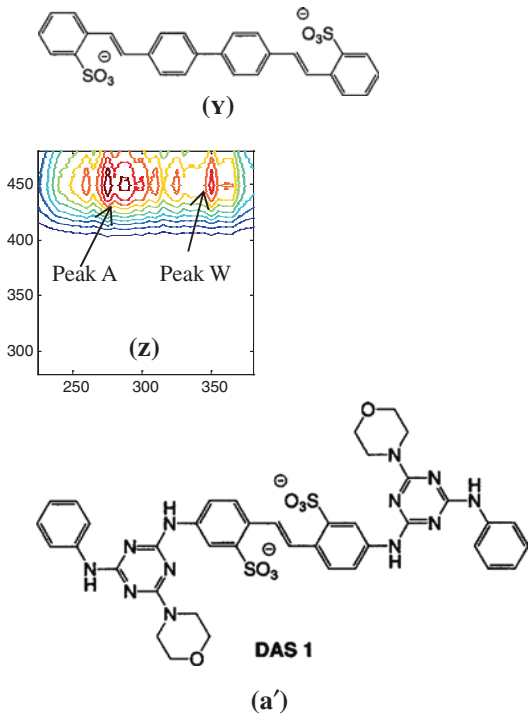

The molecular structure of DSBP (**y**). **z**, **a′** The fluorescent components of standard DAS1 (**z**) identified using PARAFAC modeling on EEM data of its aqueous samples (*Data source* Mostofa and Sakugawa 2009). The molecular structure of DAS1 (y).

with two fluorescence peaks at Ex/Em = 335–345/430–437 nm (peak C-region) and at 240–255/425–447 nm (peak A-region), respectively (Fig. 3b′). The second fluorescent component is denoted as detergent component (T_{UV}-like), with a fluorescence peak at Ex/Em = 225–230/287–296 nm (peak T_{UV}-region) (Fig. 3c′; Table 2). Detergent component (C-like) has been detected at Ex/Em = 345/430–435 and 240/427–433 nm for household detergents (Nafine Chem Ind Ltd and Nice group Co Ltd, China) dissolved in Milli-Q water; at 335–350/432–437 and at 250–255/425–447 nm in river waters; at 335–345/422–437 and 240–250/422–443 nm in sewerage waters; and at 340/440 and 250/440 nm in drinking water treatment plants (Tables 1, 2) (Mostofa et al. 2010; Baghoth et al. 2010; Guo et al. 2010). The detergent component (T_{UV}-like) has been detected at Ex/Em = 225–230/291–296 nm in sewerage waters (Table 2) (Mostofa et al. 2010). Household detergents are generally detected by EEM spectroscopy (Mostofa et al. 2005a, 2010; Komaki and Yabe 1982) and other spectroscopic methods (Kramer et al. 1996) in effluent discharged by households located in towns. The detergent component (C-like) is rapidly decomposed by natural sunlight whist it is refractory to microbial degradation (Mostofa et al. 2010). On the other hand, the detergent

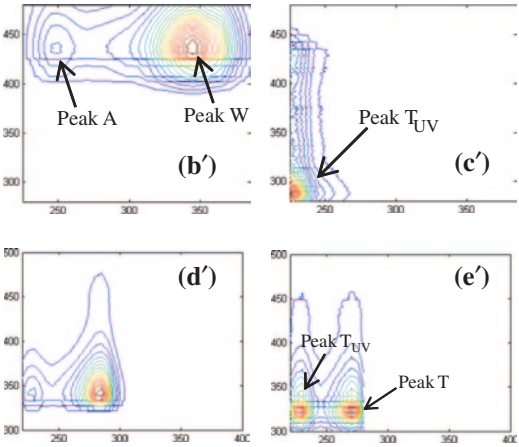

The fluorescent components of commercial or household detergents (**b**′, **c**′) indentified using PARAFAC modeling on EEM data of its aqueous samples (*Data source* Mostofa et al. 2010). The fluorescent components of lake green algae (**d**′, **e**′) isolated and resuspensions in aqueous media (Milli-Q and river waters) identified using PARAFAC modeling on respective EEM data (*Data source* Mostofa KMG et al., unpublished data).

component (T_{UV}-like) is refractory to photoinduced degradation but it is labile to microbial degradation (Mostofa et al. 2010). The form and composition of detergents is variable and recently includes synthetic or naturally occurring polymers with molecular weight ranging from <1000 to >1,000,000 Da (McCullen 1996). Surfactants can have different functionalities (anionic, nonionic and cationic) and commonly used commercial ones are linear alkylbenzene sulphonates, alkyl ethoxy sulphates, alkyl sulphates, alkylphenol ethoxylates, akyl ethoxylates, and quaternary ammonium compounds (McCullen 1996; Ying 2006).

Algae or Phytoplankton

Algae or phytoplankton show several peaks such as 280–285/340–346 nm at peak T-region and 230/327–346 or 230/305 nm at peak T_{UV}-region when resuspended in water (Tables 1, 2) (Mostofa KMG et al., unpublished data; Determann et al. 1998). PARAFAC modeling on the EEM spectra of algae in Milli-Q water show the two fluorescent components of algae (Fig. 3d′, e′; Table 2). The first algae component has a strong fluorescence peak at Ex/Em = 280–285/340–346 nm (peak T-region) and at 230/346 nm (peak T_{UV}-region) (Fig. 3d′), and is similar to the protein-like component that has a much more intense fluorescence at peak T-region than at peak T_{UV}-region (Fig. 3m, n). The second fluorescent component of algae shows a fluorescence peak at Ex/Em = 270/327–336 nm (peak T-region) and at 230/327–336 nm (peak T_{UV}-region) (Fig. 3e′; Table 2). The algae or bacteria collected from marine waters can exhibit fluorescence at Ex/Em = 280/340 nm (peak T-region)

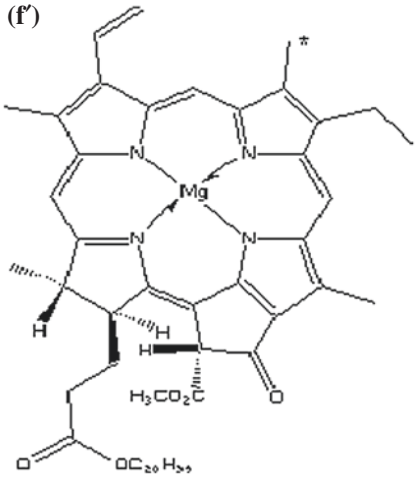

The molecular structure of chlorophyll *a* (**f′**) (*Data source* Clarke et al. 1976)

and two peaks at Ex/Em = 230/340 and 230/305 nm (peak T_{UV}-region) (Determann et al. 1998). Note that green algae have been collected from surface waters of Lake Hongfeng (China) during the summer season using GF/F filters, and their EEM properties have been determined after re-suspension in Milli-Q and river waters.

Chlorophyll a and Chlorophyll b

Chlorophyll *a* (Chl *a*) shows fluorescence at Ex/Em = 431/670 nm and chlorophyll *b* at Ex/Em = 435/659 nm (Moberg et al. 2001). The molecular formula of Chl *a* is $C_{55}H_{72}MgN_4O_5$ and it molecular weight is 893.49; its chemical structure is depicted in Fig. 3f′. The molecular formula of chlorophyll *b* is $C_{55}H_{70}MgN_4O_6$ and its molecular weight is 906.51. The chemical structure of chlorophyll *b* is similar to that of Chl *a*, just with the replacement of a methyl group [$–CH_3$, marked with an asterisk (*)] with an aldehyde one (–CHO). Photoexperiments conducted on sedimentary chloropigments using ^{14}C-labeled algal cells in combination with field observations, demonstrate that a major fraction of Chl *a* is rapidly degraded to soluble colorless compounds (Mostofa et al. 2009a; Klein et al. 1986; Bianchi et al. 1988; Sun et al. 1993). Only a minor fraction of Chl *a* (~30–40 %) is degraded to pheophytin *a* (Klein et al. 1986; Bianchi et al. 1988; Sun et al. 1993).

Identification of Allochthonous Fulvic and Humic Acids from Autochthonous Fulvic Acid (C-like and M-like) Using Fluorescence Index

The key component of autochthonous DOM is termed as marine humic-like substances (Coble 1996), sedimentary fulvic acid (Hayase et al. 1987, 1988) or

marine fulvic acids (Malcolm 1990), without a coherent terminology. Recent studies demonstrate that the two fluorescent components, termed as autochthonous fulvic acid (C-like) (Fig. 3h–j) and as autochthonous fulvic acid (M-like) (Fig. 3k, l), are primarily produced under photoinduced or microbial respiration (or assimilation) of algae or phytoplankton biomass (Mostofa et al. 2009b; Stedmon and Markager 2005a; Zhang et al. 2009a). PARAFAC modeling on EEM spectra of algal-originated DOM suggests that the fluorescence peaks and the images of the first fluorescent component are similar to allochthonous fulvic acid (C-like) (Figs. 2a, 3a). Therefore, this component is indicated as autochthonous fulvic acid (C-like) of algal origin (Fig. 3h–j). On the other hand, the fluorescence peaks and the images of the second fluorescent component (Fig. 3k, l) are similar to allochthonous fulvic acid (M-like) (Fig. 3c) and to the marine humic-like substances (Coble 1996). Therefore, this component is denoted as autochthonous fulvic acid (M-like) of algal origin. The fluorescence intensities and the excitation–emission maxima of these two fluorescent components are significantly different depending on the respective peak positions. Considering the similarities between EEM images of the algal originated fluorescent component and allochthonous fulvic acid (C-like), it is suggested to denote the first and the second fluorescent components as 'autochthonous fulvic acid (C-like)' and 'autochthonous fulvic acid (M-like)', respectively (Fig. 3h–l). Similarly, allochthonous fulvic acids can be denoted as 'allochthonous fulvic acid (C-like)' and 'allochthonous fulvic acid (A-like)', respectively (Fig. 3a, b). The allochthonous fulvic acid (A-like) shows only one shoulder or strong fluorescence intensity at peak A-region, which may not be classified as a peak in standard SRFA and SRHA as well as in field observations (Tables 1, 2; Fig. 3b). Apparently, autochthonous fulvic acids often show higher fluorescence intensities at peak C-region than at peak A-region (Fig. 3h–l), whilst allochthonous fulvic acids (C-like) often show opposite behavior (Fig. 3a–c). The differences in fluorescence intensities at peak C- and A-regions could be useful to distinguish between allochthonous and autochthonous fulvic acids using the fluorescence index (Mostofa et al. 2009b; Huguet et al. 2009; Battin 1998; Zsolnay et al. 1999; McKnight et al. 2001). The fluorescence index ($f_{450/500}$) is defined as the ratio of fluorescence intensity at Ex/Em 370/450 nm to that at Ex/Em = 370/500 nm, which can provide a basis for estimating the degree of aromaticity—and potentially for discriminating the sources—of DOM (Battin 1998; McKnight et al. 2001). However, the index $f_{450/500}$ does not distinguish the autochthonous fulvic acid (C-like) of algal origin (1.75–2.59) from allochthonous fulvic acid (1.30–3.22) and allochthonous humic acid (1.28–1.51), which can be identified using PARAFAC modeling of a variety of DOM sources in natural waters (Fig. 4; Table 3) (Mostofa et al. 2005a, 2007a, 2005b; Mostofa KMG et al., unpublished data; Fu et al. 2010; Li et al., Characteristics of sediment pore water dissolved organic matter in four Chinese lakes using EEM spectroscopy and PARAFAC modeling, unpublished data). Further, this index can also fail when applied to a variety of natural waters (Huguet et al. 2009; Jaffé et al. 2004). Another fluorescence index (HIX) has been developed to estimate the degree of maturation of DOM in soil (Zsolnay et al. 1999). HIX is defined as the ratio H/L

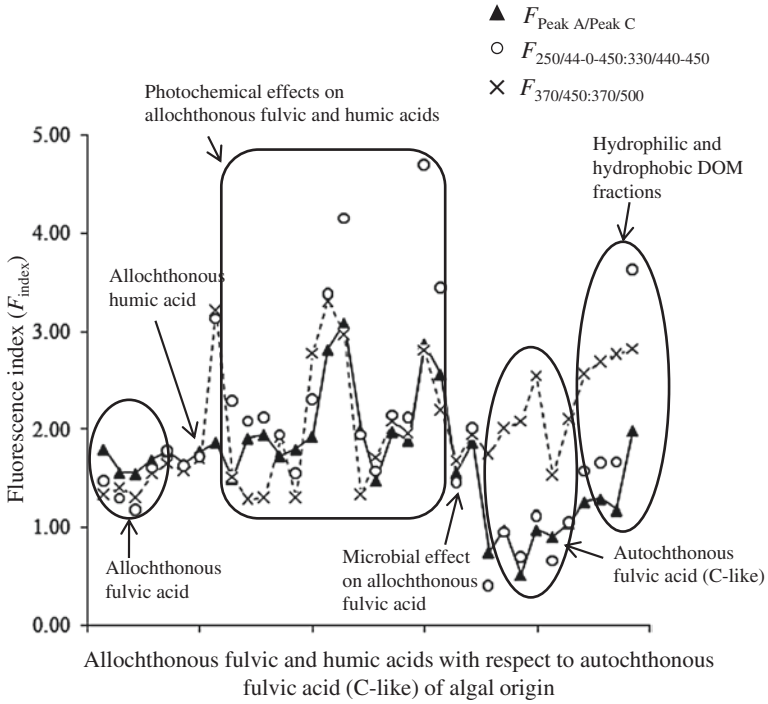

Fig. 4 The fluorescence index (F_{index}) values of allochthonous fulvic and humic acids as well as their photochemical and microbial changes with respect to autochthonous fulvic acid (C-like) of algal origin in waters

of two spectral region areas from the emission spectrum scanned for an excitation at 254 nm. The two areas are calculated between emission wavelengths 300 and 345 nm for L and between 435 and 480 nm for H. The HIX index has recently been applied to a variety of aquatic samples (Huguet et al. 2009; Vacher 2004). High HIX values (between 10 and 16) are a sign of strongly humified OM, mainly of terrestrial origin, whereas low values (<4) are associated with autochthonous OM (Huguet et al. 2009). However, HIX does not distinguish the allochthonous fulvic acid from autochthonous fulvic acid (C-like), identified using PARAFAC modeling on EEM samples in natural waters (Table 3). Indeed, HIX often shows negative values for autochthonous fulvic acid (C-like), and is thus unable to distinguish them from allochthonous fulvic acid.

To identify the PARAFAC fluorescent components, a new fluorescence index ($F_{250:330/440–450}$) has been used and is defined as the ratio of the fluorescence intensity at Ex/Em = 250/440–450 nm and at Ex/Em = 330/440–450 nm. In the case of the emission wavelengths (400–450 nm), average fluorescence intensities are used (Mostofa et al. 2009b). In the case of standard fulvic acid, the $F_{250:330/440–450}$ values vary significantly depending on the number of samples identified using PARAFAC modeling (Table 1; Fig. 4). A very useful fluorescence index

Table 3 The fluorescence index (F_{index}) of allochthonous fulvic and humic acids in contrast to autochthonous fulvic acid (C-like) of algal origin and their various sources identified using PARAFAC modelling on EEM spectra in water samples

DOM sources	Fluorescence index (F_{index})				References
	$F_{Peak\ A/Peak\ C}$	$F_{250:330/440–450}$	$f_{450/500}$	HIX**	
Fulvic acid of forest origin					
Standard Suwannee River Fulvic Acid (n = 3; 1–2 mg L^{-1})	1.80	1.47	1.33	23	Mostofa et al. (2005a)[a]
Standard Suwannee River Fulvic Acid (n = 4; 1–5 mg L^{-1})	1.56	1.29	1.40	25	Mostofa et al. (2005a)[a]
Standard Suwannee River Fulvic Acid (n = 5; 0.5–5 mg L^{-1})	1.55	1.18	1.30	−59	Mostofa et al. (2005a)[a]
Standard Suwannee River Humic Acid (n = 3; 1–5 mg L^{-1})	1.91	2.08	1.28	14	Mostofa et al. (2005a)[a]
Standard Suwannee River Humic Acid (n = 4; 1–5 mg L^{-1})	1.95	2.12	1.30	12	Mostofa et al. (2005a)[a]
Fulvic acid, upstream: Nishi-Mataya and Higashi-Mataya (n = 6)	1.69–1.78	1.60–1.78	1.55–1.65	12, 35	Mostofa et al. (2005b)[a]
Fulvic acid-like, upper branch waters (Z), Yellow River, China (n = 7)	1.30	1.36	2.02	25	Mostofa KMG et al., (unpublished data)
Fulvic acid, upper main channel waters (G), Yellow River, China (n = 18)	1.87	3.13	3.22	8	Mostofa KMG et al., (unpublished data)
Fulvic acid, downstream: Amano, Echi and Ane Rivers (n = 6)	1.65–1.78	1.62–1.72	1.58–1.70	4, 12, 17	Mostofa et al. (2005b)[a]
Photochemical effects on standards and river waters					
Irradiated standard Suwannee River Fulvic Acid (n = 2; 10 h and 20 h)	1.73	1.94	1.91	5	Mostofa KMG et al., (unpublished data)
Irradiated standard Suwannee River Humic Acid (10 h)	1.94	2.00	1.33	7	Mostofa KMG et al., (unpublished data)
Irradiated upstream river waters, Kago upstream, Lake Biwa watershed, Japan	1.8	1.55	1.30	2	Mostofa et al. (2007a)[a]
Irradiated fulvic acid, upper branch waters (Z), Yellow River, China (3 h, n = 2)	1.93	2.3	2.78	−8	Mostofa KMG et al., (unpublished data)

(continued)

Table 3 (continued)

DOM sources	Fluorescence index (F_{index})				References
	$F_{Peak\ A/Peak\ C}$	$F_{250:330/440–450}$	$f_{450/500}$	HIX**	
Irradiated fulvic acid, upper main channel waters (G), Yellow River, China (3 h, n = 2)	2.82	3.38	3.32	−14	Mostofa KMG et al., (unpublished data)
Irradiated downstream river waters, Yasu River, Lake Biwa watershed, Japan	3.09	4.15	2.98	−31	Mostofa et al. (2007a)[a]
Microbial effects on River fulvic acid					
Fulvic acid, upper branch waters (Z), Yellow River, China (12 days)	1.77	2.78	3.55	3	Mostofa KMG et al., (unpublished data)
Fulvic acid, upper main channel waters (G), Yellow River, China (12 days)	2.04	3.68	3.98	3	Mostofa KMG et al., (unpublished data)
Fulvic acid affected by agricultural and sewerage activities					
Fulvic acid, Yasu River, Lake Biwa watershed (n = 5)	2.18	2.36	1.8	−21	Mostofa et al. (2005b)
Extracted DOM fractions from Lake Hongfeng, China					
Fulvic acid, extracted from lake surface waters	1.30	1.90	2.20	–	Mostofa KMG et al., (unpublished data)
Humic acid, extracted from lake surface waters	1.50	2.29	1.51	–	Mostofa KMG et al., (unpublished data)
Hydrophilic acids (HIA), extracted from lake surface waters	1.26	1.57	2.57	–	Mostofa KMG et al., (unpublished data)
Hydrophilic bases (HIB), extracted from lake surface waters	1.29	1.65	2.70	–	Mostofa KMG et al., (unpublished data)
Hydrophilic neutrals (HIN), extracted from lake surface waters	1.18	1.66	2.77	–	Mostofa KMG et al., (unpublished data)
Hydrophobic neutrals (HON), extracted from lake surface waters	1.99	3.63	2.83	–	Mostofa KMG et al., (unpublished data)
Photobleaching allochthonous fulvic acid in lake					
Fulvic acid: 0–20 m, summer period, Lake Biwa	1.67–1.82	1.84–2.07	1.89–2.08	4, 6, 9	Mostofa et al. (2005b)[a]

(continued)

Table 3 (continued)

DOM sources	Fluorescence index (F_{index})				References
	$F_{Peak\ A/Peak\ C}$	$F_{250:330/440–450}$	$f_{450/500}$	HIX**	
Fulvic acid: 40–80 m, summer period, Lake Biwa	1.58–1.80	1.69–1.95	1.78–1.94	4, 6, 10	Mostofa et al. (2005b)[a]
Fulvic acid: 0–20 m, winter and vertical mixing period, Lake Biwa	1.48–1.98	1.57–2.14	1.71–2.02	4, 5	Mostofa et al. (2005b)[a]
Fulvic acid: 40–80 m, winter and vertical mixing period, 40–70 m, Lake Biwa	1.56–1.87	1.45–2.01	1.68–1.87	6, 7, 9	Mostofa et al. (2005b)[a]
Autochthonous fulvic acid (C-like) during photo- and microbial assimilations of algae					
Algal biomass + Milli-Q water, photo-assimilations: 6-h	0.98	0.95	2.01	11	Mostofa KMG et al., (unpublished data)
Algal biomass + River waters, photo-assimilations: 6-h	0.75	0.40	1.75	−96	Mostofa KMG et al., (unpublished data)
Algal biomass + Milli-Q waters, microbial-assimilations: 1–10 days (n = 5)	0.52	0.96	2.55	−3	Mostofa KMG et al., (unpublished data)
Algal biomass + Milli-Q waters, microbial-assimilations: 20–70 days (n = 6)	0.52	0.7	2.51	−54	Mostofa KMG et al., (unpublished data)
Algal biomass + River waters, microbial-assimilations: 1–10 days (n = 5)	1.53	1.23	2.59	−32	Mostofa KMG et al., (unpublished data)
Algal biomass + River waters, microbial-assimilations: 20–70 days (n = 6)	0.98	0.94	2.47	−37	Mostofa KMG et al., (unpublished data)
Algal biomass + River waters, microbial-assimilations: 80–180 days (n = 7)	0.87	1.11	2.08	−31	Mostofa KMG et al., (unpublished data)
Autochthonous fulvic acid (C-like) in river waters					
Autochthonous fulvic acid (C-like), Main channel of NenJiang (MNJ) River, China	1.04	0.8	0.35	−57	Mostofa KMG et al., (unpublished data)

(continued)

Table 3 (continued)

DOM sources	Fluorescence index (F_{index})				References
	$F_{Peak\ A/Peak\ C}$	$F_{250:330/440–450}$	$f_{450/500}$	HIX**	
Autochthonous fulvic acid (C-like), Tributaries of NenJiang (TNJ) River, China	0.85	1.05	0.37	−49	Mostofa KMG et al., (unpublished data)
Autochthonous fulvic acid (C-like), The Second SongHua (SH) River, China	1.14–1.31	0.98–1.21	1.54–1.71	−178	Mostofa KMG et al., (unpublished data)
Autochthonous fulvic acid (C-like), LiaoHe (LH) River, China	1.24	1.12	0.46	29	Mostofa KMG et al., (unpublished data)
Autochthonous and allochthonous lake DOM					
Epilimnion, 0–8 m (Summer: May–Sept), Lake Hongfeng	1.27–1.59	0.97–1.21	1.58–1.86	–	Fu et al. (2010)[a]
Epilimnion, 0–8 m (Winter: Nov–Feb.), Lake Hongfeng	1.57–1.61	1.20–1.50	1.83–2.25	–	Fu et al. (2010)[a]
Hypolimnion, 10–25 m (Summer: May–Sept), Lake Hongfeng	1.28–1.52	0.95–1.20	1.53–1.80	–	Fu et al. (2010)[a]
Hypolimnion, 10–25 m (Winter: Nov–Feb), Lake Hongfeng	1.52–1.64	1.20–1.25	1.80–2.22	–	Fu et al. (2010)[a]
Epilimnion, 0–8 m (Summer: May–Sept), Lake Baihua	1.37–1.55	1.10–1.26	1.82–2.14	–	Fu et al. (2010)[a]
Epilimnion, 0–8 m (Winter: Nov–Feb), Lake Baihua	1.25–1.33	1.25–1.30	2.19–2.23	–	Fu et al. (2010)[a]
Hypolimnion, 10–25 m (Summer: May–Sept), Lake Baihua	1.38–1.39	0.91–1.57	1.77–1.82	–	Fu et al. (2010)[a]
Hypolimnion, 10–25 m (Winter: Nov–Feb), Lake Baihua	1.39	1.53	1.73	–	Fu et al. (2010)[a]
Photobleaching allochthonous fulvic acid (C-like) in seawaters					
Fulvic acid-like: 0–15 m, Station 0, Seto Inland Sea, Japan (n = 11)	1.90	2.12	1.96	–	Mostofa KMG et al., (unpublished data)
Fulvic acid-like: 0–30 m, Stations 2 and 4, Seto Inland Sea, Japan (n = 12)	1.89	2.29	2.00	–	Mostofa KMG et al., (unpublished data)

(continued)

Table 3 (continued)

DOM sources	Fluorescence index (F_{index})				References
	$F_{Peak\ A/Peak\ C}$	$F_{250:330/440–450}$	$f_{450/500}$	HIX**	
Fulvic acid-like: 0–50 m, Stations 11 and 21, Seto Inland Sea, Japan (n = 13)	2.03	2.77	1.99	–	Mostofa KMG et al., (unpublished data)
Fulvic acid-like: 0–40 m, Stations 22 and 23, Seto Inland Sea, Japan (n = 12)	2.88	4.70	2.81	–	Mostofa KMG et al., (unpublished data)
Fulvic acid-like: 60–300 m, Stations 22 and 23, Seto Inland Sea, Japan (n = 9)	2.57	3.45	2.20	–	Mostofa KMG et al., (unpublished data)
Autochthonous and allochthonous fulvic acid (C-like): lake sediment pore waters					
Sediment pore waters, Lake Dianchi, China: 1–20 cm depths	2.07	1.93	2.73	–	Li et al., Characteristics of sediment pore water dissolved organic matter in four Chinese lakes using EEM spectroscopy and PARAFAC modeling, (unpublished data)
Sediment pore waters, Lake Dianchi, China: 22–40 cm depths	1.68	1.52	2.73	–	Li et al., Characteristics of sediment pore water dissolved organic matter in four Chinese lakes using EEM spectroscopy and PARAFAC modeling, (unpublished data)
Sediment pore waters, Lake Dianchi, China: 42–55 cm depths	1.21	1.25	2.05	–	Li et al., Characteristics of sediment pore water dissolved organic matter in four Chinese lakes using EEM spectroscopy and PARAFAC modeling, (unpublished data)
Sediment pore waters, Lake Chenghai, China: 1–20 cm depths	1.24	1.32	2.13	–	Li et al., Characteristics of sediment pore water dissolved organic matter in four Chinese lakes using EEM spectroscopy and PARAFAC modeling, (unpublished data)
Sediment pore waters, Lake Chenghai, China: 22–40 cm depths	1.05	0.66	1.53	–	Li et al., Characteristics of sediment pore water dissolved organic matter in four Chinese lakes using EEM spectroscopy and PARAFAC modeling, (unpublished data)
Sediment pore waters, Lake Chenghai, China: 42–87 cm depths	1.06–1.17	0.86–1.12	1.76–2.12	–	Li et al., Characteristics of sediment pore water dissolved organic matter in four Chinese lakes using EEM spectroscopy and PARAFAC modeling, (unpublished data)

(continued)

Table 3 (continued)

DOM sources	Fluorescence index (F_{index})				References
	$F_{Peak\ A/Peak\ C}$	$F_{250:330/440–450}$	$f_{450/500}$	HIX**	
Sediment pore waters, Lake Qinghai, China: 1–20 cm depths	0.91	0.80	1.67	–	Li et al., Characteristics of sediment pore water dissolved organic matter in four Chinese lakes using EEM spectroscopy and PARAFAC modeling, (unpublished data)
Sediment pore waters, Lake Qinghai, China: 22–40 cm depths	0.91	0.83	2.05	–	Li et al., Characteristics of sediment pore water dissolved organic matter in four Chinese lakes using EEM spectroscopy and PARAFAC modeling, (unpublished data)
Sediment pore waters, Lake Qinghai, China: 41–50 cm depths	0.92	0.77	2.00	–	Li et al., Characteristics of sediment pore water dissolved organic matter in four Chinese lakes using EEM spectroscopy and PARAFAC modeling, (unpublished data)
Sediment pore waters, Lake Bosten, China: 1–20 cm depths	1.22	1.25	2.13	–	Li et al., Characteristics of sediment pore water dissolved organic matter in four Chinese lakes using EEM spectroscopy and PARAFAC modeling, (unpublished data)
Sediment pore waters, Lake Bosten, China: 22–40 cm depths	0.97	0.76	1.62	–	Li et al., Characteristics of sediment pore water dissolved organic matter in four Chinese lakes using EEM spectroscopy and PARAFAC modeling, (unpublished data)
Sediment pore waters, Lake Bosten, China: 41–50 cm depths	1.03	1.05	2.11	–	Li et al., Characteristics of sediment pore water dissolved organic matter in four Chinese lakes using EEM spectroscopy and PARAFAC modeling, (unpublished data)

$F_{250:330/340–450}$ is defined by Mostofa et al. (2009b); $F_{370/350}$ is defined by McKnight et al. (2001); HIX is defined by Zsolnay et al. (1999)
$F_{peak\ A/Peak\ C}$ indicates the ratios of the maximum fluorescence intensity at peak A-region and peak C-region
HIX** Indicates that values are determined at excitation wavelength 255 nm instead of 254 nm
[a]Results obtained after applying the PARAFAC modeling on the publish sample's EEM spectra

is $F_{\text{Peak A/Peak C}}$, which is simple and can be easily applied to fluorescent components identified using PARAFAC modeling (Table 3; Fig. 4). The $F_{\text{Peak A/Peak C}}$ is defined as the ratio of the maximum fluorescence intensity at peak A (peak A-region) to that at peak C (peak C-region). For example, the maximum fluorescence intensity of peak A for standard Suwannee River Fulvic Acid (n = 5: 0.5–5 mg L^{-1}) identified using PARAFAC modeling (component 1) is 60 a.u. at Ex/Em = 260/463 nm and that for peak C is 39 a.u. at Ex/Em = 330/463 nm for the same component, which leads to $F_{\text{Peak A/Peak C}} = 1.55$ (Table 1). The comparisons of the $F_{\text{Peak A/Peak C}}$ values with other indices demonstrate that this new index is very useful to identify the allochthonous fulvic acid (C-like) (1.30–1.80) and allochthonous humic acid (1.50–1.95) from autochthonous fulvic acid of algal origin (0.52–0.98) (Table 3, Fig. 4). Note that the $F_{\text{Peak A/Peak C}}$ of autochthonous fulvic acid (C-like) is relatively high (1.53) in the initial 10 days of microbial assimilation of algae mixed with river waters (Table 3). Photoinduced degradation of fulvic acid in surface waters mostly causes a decrease in fluorescence intensity, which is more marked at peak C than at peak A and ultimately causes an increase of the $F_{\text{Peak A/Peak C}}$ values. This has also been found in irradiated SRFA (1.73), irradiated SRHA (1.94), irradiated fulvic acid in Kago upstream (1.80), Yellow River upper waters (1.93), Yellow River downstream waters (2.82), Yasu River waters (3.09) and lake surface waters (0–20 m) during the summer stratification period in Lake Biwa (1.67–1.82). Therefore, high values (>1.30) of $F_{\text{Peak A/Peak C}}$ can indicate the presence of photobleached fulvic or humic acid whilst low values (<1) are associated with autochthonous fulvic acid (C-like) of algal origin.

Low values of $F_{\text{Peak A/Peak C}}$ for autochthonous fulvic acid (C-like) of algal origin also suggests the presence of high aromaticity with more functional groups or fluorophores at peak C-region than at peak A region. Indeed, the highest fluorescence intensity of algal-origin autochthonous DOM is often detected at peak C-region than at peak A-region (Fig. 3h–j). On the other hand, fulvic acid (terrestrial in origin) shows lower fluorescence intensity at peak C-region than at peak A-region (Fig. 3a), which indicates the presence of relatively low aromaticity with a low number of functional groups or fluorophores and higher content of aliphatic carbon (Mostofa et al. 2009a, b; Malcolm 1985). Such differences in fluorescence intensities or fluorophores (functional groups) are attributed to differences in the f_{index} values, which would be useful in characterizing allochthonous fulvic acid and autochthonous fulvic acid. However, there is no study conducted on the chemical composition of algal-origin autochthonous DOM, which would be the focus for future research. Some researchers believe that autochthonously produced fulvic acid is similar to terrestrial fulvic acid, because autochthonous DOM shows a yellow color as well as similar fluorescence properties. Therefore, the f_{index} values can be useful to distinguish between the two materials. On the other hand, allochthonous fulvic acid (M-like) can merely be distinguished from the maximum fluorescence intensity of peak A (peak A-region) and low fluorescence intensity of peak C (peak C-region) (Fig. 3c) whilst autochthonous fulvic acid (M-like) of algal (or phytoplankton) origin

shows an entirely opposite behavior (maximum fluorescence at peak C and low fluorescence at peak A) (Fig. 3k, l).

2.6 Relationship Between FDOM and DOM

Fulvic acid-like fluorescence intensity (FI) is significantly correlated with DOC concentration both linearly and non-linearly as a consequence of the effects of sunlight on river water. However, non-linear correlation is more significant than the linear one (Fig. 5). The extrapolation of the linear relationship suggests that fulvic acid contributes approximately 45–63 % of the total DOM in Kago (KG) upstream, approximately 53 % in Nishi-Mataya (NM) upstream and approximately 73 % in the downstream waters of the Yasu River (YR) (Mostofa et al. 2007a). The fulvic acid contribution in Japanese rivers estimated from DOC and fulvic acid-like FI is similar to that reported in other studies of river water (40–80 %) (Mostofa et al. 2009a; Malcolm 1985; Peuravuori and Pihlaja 1999; Mostofa 2005). The higher presence of allochthonous fulvic acid and humic acids in river water is responsible for the good correlations with DOM found in natural waters (Mostofa et al. 2005a; Fu et al. 2007, 2010; Westerhoff et al. 2001). A gradual decrease in fulvic acid-like FI with decreasing DOC concentration (Fig. 5) can be explained if losses in FI and DOC are mostly involving the fluorophores in fulvic acid. The latter consist of some repeating functional groups with highly variable composition, having aromatic rings and highly unsaturated aliphatics with extensive π-electron systems (Mostofa et al. 2009b, 2010; Senesi 1990a; Malcolm 1985; Corin et al. 1996; Wu et al. 2005). The fluorophores present in

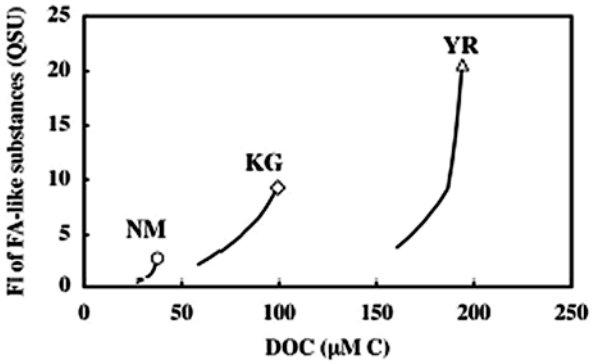

Fig. 5 Changes in DOC concentration and fulvic acid (FA)-like fluorescence intensity (FI) during photodegradation of DOM modeled by the first-order kinetics. Initial DOC concentration and FI are presented by the *open circle* (the Nishi-Mataya, NM upstream); *open diamond* (the Kago, KG upstream); and *open triangle* (Yasu River, YR downstream) for their respective samples collected from Lake Biwa watershed, Japan. *Data source* Mostofa et al. (2007a)

any macromolecule (e.g., fulvic acids and humic acids) at any peak C- or peak A-regions can be referred to as 'fluorochrome'. Any changes of the fluorochrome by photoinduced or microbial degradation can cause changes in the fluorescence properties of that molecule. Conversely, any DOM fraction that does not show fluorescence and is mostly composed of aliphatic C chain, which is photolytically inactive, is termed as 'non-fluorochrome'. On the basis of fluorescence characteristics, DOM can be separated into two major parts: fluorochrome and non-fluorochrome. They allow the photolytically sensitive fractions of DOM in waters to be distinguished. Therefore, any changes in the chemical composition of DOM by photoinduced processes can be examined by the determination of fluorescence characteristics in the asquatic environments (Mostofa et al. 2007a; Ma and Green 2004; Moran et al. 2000; Wu et al. 2007).

3 Factors Affecting the Fluorescence Properties of FDOM in Natural Waters

The fluorescence properties of FDOM are significantly affected by several factors in natural waters. They are: (i) Autochthonous origin of FDOM; (ii) Photodegradation of FDOM; (iii) Microbial degradation of FDOM; (iv) Complex formation between trace elements and FDOM; (v) Salinity; (vi) pH, and (vii) Temperature.

3.1 Autochthonous Origin of FDOM in Natural Waters

Photorespiration or photoinduced assimilation of organic matter (e.g. algal or phytoplankton biomass) can produce new DOM or FDOM in the aquatic environments (Fig. 3i, j) (Mostofa et al. 2009b; Fu et al. 2010; Aoki et al. 2008; Thomas and Lara 1995; Rochelle-Newall and Fisher 2002; Hiriart-Baer and Smiith 2005). It has been shown that the fluorescence intensity of FDOM is gradually increased upon 6 h sunlight irradiation in the presence of re-suspended algal biomass, collected by filtration of water (~0 m depth) from Lake Hongfeng (China) using GF/F filters during the summer season (Mostofa et al. 2009b). These results imply that photoinduced processes play an important role both in the decomposition of FDOM and in its production. They also play a key role in the biogeochemical cycles in the aquatic environments. Also the microbial degradation or assimilation of organic matter (e.g. algal or phytoplankton biomass) in in vitro experiments or under dark incubation may produce new DOM or FDOM in natural waters (Fig. 3h, j–l) (Mostofa et al. 2009b; Stedmon and Markager 2005a; Fu et al. 2010; Zhao et al. 2009; Aoki et al. 2008; Zhang et al. 2009b; Rochelle-Newall and Fisher 2002; Yamashita and Tanoue 2004, 2008; Miller et al. 2009). The fluorescence intensity of microbiologically produced FDOM was gradually increased after 20 days dark incubation at room temperature or upon resuspension

of algal biomass, which was collected through filtration of surface lake waters (~0 m) of Lake Hongfeng (China) using GF/F filters during the summer season (Mostofa et al. 2009b). One generally observes high fluorescence intensity in deeper lake or oceanic environments (Hayase et al. 1987, 1988; Hayase and Shinozuka 1995; Mostofa et al. 2005b), which might be the effect of microbial release of FDOM.

Studies on phytoplankton shows that fulvic-like and protein-like fluorescent components are released during the cultivation of three kinds of phytoplankton (*Microcystis aeruginosa* and *Staurastrum dorcidentiferum* of green algae and *Cryptomonas ovata* of dark-brown whip-hair algae collected from lake waters) under a 12:12 h light/dark cycle in an MA medium and an improved VT medium at 20 °C (Aoki et al. 2008). The results demonstrate that produced new DOM from three phytoplanktons can exhibit the different Ex/Em fluorescence properties whereas *Microcystis* can produce the hydrophilic DOM fraction with fluorescence peak at Ex/Em = 340/430 nm (peak C) and Ex/Em = 260/445 nm (peak A) whilst hydrophobic acid (or autochthonous fulvic acids) fraction at Ex/Em = 330/440 nm and 250/455 nm. These two fractions also show the protein-like peak at Ex/Em = 290/335 nm and 280/350 nm (peak T) and the autochthonous fulvic acid (M-like) at 320/385 nm and 330/385 nm (peak C-region), respectively (Table 2) (Aoki et al. 2008). Correspondingly, *Staurastrum* can produce hydrophilic DOM fraction at Ex/Em = 340/420 nm and 280/425 nm and hydrophobic acid fraction at Ex/Em = 340/435 nm and 290/430 nm whereas these two fractions display merely the protein-like peak at Ex/Em = 270/375 nm and 290/365 nm, respectively and do not show any autochthonous fulvic acid (M-like) fluorescence (Table 2) (Aoki et al. 2008). Finally, *Cryptomonas* can produce the hydrophilic DOM fraction at Ex/Em = 350/440 nm and 280/440 nm and the hydrophobic acid fraction at Ex/Em = 350/440 nm and 290/450 nm whereas these two fraction also exhibit the protein-like peak at Ex/Em = 270/355 nm and 270/350 nm, respectively and do not exhibit the autochthonous fulvic acid (M-like) fluorescence (Table 2) (Cammack et al. 2004). Similarly, cultivation of three kinds of phytoplankton (*Prorocentrum donghaiense, Heterosigma akashiwo* and *Skeletonema costatum* collected from sea water) can produce the visible humic-like (C-like and M-like) and the protein-like or the tyrosine-like components in waters (Zhao et al. 2009, 2006). Therefore, production of the autochthonous DOM is largely dependent on the phytoplankton communities in natural waters.

3.2 Photodegradation of FDOM in Natural Waters

Photodegradation can sequentially change the optical properties (fluorescence peak and fluorescence intensity) of FDOM in waters. Photodegradation can change the fluorescence peak position (Ex/Em) of various FDOM components in waters (Mostofa et al. 2005a, 2010, 2007b, 2011; Moran et al. 2000; Miller et al. 2009). For instance, photodegradation can alter the terrestrial fulvic acid (C-like)

fluorescence of peak C into the photo-bleached fluorescence peak (peak M_p), which can show the highest fluorescence intensity in some natural waters (Mostofa et al. 2007a, 2005b; Moran et al. 2000; Komada et al. 2002; Burdige et al. 2004). Due to photodegradation, the new photo-bleached peak M_p is shifted at shorter excitation–emission wavelengths (Fig. 3a, d, e). Such a change in the fluorescence peak caused by photodegradation is termed as `blue-shift`. Blue-shift is commonly observed in surface lake or seawaters where photodegradation is important due to exposure to natural sunlight (Fig. 3d, e). Photoinduced effects can decrease the fluorescence intensity (FI) of fulvic acid-like (peak C), FWAs-like (peak W), and tryptophan-like (peak T) compounds, which are commonly observed in natural waters in field and experimental observations (Fig. 5; Table 4) (Hayase and Shinozuka 1995; Mostofa et al. 2005a; 2005b, 2010, 2007a, 2011; Stedmon et al. 2007a; Brooks et al. 2007; Garcia et al. 2005; Winter et al. 2007; Mostofa KMG et al., unpublished data; Skoog et al. 1996; Moran et al. 2000; Osburn et al. 2009; Lepane et al. 2003; Abboudi et al. 2008; Poiger et al. 1999; Fu et al. 2010; Borisover et al. 2009; Yamashita and Tanoue 2008; Vodacek et al. 1997; Yamashita et al. 2007; Shank et al. 2010).

Fulvic Acid-like Components in Natural Waters

Fluorescence intensity losses of fulvic acid-like substances by photoinduced degradation are 1–84 % in rivers, 16–83 % in lakes, 19–67 % in estuaries, and 9–84 % in sea waters studied experimentally in the course of short (hours) to long-term (days or months) irradiation (Table 4). In lake water after 12 days irradiation, the losses of fulvic acid-like fluorescence intensity have been 36 % at the surface (2.5 m) and 48 % in deeper waters (70 m) for DOM fractions of <0.1 μm. In the case of DOM molecular-weight fractions below 5 kDa, the corresponding losses have been 16 % in surface waters (2.5 m) and 50 % in deeper waters (70 m). The low fluorescence intensity decrease in the case of surface-water DOM with molecular weight below 5 kDa may be explained by the fact that the corresponding samples have been collected during an ongoing summer stratification period (September). Therefore, the photosensitive DOM fractions had probably already undergone photoinduced decomposition before sample collection. The higher fluorescence intensity decrease observed for deep-water DOM may be accounted for by the fact that deep waters undergo photoinduced degradation processes to a lesser extent because of the reduced sunlight irradiance compared to surface waters (Laurion et al. 2000). As a consequence, deep-water samples may contain significant amounts of photosensitive DOM components, which have not been degraded in the natural environment and can undergo photoinduced decomposition when irradiated in the laboratory (Table 4). For similar reasons, photoinduced DOM mineralization is very difficult to be observed in surface lake water samples and is much easier to be detected upon irradiation of groundwater (Vione et al. 2009). In estuarine water it has been observed a fluorescence intensity decrease in fulvic acid-like

Table 4 Photochemical and microbial changes of fluorescence intensity (FI) of fulvic acid-like (peak C), fluorescent whitening agents (FWAs)-like (peak W) tryptophan-like, tyrosine-like or protein-like (peak T) substances as a result of photoirradiation experiments conducted on standard substance and natural waters

Type of samples/locations	Origin of DOM	Filtration size/type (μm)	Irradiation time (h/days)	Solar intensity (MJm^{-2})	Changes in fluorescence intensities				References
					Photoirradiation	Microbial	Photoirradiation	Microbial	
					Peak C-region		Peak T- and T_{UV}-regions		
					%		%		
Suwannee River Fulvic Acid (SRFA): 1 mg L^{-1}	Allochthonous/plant material	MQ water	10 h (Xe lamp)	nd	−42	(+) 0.1	na	na	Mostofa et al. (2011)
SRFA:1 mg L^{-1}	Allochthonous/plant material	MQ water	3 h (Xe lamp)	nd	−19	nd	na	na	Mostofa et al. (2011)
SRFA:1 mg L^{-1} + 50 μM NO_2^-	Allochthonous/plant material	MQ water	3 h (Xe lamp)	nd	−22	nd	na	na	Mostofa et al. (2011)
SRFA: 3 mg L^{-1}	Allochthonous/plant material	MQ water	3 h (Xe lamp)	nd	−23	nd	na	na	Mostofa et al. (2011)
SRFA: 5 mg L^{-1}	Allochthonous/plant material	MQ water	3 h (Xe lamp)	nd	−20	nd	na	na	Mostofa et al. (2011)
Suwannee River Humic Acid (SRHA): 1 mg L^{-1}	Allochthonous/plant material	MQ water	10 h (Xe lamp)	nd	(+) 70	nd	na	na	Mostofa et al. (2011)
SRHA: 3 mg L^{-1}	Allochthonous/plant material	MQ water	3 h (Xe lamp)	nd	−17	nd	na	na	Mostofa et al. (2011)
SRHA: 5 mg L^{-1}	Allochthonous/plant material	MQ water	3 h (Xe lamp)	nd	(+) 5	nd	na	na	Mostofa et al. (2011)
Tryptophan standard: 1 mg L^{-1}	–	MQ water	10 h (Xe lamp)	nd	na	nd	−63	−0.1	Mostofa et al. (2011)
Tryptophan standard: 3 mg L^{-1}	–	MQ water	3 h (Xe lamp)	nd	na	nd	−23	nd	Mostofa et al. (2011)
Tryptophan standard: 5 mg L^{-1}	–	MQ water	3 h (Xe lamp)	nd	na	nd	−20	nd	Mostofa et al. (2011)
Tyrosine standard: 1 mg L^{-1}	–	MQ water	10 h (Xe lamp)	nd	na	nd	−4	(+) 5	Mostofa KMG et al., (unpublished data)
Tyrosine standard: 3 mg L^{-1}	–	MQ water	3 h (Xe lamp)	nd	na	nd	−36	nd	Mostofa KMG et al., (unpublished data)
DSBP standard: 1 mg L^{-1}	–	MQ water	10 h (Xe lamp)	nd	−94	(+) 0.1	na	na	Mostofa et al. (2011)
DSBP standard: 1 mg L^{-1}	–	MQ water	0.5 h (Xe lamp)	nd	−40	nd	nd	nd	Mostofa et al. (2005a)
DSBP standard: 3 mg L^{-1}	–	MQ water	3 h (Xe lamp)	nd	−73	nd	nd	nd	Mostofa et al. (2011)
DSBP standard: 5 mg L^{-1}	–	MQ water	3 h (Xe lamp)	nd	−60	nd	nd	nd	Mostofa et al. (2011)

(continued)

Table 4 (continued)

Type of samples/locations	Origin of DOM	Filtration size/type (μm)	Irradiation time (h/days)	Solar intensity (MJm^{-2})	Changes in fluorescence intensities				References
					Photoirradiation	Microbial	Photoirradiation	Microbial	
					Peak C-region		Peak T- and T_{UV}-regions		
					%		%		
DAS1 standard: 1 mg L^{-1}	–	MQ water	10 h (Xe lamp)	nd	−93	nd	nd	nd	Mostofa et al. (2011)
DAS1 standard: 1 mg L^{-1}	–	MQ water	0.5 h (Xe lamp)	nd	−45	nd	nd	nd	Mostofa et al. (2011)
Fulvic acid, extracted from Göta River: 6.3 mg L^{-1}	Allochthonous/plant material	NaOH + MQ water	13 (UV-B lamp)	nd	−32	na	nd	nd	Lepane et al. (2003)
Humic acid, extracted from Göta River: 6.5 mg L^{-1}	Allochthonous/plant material	NaOH + MQ water	13 (UV-B lamp)	nd	(+) 4	na	nd	nd	Lepane et al. (2003)
Fulvic acid, extracted from Göta River: 6.3 mg L^{-1}	Allochthonous/plant material	NaOH + MQ water	9 (dark)	nd	na	(+) 8	nd	nd	Lepane et al. (2003)
Humic acid, extracted from Göta River: 6.5 mg L^{-1}	Allochthonous/plant material	NaOH + MQ water	9 (dark)	nd	na	(+) 6	nd	nd	Lepane et al. (2003)
Aldrich fulvic acid	Allochthonous/plant material	Deionized water	13 (irradiated)	nd	−(26–41)	na	nd	nd	Winter et al. (2007)
Aldrich fulvic acid	Allochthonous/plant material	Deionized water	13 (irradiated)	nd	−(21–45)	na	nd	nd	Winter et al. (2007)
Kago upstream, Japan (35°N)	Allochthonous/plant material	0.45	12 (irradiated)	192	−74	na	np	np	Mostofa et al. (2005b)
Kago upstream, Japan (35°N)	Allochthonous/plant material	0.45	12 (dark)	192	na	(+) 3	np	np	Mostofa et al. (2005b)
Kago upstream, Japan (35°N)	Allochthonous/plant material	0.45	13 (irradiated)	176	−72	na	np	np	Mostofa et al. (2007a)
Kago upstream, Japan (35°N)	Allochthonous/plant material	0.45	13 (dark)	176	na	(+) 15	np	np	Mostofa et al. (2007a)
Nishi-Mataya upstream, Japan (35°N)	Allochthonous/plant material	0.45	13 (irradiated)	176	−84	na	np	np	Mostofa et al. (2007a)
Nishi-Mataya upstream, Japan (35°N)	Allochthonous/plant material	0.45	13 (dark)	176	na	(+) 6	np	np	Mostofa et al. (2007a)
Nishi-Mataya upstream, Japan (35°N)	Allochthonous/plant material	0.45	12 (irradiated)	192	−78	na	−40	na	Mostofa et al. (2007a)

(continued)

Table 4 (continued)

Type of samples/locations	Origin of DOM	Filtration size/type (μm)	Irradiation time (h/days)	Solar intensity (MJm^{-2})	Changes in fluorescence intensities				References
					Photoirradiation	Microbial	Photoirradiation	Microbial	
					Peak C-region		Peak T- and T_{UV}-regions		
					%		%		
Nishi-Mataya upstream, Japan (35°N)	Allochthonous/plant material	0.45	12 (dark)	192	na	(+) 5	na	np	Mostofa et al. (2007a)
Yasu River, Japan (35°N)	Allochthonous/ autochthonous	0.45	13 (irradiated)	176	−80	na	−59	na	Mostofa et al. (2007a)
Yasu River, Japan (35°N)	Allochthonous/ autochthonous	0.45	13 (dark)	176	na	(+) 14	na	(+) 6	Mostofa et al. (2007a)
Kurose River (Izumi site), 34°N	Allochthonous/ anthropogenic	0.20	6 (irradiated)	118.5	−77	na	−10	na	Mostofa et al. (2011)
Kurose River (Izumi site), 34°N	Allochthonous/ anthropogenic	0.45	6 (dark)	118.5	na	(+) 6	na	(+) 4	Mostofa et al. (2011)
Kurose River (Izumi site), 34°N	Allochthonous/ anthropogenic	Unfiltered	6 (irradiated)	118.5	−77	na	−5	na	Mostofa et al. (2011)
Kurose River (Izumi site), 34°N	Allochthonous/ anthropogenic	Unfiltered	6 (dark)	118.5	na	nd	na	−17	Mostofa et al. (2011)
Kurose River (Hinotsume site), 34°N	Allochthonous/ anthropogenic	0.20	10 (irradiated)	152.5	−76	na	−21	na	Mostofa et al. (2011)
Kurose River (Hinotsume site), 34°N	Allochthonous/ anthropogenic	0.45	10 (dark)	152.5	na	nd	na	−11	Mostofa et al. (2011)
Kurose River (Hinotsume site), 34°N	Allochthonous/ anthropogenic	Unfiltered	10 (irradiated)	152.5	−81	na	−19	na	Mostofa et al. (2011)
Kurose River (Hinotsume site), 34°N	Allochthonous/ anthropogenic	Unfiltered	10 (dark)	152.5	na	nd	na	−13	Mostofa et al. (2011)
Nanming River, (Near Institute), 26°N	Allochthonous/ anthropogenic	Unfiltered	3 h (irradiated)	nd	−27	na	−32	na	Mostofa et al. (2010)
Detergent component (C-like), drain samples, (near institute), 26°N	–	Unfiltered	3 h (irradiated)	nd	−34	na	−50	na	Mostofa et al. (2010)

(continued)

Table 4 (continued)

Type of samples/locations	Origin of DOM	Filtration size/type (μm)	Irradiation time (h/days)	Solar intensity (MJm^{-2})	Changes in fluorescence intensities				References
					Photoirradiation	Microbial	Photoirradiation	Microbial	
					Peak C-region		Peak T- and T_{UV}-regions		
					%		%		
Detergent component (T_{UV}-like), drain samples, (near institute), 26°N	–	Unfiltered	3 h (irradiated)	nd	na	na	na	(+) 4	Mostofa et al. (2010)
Detergent component (C-like), component 2, commercial detergents	–	MQ water	3 h (irradiated)	nd	−88	na	np	na	Mostofa et al. (2010)
Detergent component (T_{UV}-like), component 2, commercial detergents	–	MQ water	3 h (irradiated)	nd	na	na	na	(+) 9	Mostofa et al. (2010)
Detergent component (C-like), river water + commercial detergent	–	Unfiltered	10 (dark)	nd	na	(+) 21	na	na	Mostofa et al. (2010)
Tryptophan-like (T-like): River water + commercial detergent	–	Unfiltered	10 (dark)	nd	na	na	na	−24	Mostofa et al. (2010)
Detergent component (T_{UV}-like): river water + commercial detergent	–	Unfiltered	10 (dark)	nd	na	na	na	−84	Mostofa et al. (2010)
Detergent component (C-like), drain samples, (near institute), 26°N	–	Unfiltered	10 (dark)	nd	na	(+) 8	na	na	Mostofa et al. (2010)
Tryptophan-like or protein-like (T-like), drain samples, (near institute), 26°N	Sewerage	Unfiltered	10 (dark)	nd	na	na	na	−67	Mostofa et al. (2010)
Detergent component (T_{UV}-like), drain samples, (near institute), 26°N	Sewerage	Unfiltered	10 (dark)	nd	na	na	na	−90	Mostofa et al. (2010)
Commercial detergent (C-like), component 1	–	MQ water	10 (dark)	nd	na	(+) 14	na	na	Mostofa et al. (2010)

(continued)

Table 4 (continued)

Type of samples/locations	Origin of DOM	Filtration size/type (μm)	Irradiation time (h/days)	Solar intensity (MJm^{-2})	Changes in fluorescence intensities				References
					Photoirradiation	Microbial	Photoirradiation	Microbial	
					Peak C-region		Peak T- and T_{UV}-regions		
					%		%		
Commercial detergent (T_{UV}-like), component 2	–	MQ water	10 (dark)	nd	na	na	na	−15	Mostofa et al. (2010)
River water + DSBP	–	River water	12 h (summer)	nd	−31	na	nd	nd	Poiger et al. (1999)
River water + DAS1	–	River water	12 h (summer)	nd	−12	na	nd	nd	Poiger et al. (1999)
Fulvic acid (C-like: comp 1), Yellow River, China	Allochthonous/plant material	River water	3 h (summer)	nd	−(43–46)	na	nd	nd	Mostofa KMG et al., (unpublished data)
Fulvic acid (M-like: comp 2), Yellow River, China	Allochthonous/plant material	River water	3 h (summer)	nd	−(5–68)	na	nd	nd	Mostofa KMG et al., (unpublished data)
Fulvic acid (C-like: comp 1), Yellow River, China	Allochthonous/plant material	River water	12 (dark)	nd	na	(+) (52–81)	nd	nd	Mostofa KMG et al., (unpublished data)
Fulvic acid (M-like: comp 2), Yellow River, China	Allochthonous/plant material	River water	12 (dark)	nd	na	−100	nd	(−) 8; (+) 33	Mostofa KMG et al., (unpublished data)
Mackenzie River, 68°N	Allochthonous/plant material	0.20	72 h (summer)	nd	−(13–45)	nd	nd	nd	Osburn et al. (2009)
Mackenzie River, 68°N	Allochthonous/plant material	0.20	72 h (spring)	nd	−33	nd	nd	nd	Osburn et al. (2009)
Mackenzie River, 68°N	Allochthonous/plant material	0.20	72 h (autumn)	nd	−(1–10)	nd	nd	nd	Osburn et al. (2009)
Laramie River-DOM, 41°N	Allochthonous/plant material	River water	72 h (sunlight)	nd	−23	na	nd	nd	Brooks et al. (2007)
Chimney Park Wetland-DOM, 41°N	Allochthonous/plant material	River water	72 h (sunlight)	nd	−7	na	nd	nd	Brooks et al. (2007)
Lake Biwa, 35°N: surface water (2.5 m)	Allochthonous/ autochthonous	0.10	12 (irradiated)	137	−36	na	−18	na	Mostofa et al. (2011)
Lake Biwa, 35°N: surface water (2.5 m)	Allochthonous/ autochthonous	0.10	12 (dark)	nd	na	(+) 31	na	(+) 68	Mostofa et al. (2011)
Lake Biwa, 35°N: deeper water (70 m)	Allochthonous/ autochthonous	0.10	12 (irradiated)	nd	−48	na	−7	na	Mostofa et al. (2011)

(continued)

Table 4 (continued)

Type of samples/locations	Origin of DOM	Filtration size/type (μm)	Irradiation time (h/days)	Solar intensity (MJm^{-2})	Changes in fluorescence intensities				References
					Photoirradiation	Microbial	Photoirradiation	Microbial	
					Peak C-region		Peak T- and T_{UV}-regions		
					%		%		
Lake Biwa, 35°N: deeper water (70 m)	Allochthonous/ autochthonous	0.10	12 (dark)	nd	na	0	na	(+) 5	Mostofa et al. (2011)
Lake Biwa, 35°N: surface water (2.5 m)	Allochthonous/ autochthonous	<5 kDa	12 (irradiated)	nd	−16	na	(+) 4	na	Mostofa et al. (2011)
Lake Biwa, 35°N: surface water (2.5 m)	Allochthonous/ autochthonous	<5 kDa	12 (dark)	nd	na	(+) 102	na	(+) 51	Mostofa et al. (2011)
Lake Biwa, 35°N: deeper water (70 m)	Allochthonous/ autochthonous	<5 kDa	12 (irradiated)	nd	−50	na	−19	na	Mostofa et al. (2011)
Lake Biwa, 35°N: deeper water (70 m)	Allochthonous/ autochthonous	<5 kDa	12 (dark)	nd	na	(+) 20	na	(+) 28	Mostofa et al. (2011)
Four Lakes (45ºN)	Allochthonous/ autochthonous	0.45	13	nd	−(22–31)	−(0–5)	nd	nd	Garcia et al. (2005)
Lake Taihu, China	Allochthonous/ autochthonous	0.22	12	nd	−70	nd	−60	nd	Zhang et al. (2009b)
Fulvic acid, Mill Creek: surface water, 43ºN	Allochthonous/ autochthonous	0.45	12	nd	−(48–79)	na	na	na	Winter et al. (2007)
Fulvic acid, Bannister Lake: surface water, 43ºN	Allochthonous/ autochthonous	0.45	12	nd	−(75–83)	na	na	na	Winter et al. (2007)
Fulvic acid and tryptophan, Lake Erie: surface water, 42ºN	Allochthonous/ autochthonous	0.45	12	nd	−(74–77)	na	na	na	Winter et al. (2007)
Fulvic acid, Sanctuary Pond: surface water, 41ºN	Allochthonous/ autochthonous	0.45	12	nd	−(71–79)	na	na	na	Winter et al. (2007)
Humic acid, Luther Marsh: surface water, 43ºN	Allochthonous/ autochthonous	0.45	12	nd	−(64–65)	na	na	na	Winter et al. (2007)
Humic acid, Mill Creek: surface water, 43ºN	Allochthonous/ autochthonous	0.45	12	nd	−(91–100)	na	na	na	Winter et al. (2007)
Humic acid, Bannister Lake: surface water, 43ºN	Allochthonous/ autochthonous	0.45	12	nd	−71	na	na	na	Winter et al. (2007)

(continued)

Table 4 (continued)

Type of samples/locations	Origin of DOM	Filtration size/type (μm)	Irradiation time (h/days)	Solar intensity (MJm^{-2})	Changes in fluorescence intensities				References
					Photoirradiation	Microbial	Photoirradiation	Microbial	
					Peak C-region		Peak T- and T_{UV}-regions		
					%		%		
Humic acid, Lake Erie: surface water, 42ºN	Allochthonous/ autochthonous	0.45	12	nd	np	na	na	na	Winter et al. (2007)
Humic acid, Sanctuary Pond: surface water, 41ºN	Allochthonous/ autochthonous	0.45	12	nd	−(63–81)	na	na	na	Winter et al. (2007)
Tryptophan, Luther Marsh: surface water, 43ºN	Allochthonous/ autochthonous	0.45	12	nd	na	na	(+) 62	0	Winter et al. (2007)
Tryptophan, Mill Creek: surface water, 43ºN	Allochthonous/ autochthonous	0.45	12	nd	na	na	−(81–88)	0	Winter et al. (2007)
Tryptophan, Lake Erie: surface water, 42ºN	Allochthonous/ autochthonous	0.45	12	nd	na	na	−(72–82)	0	Winter et al. (2007)
Tryptophan, Fish food	Allochthonous/ autochthonous	0.45	12	nd	na	na	−(54–66)	(+) (20–40)	Winter et al. (2007)
Tyrosine, Bannister Lake: surface water, 43ºN	Allochthonous/ autochthonous	0.45	12	nd	na	na	(+) 68, −34	0	Winter et al. (2007)
Tyrosine, Lake Erie: surface water, 42ºN	Allochthonous/ autochthonous	0.45	12	nd	na	na	(+) 1, −19	0	Winter et al. (2007)
Tyrosine, Sanctuary Pond: surface water, 41ºN	Allochthonous/ autochthonous	0.45	12	nd	na	na	−(73–100)	0	Winter et al. (2007)
Satilla Estuary	Allochthonous/ autochthonous	0.20	70 (irradiated)	nd	−61	na	−45	na	Moran et al. (2000)
Satilla Estuary	Allochthonous/ autochthonous	0.20	70 (irradiated)	nd	−67	"	−37	"	Moran et al. (2000)
Satilla Estuary	Allochthonous/ autochthonous	0.20	51 (dark)	nd	na	−12	na	(+) 112	Moran et al. (2000)
Satilla Estuary	Allochthonous/ autochthonous	0.20	51 (dark)	nd	na	−1	na	(+) 23	Moran et al. (2000)
Estuary, Beaufort Sea, 69ºN	Allochthonous/ autochthonous	0.20	72 h (summer)	nd	−(47–60)	nd	nd	nd	Osburn et al. (2009)

(continued)

Table 4 (continued)

Type of samples/locations	Origin of DOM	Filtration size/type (μm)	Irradiation time (h/days)	Solar intensity (MJm^{-2})	Changes in fluorescence intensities				References
					Photoirradiation	Microbial	Photoirradiation	Microbial	
					Peak C-region		Peak T- and T_{UV}-regions		
					%		%		
Estuary, Beaufort Sea, 69°N	Allochthonous/ autochthonous	0.20	72 h (spring)	nd	−33	nd	nd	nd	Osburn et al. (2009)
Estuary, Beaufort Sea, 69°N	Allochthonous/ autochthonous	0.20	72 h (autumn)	nd	−19	nd	nd	nd	Osburn et al. (2009)
Shelf, Beaufort Sea, 69–70°N	Allochthonous/ autochthonous	0.20	72 h (summer)	nd	−(67–75)	nd	nd	nd	Osburn et al. (2009)
Shelf, Beaufort Sea, 70°N	Allochthonous/ autochthonous	0.20	72 h (spring)	nd	−(46–61)	nd	nd	nd	Osburn et al. (2009)
Shelf, Beaufort Sea, 70–71°N	Allochthonous/ autochthonous	0.20	72 h (autumn)	nd	−(29–84)	nd	nd	nd	Osburn et al. (2009)
Gulf, Beaufort Sea, 70°N	Allochthonous/ autochthonous	0.20	72 h (spring)	nd	−66	nd	nd	nd	Osburn et al. (2009)
Gulf, Beaufort Sea, 70–71°N	Allochthonous/ autochthonous	0.20	72 h (autumn)	nd	−(50–61)	nd	nd	nd	Osburn et al. (2009)
Gulf, Beaufort Sea, 70–71°N	Allochthonous/ autochthonous	0.20	72 h (winter)	nd	−(21–67)	nd	nd	nd	Osburn et al. (2009)
Fulvic acid (C-like)?, component 1, Baltic Sea: 55–65°N	Allochthonous/ autochthonous	0.20	48 h (UV−A lamp)	nd	−65	na		na	Stedmon et al. (2007a)
Autochthonous fulvic acid (M-like)?, component 2	Allochthonous/ autochthonous	0.20	48 h (UV-A lamp)	nd	−69	na	na	na	Stedmon et al. (2007a)
Protein-like?, component 4	Allochthonous/ autochthonous	0.20	48 h (UV-A lamp)	nd	−54	na	na	na	Stedmon et al. (2007a)
Tyrosine-like?, component 5	Allochthonous/ autochthonous	0.20	48 h (UV-A lamp)	nd	na	na	−26	na	Stedmon et al. (2007a)
Fulvic acid (A-like)?, component 6	Allochthonous/ autochthonous	0.20	48 h (UV-A lamp)	nd	(+) (252–2740)	na	na	na	Stedmon et al. (2007a)
Baltic Sea, BY15: 0–30 m depth	Allochthonous/ autochthonous	0.20 (unfiltered)	5	nd	−(44–52)	nd	nd	nd	Skoog et al. (1996)
Baltic Sea, BY15: 100–240 m depth	Allochthonous/ autochthonous	0.20 (unfiltered)	5	nd	−(58–65)	nd	nd	nd	Skoog et al. (1996)

(continued)

Table 4 (continued)

Type of samples/locations	Origin of DOM	Filtration size/type (μm)	Irradiation time (h/days)	Solar intensity (MJm^{-2})	Changes in fluorescence intensities				References
					Photoirradiation	Microbial	Photoirradiation	Microbial	
					Peak C-region		Peak T- and T_{UV}-regions		
					%		%		
Baltic Sea, BY32: 0–50 m depth	Allochthonous/ autochthonous	0.20 (unfiltered)	12	nd	−(61–70)	nd	nd	nd	Skoog et al. (1996)
Baltic Sea, BY32: 0–50 m + chloroform	Allochthonous/ autochthonous	0.20 (unfiltered)	12	nd	−(59–81)	nd	nd	nd	Skoog et al. (1996)
Baltic Sea, BY32: 100–190 m depth	Allochthonous/ autochthonous	0.20 (unfiltered)	12	nd	−(73–75)	nd	nd	nd	Skoog et al. (1996)
Baltic Sea, BY32: 100–190 m + Chloroform	Allochthonous/ autochthonous	0.20 (unfiltered)	12	nd	−(83–84)	nd	nd	nd	Skoog et al. (1996)
Baltic Sea, F15: 0–50 m depth	Allochthonous/ autochthonous	0.20 (unfiltered)	4	nd	−(48–49)	nd	nd	nd	Skoog et al. (1996)
Baltic Sea, F15: 0–50 m depth	Allochthonous/ autochthonous	0.20 (unfiltered)	4	nd	−50	nd	nd	nd	Skoog et al. (1996)
Baltic Sea, F15: 0–50 m depth	Allochthonous/ autochthonous	0.20 (filtered)	4	nd	−(50–51)	nd	nd	nd	Skoog et al. (1996)
Baltic Sea, F15: 100 m depth	Allochthonous/ autochthonous	0.20 (filtered)	4	nd	−56	nd	nd	nd	Skoog et al. (1996)
Mediterranean Sea, 42°N: Canet lagons	Allochthonous/ autochthonous	0.20 (filtered)	8 h (summer)	nd	−22	(+) 8	nd	nd	Abboudi et al. (2008)
Mediterranean Sea, 42°N: Leucate lagons	Allochthonous/ autochthonous	0.20 (filtered)	8 h (summer)	nd	−9	(+) 0.4	nd	nd	Abboudi et al. (2008)
Mediterranean Sea, 42°N: coastal waters (SOLA)	Allochthonous/ autochthonous	0.20 (filtered)	8 h (summer)	nd	−34	−2	nd	nd	Abboudi et al. (2008)
Seawater, Gotland Deep: 40 m, 57°N	Allochthonous/ autochthonous	0.45	13 (UV-B lamp)	nd	−32	nd	nd	nd	Lepane et al. (2003)

nd not detected, *na* not applicable, *np* no significant fluorescence peak observed in samples

(−) and (+) means a decrease in fluorescence and an increase in fluorescence, respectively, of the respective peaks

Irradiation time-hours (h) mentioned with each time as 'h' and 'days' mentioned as a whole digit only

substances of 19–67 % during 72 h to 70 days irradiation (Table 4) (Moran et al. 2000; Osburn et al. 2009). In unfiltered seawater samples from the Baltic Sea irradiated for 4–5 days, the corresponding fluorescence intensity decrease has been of 44–52 % at the surface (0–50 m) and 56–65 % in the deeper layers (100–240 m). In some cases the decrease has been more marked, i.e. 61–70 % at the surface (0–50 m) and 73-75 % in the deeper layer (100–190 m). Interestingly the addition of chloroform significantly enhanced photodegradation, yielding a fulvic acid-like fluorescence decrease of 59–81 % in surface samples (0–50 m) and of 83–84 % in deep-water ones (Table 4) (Skoog et al. 1996). The mechanism behind the increased FDOM photodegradation upon addition of chloroform may be the production of phosgene in the presence of O_2 ($CHCl_3 + O_2 + h\upsilon \rightarrow COCl_2 + H Cl$). Phosgene is highly reactive toward the degradation of the fluorophores, such as the amino groups ($RNH_2 + COCl_2 \rightarrow RN = CO + 2HCl$) or carboxylic acids ($RCO_2H + COCl_2 \rightarrow RC(O)Cl + HCl + CO_2$) (Mostofa et al. 2011; Shriner et al. 1943). Such processes would contribute to the decrease of DOM fluorescence in natural waters (Mostofa et al. 2009a, 2011).

Photoinduced degradation of Mediterranean Sea samples (8 h sunlight exposure) showed a decrease in the fluorescence of fulvic acid-like or humic-like fluorophores (peak C), in the range of 9–22 % for lagoon water and approaching 34 % for coastal water (Table 4) (Abboudi et al. 2008). Similarly, photoinduced degradation of waters collected from Mackenzie River and Beaufort Sea (Estuary, Shelf and Gulf) demonstrates that the degradation of fulvic acid-like fluorophores (peak C) is usually higher during summer irradiation than in spring, autumn and winter (Table 4). The photodegradation of fulvic acid-like fluorophore (peak C) is relatively higher in Beaufort Sea samples (47–60 % in Estuary during summer; 67–75 % in Shelf during summer; 66 % in Gulf during spring; 72 h irradiation) than in Satilla Estuary (61–67 %, 70 days), Baltic Sea (44–52 % in surface waters, 4–5 days), and Gotland Deep seawater (32 %, 13 days) (Table 4) (Stedmon et al. 2007a; Skoog et al. 1996; Moran et al. 2000; Osburn et al. 2009; Lepane et al. 2003). The high photodegradation of fulvic acid-like substances in Beaufort Sea samples has been explained by the occurrence of two phenomena. Firstly, in many cases a significant fraction of the fulvic acid-like substances are of autochthonous origin, which makes them highly susceptible to photodegradation (Mostofa KMG et al., unpublished data; Johannessen et al. 2007). Secondly, in the case of the Beaufort Sea the fulvic acid-like substances have allochthonous origin as they mainly derive from riverine input. Photoinduced degradation of these compounds is poorly effective due to low water temperature in the Beaufort Sea (−0.54 to 21.81 °C in Estuary, −1.36 to 9.23 °C in Shelf, and −1.68 to 0.12 °C in Gulf samples) (Osburn et al. 2009). Therefore, unaffected allochthonous fulvic acid-like substances are highly susceptible to degradation upon laboratory irradiation. The case of the Beaufort Sea may be a particular one, however, because it has been reported that DOM (or FDOM) components are produced from microbial assimilation of phytoplankton biomass or organic matter in natural waters (Mostofa et al. 2009a; Parlanti et al. 2000; Stedmon et al. 2007a, 2007b; Fu et al. 2010; Rochelle-Newall and Fisher 2002; Yamashita and Tanoue 2004; Rochelle-Newall

et al. 1999). Photoinduced degradation thus leads to hypotheses about several characteristic chemical and optical features of FDOM, which can be listed as follows (Mostofa et al. 2011): (i) In upstream and downstream rivers the fluorescence is predominantly caused by fulvic and humic acids. In contrast, in the surface layer of lakes and oceans the fluorescence of various FDOM components is rapidly depleted by exposure to natural sunlight (Hayase and Shinozuka 1995; Mostofa et al. 2005b; Fu et al. 2010; Yamashita and Tanoue 2008). As a consequence, the FDOM sampled from these environments is relatively less susceptible to undergo further photoinduced degradation in the laboratory, as was for instance the case for Lake Biwa (Table 4). (ii) High losses of fulvic acid-like fluorescence have been observed upon irradiation of water samples from the deeper layers of lakes and seas. They are more pronounced compared to surface water. A reasonable explanation for this phenomena can include two facts. First, the higher occurrence of fulvic or humic acids in the deeper layers may result directly from terrestrial sources through riverine input without degradation in surface waters (Table 4) (Mopper et al. 1991). Second, the releases of autochthonous fulvic acid (C-like) can occur microbially from algal biomass or phytoplankton in deeper waters (Mostofa et al. 2009a, b; Zhang et al. 2009a; Yamashita and Tanoue 2004, 2008). Autochthonous material is highly susceptible to undergo photoinduced decomposition. It has recently been shown that algal-derived CDOM is a more efficient photoinduced substrate than allochthonous fulvic acid (Mostofa KMG et al., unpublished data; Johannessen et al. 2007; Hulatt et al. 2009). (iii) By comparison of the initial and final photo-bleached components of fulvic acid (C-like) using PARAFAC analysis, it is estimated that the decrease in fluorescence was highest (28–30 %) in the longer wavelength regions (Ex/Em = 335–350/430–450 nm) than at peak M (17 % at 310/450 nm) and peak A (20 % at 250/440 nm) in downstream river (Mostofa et al. 2010). This suggests that the fluorophore at the longer Ex/Em wavelength in fulvic acid is susceptible to undergo rapid photoinduced degradation in aqueous media. Thus, photodegradation would be useful in the removal of major anthropogenic fluorescent organic contaminants, particularly the fluorophores at the longer Ex/Em wavelengths in rivers (Mostofa et al. 2010). (iv) Photo-induced losses of fulvic acid-like fluorescence intensity are gradually reduced in the transition from river to lake, estuary and sea water (Yamashita and Tanoue 2003a; Mostofa et al. 2007a, 2005b; Vodacek et al. 1997; Cory et al. 2007). The cause might be linked to the prior losses of fluorescence intensity in stagnant lake or seawaters by photodegradation. In contrast, photodegradation in rivers is less effective due to continuous transport of water. Photodegradation changes the excitation–emission spectra by introducing a shift to shorter wavelengths. This might constitute evidence of the alteration of existing fluorophores or of the appearance of new fluorescent organic substances (Mostofa et al. 2009a). Examples of fluorescent substances arising from FDOM photodegradation could be salicylic acid (Ex/Em = 314/410 nm), 3-hydroxybenzoic acid (Ex/Em = 314/423 nm), and 3-hydroxycinnamic acid (Ex/Em = 310/407 nm). These molecules are characterized by fluorescence at relatively short wavelengths (Mostofa et al. 2009a).

Photodegradation of Fulvic Acid and Humic Acid

The fluorescence of standard or extracted fulvic and humic acids is typically decreased by photoinduced degradation under sunlight. The fluorescence of SRFA dissolved in Milli-Q water is photolytically decreased under simulated sunlight (by 42 % in 1 mg L^{-1} SRFA for 10 h, 23 % for 3 mg L^{-1} and 3 h, 20 % for 5 mg L^{-1} and 3 h, and by 22 % with 1 mg L^{-1} SRFA + 50 μM NO_2^- for 3 h) (Table 4). Extracted fulvic acid from Göta River shows a decrease in fluorescence (32 %) in alkaline samples (6.3 mg L^{-1} fulvic acid in 0.5 M NaOH solution) after 13 days UV-B irradiation (Table 4). A 6-h summer sunlight exposure of fulvic and humic acids extracted from lake, pond and marsh showed that the decrease of humic acid fluorescence was relatively higher (64–100 %) compared to fulvic acid (48–83 %) (Table 4). It is reported that the fluorescence of humic acid is highly depleted in acidic samples, and undergoes a more pronounced decrease compared to fulvic acid even at higher pH (Wu et al. 2005). Correspondingly, photoirradiation can decompose 35 % of extracted Nordic Reference humic acid (NoHA) and 24 % of extracted Nordic Reference fulvic acid (NoFA) from humus-rich pond water in photoexperiments conducted using a solar simulator (Corin et al. 1996). The reported results suggest that the photoinduced degradation of humic acid is pH and concentration dependent, but the reason behind this phenomenon is still unknown. However, the relatively high photolability of humic acid can be in agreement with the high level of aromaticity (30–51 %), in particular when compared to fulvic acid (14–21 %) (Malcolm 1985; Gron et al. 1996; Wu et al. 2005).

The rate constants for the decrease in fluorescence and for DOC loss are significantly higher for humic than for fulvic acid, as obtained by photoexperiments carried out at different pH levels on extracted humic and fulvic acid from upstreams (Wu et al. 2005). Thus, photodegradation of the humic acid fraction is significantly higher than the fulvic acid fraction and is more sensitive to pH. Interestingly, the higher photolability of humic compared to fulvic acid correlates well with the higher production rate of H_2O_2 upon irradiation of Suwannee River humic Acid (179×10^{-2} M s^{-1}) than for Suwannee River fulvic Acid (69×10^{-2} M s^{-1}) (Mostofa and Sakugawa 2009). This might imply that the production of H_2O_2 is a primary step for the photoinduced degradation of DOM in aqueous solution. Humic acid could thus be the primary target of DOM photodegradation in natural waters (Wu et al. 2005). In contrast, fulvic acid is photolytically more stable than humic acid in aqueous media and may play a vital role in biogeochemical processes due to its longer lifetime in natural waters.

It can be noted that the fluorescence intensity of humic acid is increased by irradiation in some particular cases. Thus, increases have been observed of ca. 70 % for Suwannee River Humic Acid (SRHA) (1 mg L^{-1}, 10 h), 5 % for SRHA (5 mg L^{-1}, 3 h), and 4 % in alkaline samples (6.5 mg L^{-1} Göta River humic acid in 0.5 M NaOH) (Table 4). The reason behind such a phenomenon may be the generation of aromatic photoproducts upon irradiation of humic acid (Corin et al. 1996). Some of these photoproducts may show fluorescence at peak C-region, for

example 3-hydroxybenzoic acid at Ex/Em = 314/423 nm, 3-hydroxycinnamic acid at Ex/Em = 310/407 nm, and methyl salicylate at Ex/Em = 366/448 nm (Mostofa et al. 2010). This may produce an increase of humic acid fluorescence. Weak light intensity may prolong the lifetime of humic acid and its aromatic photoproducts, which may result in a fluorescence increase. On the other hand, intense and prolonged irradiation may decompose humic acid and its photoproducts rapidly (Corin et al. 1996), which causes a decrease in fluorescence.

Photodegradation of Aromatic Amino Acids and Protein

Photodegradation experiments have shown a decrease in tryptophan-like fluorescence (peak T) of 5–59 % in river waters, 7–88 % in lake waters, 37–45 % in estuarine waters, and 54 ± 6 % in sea waters (Table 4) (Stedmon et al. 2007a; Mostofa et al. 2010, 2011; Winter et al. 2007; Moran et al. 2000). Similarly, the decrease in tyrosine-like fluorescence intensity upon irradiation was 19–100 % in lakes, 26 ± 9 % in sea waters and 4–36 % for standard tyrosine dissolved in Milli-Q water. A photolytically-induced increase of tyrosine like fluorescence (1–68 %) was also observed in some lake waters (Table 4) (Stedmon et al. 2007a; Winter et al. 2007). A decrease of fluorescence upon irradiation has also been observed as 63 % for standard tryptophan at 1 mg L^{-1} in milli-Q water and 10 h, 23 % for 3 mg L^{-1} and 3 h, and 20 % for 5 mg L^{-1} and 3 h (Table 4) (Mostofa et al. 2011). Some amino acids including tryptophan are degradable by photoinduced processes due to their high chemical reactivity (Yamashita and Tanoue 2003a; Rosenstock et al. 2005). The decrease in tryptophan-like fluorescence intensity was lower (59 %) compared than that of fulvic acid (80 %) in rivers (Mostofa et al. 2007b). Therefore, protein- or tryptophan-like components are photolytically degradable but they are less susceptible to photoinduced degradation compared to fulvic acid in natural waters.

Photodegradation of FWAs and Other Substances in Aqueous Media

The FWAs (DAS1 and DSBP) and household detergents are present in significant amount in some polluted rivers, lakes, coastal sea waters and sediments (Mostofa et al. 2005a, 2010, 2011; Poiger et al. 1999, 1996; Komaki and Yabe 1982; Managaki and Takada 2005; Kramer et al. 1996; Stoll et al. 1998; Stoll and Giger 1998; Baker 2002; Yamaji et al. 2010). The observed fluorescence intensity losses of FWAs or detergent components after up to 10 days irradiation have been 12–81 % in rivers, 34 % in drain samples, and 60–94 % in Milli-Q water (Table 4) (Mostofa et al. 2005a, 2010, 2011). It has been shown that losses in fluorescence intensity of peak W are 76–81 % during 6–10 days irradiation in river water (Table 4). In the case of distyryl biphenyl (DSBP), the decrease in fluorescence intensity is 94 % for 1 mg L^{-1} and 10 h, 73 % for 3 mg L^{-1} and 3 h, 60 % for 5 mg L^{-1} and 3 h; and 31 %

in river water mixed with DSBP during 12 h summer irradiation (Poiger et al. 1999; Mostofa et al. 2011). For diaminostilbene (DAS1) it has been observed a 93 % decrease at 1 mg L^{-1} initial concentration and 10 h irradiation under a solar simulator; and a 12 % decrease in river water mixed with DSBP during 12 h summer irradiation (Table 4) (Poiger et al. 1999; Mostofa et al. 2011). Photoinduced degradation can also decrease 53 % of DAS1 and 81 % of DSBP contents in lake surface waters (Stoll et al. 1998). Irradiation experiments for the standard DSBP and DAS1 using a solar simulator indicate that the fluorescence intensities of FWAs are rapidly decreased, by 40 % for DSBP and 45 % for DAS1 after of 30 min irradiation, but with no shift of their Ex/Em wavelengths (Mostofa et al. 2005a). It is estimated in field observations that the observed removal of FWAs during transport (12 h residence time) is 31 and 12 % for DSBP and DAS 1, respectively, corresponding to half-lives of 0.9 and 2.7 days, respectively, under cloudless summer skies (Poiger et al. 1999). In another study, a mass balance calculation and DSBP/DAS1 ratio shows that ~95 % of DSBP and ~55 % of DAS1 supplied in sewage were decomposed photolytically by natural sunlight in inflowing rivers and in lake, while sedimentation to the lake bottom was insignificant for DSBP and reached ~35 % for DAS1 (Yamaji et al. 2010). More intense photodegradation of FWAs, especially the more photodegradable DSBP, has been observed in Lake Biwa, Japan, than in Lake Greifensee, Switzerland, possibly because of the longer residence time of water in the larger Lake Biwa (Yamaji et al. 2010). A FWAs-salinity diagram in the Tamagawa Estuary shows fairly conservative behavior of the FWAs with ~20 % and ~10 % removal of DSBP and DAS1, respectively, which is thought to be caused by photodegradation (Hayashi et al. 2002). The DSBP/DAS1 ratio also shows a decreasing trend from sewage effluents to rivers and to the Tokyo Bay, indicating selective photodegradation of DSBP (Hayashi et al. 2002). These results suggest that DSBP is more susceptible to photoinduced degradation than DAS1 in natural waters.

For commercial household detergent, the decrease in fluorescence intensity of detergent component (C-like, component 1) is 88 % at peak C-region and 70 % at peak A-region in Milli-Q water during the 3 h of direct sunlight irradiation, under noon summer clear sky conditions (Table 4) (Mostofa et al. 2010). The detergent component (T_{UV}-like) does not decompose photolytically, rather an increase in fluorescence is detected such as 4 % in sewerage drainage samples and 9 % in commercial detergents samples dissolved in Milli-Q water (Table 4) (Mostofa et al. 2010). In sewerage-impacted rivers, the fluorescence intensity of the detergent-like component (peak W) was significantly lower (28 %) at noon time (12:00–13:00 p.m.) than before sunrise (Mostofa et al. 2005a). This indicates that detergent-like compounds may have been decomposed photolytically by natural sunlight during the water transport (Mostofa et al. 2005a). In summary, FWAs and household detergents are highly susceptible to photoinduced degradation upon irradiation in the laboratory as well as in field observations (Table 4) (Mostofa et al. 2005a; Baker 2002).

Mechanism for Photodegradation of Fluorophores in FDOM in Aqueous Media

Sequential photodegradation is observed for FDOM fluorophores or functional groups in FDOM macromolecules, particularly fulvic and humic acids. The sequential degradation of fluorophores is generally caused by the presence of diverse functional groups in their molecular structure (Mostofa et al. 2009a; Senesi 1990a; Leenheer and Croué 2003; Malcolm 1985; Corin et al. 1996; Peña-Méndez et al. 2005; Seitzinger et al. 2005; Zhang et al. 2005). This phenomenon can be understood from the sequential decrease in the fluorescence intensity of fluvic acid-like components (peak C- and A-regions) with irradiation time (Mostofa et al. 2005a, 2007a; Moran et al. 2000). The sequential degradation of various functional groups bound to fulvic and humic acids has also been observed in natural waters (Shriner et al. 1943; Amador et al. 1989; Allard et al. 1994; Xie et al. 2004; Li and Crittenden 2009; Minakata et al. 2009).

Absorption of photon or light by a fluorophore (or functional group) is generally caused by its lowest energy excitation, then by the next lowest energy excitation caused by another fluorophore in the molecule and so on (Mostofa et al. 2009a; Senesi 1990a). Fluorophore excitation is the first step for the generation of H_2O_2 in aqueous media according to (Eq. 3.1). Photoirradiation converts H_2O_2 into $HO^{\bullet}$ (Eq. 3.2), photolytically or by Fenton and photo-Fenton reactions (see chapter "Photoinduced Generation of Hydroxyl Radical in Natural Waters"). The $HO^{\bullet}$ radical can then react with the initial excited fluorophore and decompose it (Eq. 3.3). Therefore, a scheme for the photoinduced degradation of flurophores in macromolecules can be depicted as below (Eqs. 3.1–3.4; see chapters "Photoinduced and Microbial Generation of Hydrogen Peroxide and Organic Peroxides in Natural Waters", "Photoinduced Generation of Hydroxyl Radical in Natural Waters" and "Photoinduced and Microbial Degradation of Dissolved Organic Matter in Natural Waters"):

$$\mathrm{FDOM} + \mathrm{O_2} + \mathrm{HO_2} + \mathrm{H^+} \xrightarrow{h\nu} \mathrm{H_2O_2} + \mathrm{FDOM^{\bullet +}} + \mathrm{O_2} + \mathrm{OH^-} \tag{3.1}$$

$$\mathrm{H_2O_2} \xrightarrow{h\nu} 2\mathrm{HO^{\bullet}} \tag{3.2}$$

$$\mathrm{FDOM^{\bullet +}} + \mathrm{HO^{\bullet}} \xrightarrow{h\nu} \left[\mathrm{FDOM^{\bullet +}HO^{\bullet}}\right]^{*} \tag{3.3}$$

$$\left[\mathrm{FDOM^{\bullet +}HO^{\bullet}}\right]^{*} \xrightarrow{h\nu} \mathrm{LMWDOM} + \mathrm{DIC} + \mathrm{CO_2} + \text{other end products} \tag{3.4}$$

One of the pathways that can lead to H_2O_2 formation is the production of $O_2^{\bullet -}$ from O_2 upon release of electrons from irradiated FDOM fluorophores or chromophores (Eq. 3.1, see chapter "Photoinduced and Microbial Generation of Hydrogen Peroxide and Organic Peroxides in Natural Waters"). Reaction (3.4) produces low molecular weight DOM (LMWDOM), dissolved inorganic carbon (DIC), CO_2, and other end products (see chapter "Photoinduced and Microbial Degradation of Dissolved Organic Matter in Natural Waters").

Radiation absorption by the next lowest energy fluorophore would then produce further reactive species and cause sequential degradation of the fluorophores, and so on till the entire degradation of the parent molecule. Photoinduced degradation of organic substances can also occur by other processes. For instance, phosgene ($COCl_2$) is highly photosensitive and highly reactive (Shriner et al. 1943) as explained previously. The sequential photodegradation mechanism is applicable to various FDOM such as fulvic acid and humic acid of plant origin, autochthonous fulvic acid of algal origin, proteins and aromatic amino acids.

Controlling Factors for Photodegradation of FDOM in Natural Waters

Photodegradation of FDOM depends on several key factors that are similar to the photodegradation of DOM (Mostofa et al. 2011). The photoinduced degradation of FDOM depends on the several factors in the aquatic environments: (i) The nature or the quality of the organic components of DOM; (ii) The concentration or the quantity of the organic DOM components; (iii) The pH of the sample solution that may affect the photo-induced generation of $HO^{\bullet}$, a strong oxidizing agent that is involved in the photodegradation of DOM (Bertilsson and Tranvik 2000; Wu et al. 2005; Kwan and Voelker 2002). pH also influences the photoactivity of Fe species that take part to DOM photomineralization (Vione et al. 2009); (iv) The presence and quantity of Fe in the water samples that may provide $HO^{\bullet}$ through photo-Fenton reaction ($H_2O_2 + Fe^{2+} \rightarrow Fe^{3+} + HO^{\bullet} + OH^{-}$) or induce DOM transformation though irradiated Fe-DOM complexes (Wu et al. 2005; Miles and Brezonik 1981; Zepp et al. 1992; Southworth and Voelker 2003); *(v)* The concentration of O_2 that can assist in the production of $HO^{\bullet}$ or H_2O_2 (Miles and Brezonik 1981); (vi) The occurrence of NO_2^{-} and NO_3^{-}, further sources of $HO^{\bullet}$ that may enhance the photoinduced decrease of DOM fluorescence (Table 4) (Zinder 1993). For example, irradiation experiments using a solar simulator have shown that addition of NO_2^{-} to standard SRFA can slightly enhance the decrease of fluorescence, which reaches approximately 22 % with 1 mg L^{-1} SRFA + 50 μM NO_2^{-} upon 3 h irradiation compared to 19 % with 1 mg L^{-1} SRFA after 3 h (Table 4). (vii) The light intensity (UV-B, UV-A and PAR: photosynthetically active radiation) is a key factor in the photoinduced reactions and controls the production of reactive transients that correspondingly enhance the photodegradation processes (Garcia et al. 2005; Bertilsson and Tranvik 2000; Granéli et al. 1998; Qian et al. 2001; Randall et al. 2005). Interestingly, the decrease of fluorescence upon addition of NO_2^{-} that is a major $HO^{\bullet}$ source (Mack and Bolton 1999) was relatively limited (3 %). This finding would be compatible with SRFA photooxidation primarily occurring because of the photo-induced generation of $HO^{\bullet}$ produced photolytically by SRFA itself, or through other processes. It can be noted that the production rate of H_2O_2 from SRFA is 69×10^{-12} M s^{-1} (Mostofa and Sakugawa 2009) and a relatively low level of H_2O_2 can accelerate the photoinduced degradation of humic acid in aqueous media (Wang et al. 2001). This hypothesis is in agreement with the assumption that part of the production of $HO^{\bullet}$ by DOM under irradiation derives from H_2O_2 photogeneration. It is also in agreement

with the results of field observations that the DOM fluorescence decreases with an increase of H_2O_2 concentration over the course of the day in marine surface waters (Obernosterer et al. 2001). An alternative possibility is that also other species different from $HO^{\bullet}$ may induce the transformation of DOM. Interestingly, the generation rate of $HO^{\bullet}$ was largely unable to account for the photoinduced mineralization of acidified lake-water or filtered groundwater DOM (Vione et al. 2009).

In addition, photodegradation of FDOM depends on several key factors such as sunlight incident doses, water chemistry, DOM contents, mixing regime and so on (White et al. 2003; Ma and Green 2004; Mostofa et al. 2011; Reche et al. 1999). Moreover, the key factors that affect the FDOM photobleaching are: (1) Solar radiation, (2) Water temperature, (3) Effects of total dissolved Fe and photo-Fenton reaction, (4) Occurrence and quantity of NO_2^- and NO_3^- ions, (5) Molecular nature of DOM, (6) pH and alkalinity of the waters, (7) Dissolved oxygen (O_2), (8) Depth of the water, (9) Physical mixing in the surface mixing zone, (10) Increasing UV-radiation during ozone hole event, and (11) Global warming. These factors are similar to those affecting the photoinduced degradation of DOM (see the chapter Photoinduced and Microbial Degradation of Dissolved Organic Matter in Natural Waters).

3.3 Microbial Degradation of FDOM in Natural Waters

Microbial degradation by autotrophs (plants, algae and bacteria) and heterotrophs (animals, fungi and bacteria) induces changes in FDOM in the deeper layers of natural waters (rivers, lakes, and oceans), pore waters and soil waters. The effects have been highlighted in field observations and experimentally under dark incubation. Microbial processes thus alter the fluorescence properties of various FDOM such as fulvic acid, humic acid, aromatic amino acids and FWAs (DAS1 and DSBP) (Fig. 5) (Mostofa et al. 2010, 2007a, 2005b, 2007b, 2011; Ma and Green 2004; Moran et al. 2000).

Fulvic Acid and Humic Acid of Terrestrial Plant Material Origin

The microbial degradation can alter the fulvic acid-like fluorescence intensities at peaks A-, C- and M-regions and their excitation–emission (Ex/Em) peak positions in natural waters (Ma and Green 2004; Moran et al. 2000; Mostofa et al. 2007b, 2011; Yamashita and Tanoue 2008). Allochthonous fulvic acid (C-like) fluorescence is increased by approximately 3–81 % in rivers due to microbial degradation, for an incubation period ranging from hours to 13 days (Table 4). Allochthonous fulvic acid (M-like) fluorescence is entirely decomposed microbially after 12 days of dark incubation at room temperature (Table 4). In lakes, the fulvic acid-like fluorescence is increased by up to 31 % in molecular fractions <0.1 μm and 102 % in <5 kDa fractions in surface waters. In deeper DOM fractions the corresponding increases are 0 and 20 % under dark incubation for 12 days (Table 4) (Mostofa et al. 2011). In contrast, fulvic acid-like

fluorescence is decreased microbially (Table 4) (Garcia et al. 2005). In estuarine water, the decrease in fulvic acid-like fluorescence is relatively high: 11 % at peak A, 1–12 % at peak C, and 1–12 % at peak M in replicate samples during a 51 days incubation period (Table 4) (Moran et al. 2000). In Mediterranean Sea samples, DOM fluorescence is either increased (0.4–8 %) after 8 h dark incubation in lagoon water, or decreased (2 %) in coastal water (Table 4) (Abboudi et al. 2008). Upon microbial processing, the fluorescence of standard SRFA does not change significantly after 10 h incubation (Table 4). A fluorescence increase after a 9-day incubation period has been detected in fulvic (8 %) and humic acid (6 %) extracted from Göta River (Table 4). These results may lead to the hypothesis that there are several characteristic chemical and optical features of fulvic acid and FWAs in natural waters, which can be classified as: (i) Fluorescent compounds, particularly fulvic and humic acids (C-like) in stream, are typically recalcitrant to microbial degradation. Microbes are not capable of decomposing the fluorophores in the longer wavelength region, particularly the peak C-region in allochthonous fulvic and humic acids. Fluorophores of humic substances at peak C-region are mostly composed of aromatic molecules associated with functional groups having extensive π-electron systems, or with specific repeating functional groups in the carbon matrix of peak C-region, which are highly recalcitrant to microbial degradation (Mostofa et al. 2009a, 2010; Malcolm 1985; Geller 1986; Münster 1991). (ii) Allochthonous fulvic acid (M-like) is highly labile to biological degradation, thus it has opposite behavior than allochthonous fulvic acid (C-like). (iii) Under dark incubation, the increase of fulvic acid-like fluorescence is typically higher in surface lake water compared to the deeper layers. This finding allows the hypothesis that surface photo-bleached fulvic acid is highly labile to microbial changes, which can lead to a significant increase in fulvic acid-like fluorescence. (iv) Finally, the decrease in fulvic acid-like fluorescence is insignificant (0–5 %). This fluorescence may presumably result from the decomposition of other fluorescent components present in the same peak position.

Autochthonous Fulvic Acid (C-like) of Algal Origin

The fluorescence intensities of peaks A and C of autochthonous fulvic acid (C-like), produced during the microbial assimilation of algal biomass (Algae + river waters) during long-term dark incubation (180 days), were maximal at the 4th day of incubation. The intensities then became lowest at the 20th day, gradually increased until the 70th day and increased again after the 80th day till the 180th (Fig. 6). This result suggests that the microbial processes can alter rapidly the fluorophores bound at peaks A- and C-regions of autochthonous fulvic acid (C-like) during the initial 20 days of incubation. It follows a slower microbial alteration of fluorophores from 20 to 70 days, and an even slower alteration from 80 to 180 days. From 20 days onward, fluorescence intensities of both peaks gradually increase. This result can be interpreted by the ratios of fluorescence intensities of peak A divided by peak C of autochthonous fulvic acid (C-like). Such a

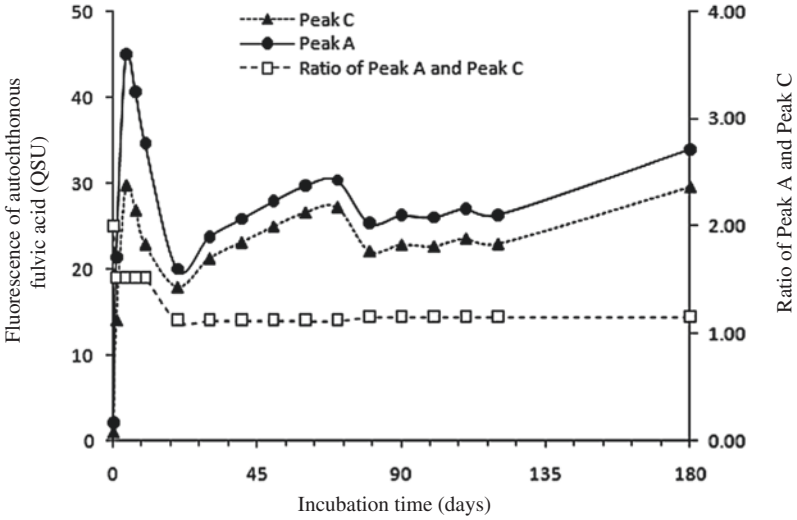

Fig. 6 The changes in the fluorescence intensities of peaks A and C and their fluorescence intensities ratios of autochthonous fulvic acid (C-like) originated under microbial assimilations of lake algal biomass during the long-term dark incubation period (1–180 days). The fluorescence intensities of both peaks A and C are the average of duplicate samples. *Data source* Mostofa KMG et al. (unpublished data)

ratio becomes high (peak A/peak C = 1.53) from 1 to 10 days, then it decreases to 0.98 from 20 to 70 days, and decreases again to 0.87 between 80 and 180 days of incubation (Table 3; Fig. 6). It is in agreement with earlier results concerning the production of CDOM in resuspension of particulate matter in an isotonic solution (0.5 ‰ salinity, no N and P). The measured spectral slope $S_{300–500}$ was highest at the 6th day, reached the lowest level at the 9th day, increased during days 12–18 and after 21 days it remained approximately constant (Zhang et al. 2009a). Time-scale variation in the release of new DOM depends on the several key factors such as contents of nutrients, occurrence of microorganisms, salinity, and nature of particulate materials. Microbial degradation can also increase the spectral slope S_{350}–S_{400} (nm^{-1}), which is an index of high molecular weight substances and can decrease S_{275}–S_{295} (nm^{-1}), which is related to low molecular weight DOM (Helms et al. 2008).

The reported findings allow three characteristic phenomena to be hypothesized for the microbial degradation of autochthonous fulvic acid (C-like) of algal origin. Firstly, autochthonous fulvic acid (C-like) is primarily released in the initial phase (4–6 days), and afterward the fluorophores bound at peaks A- and C-regions may be rapidly decomposed by microbial processes (4–20 days). The result is the decrease either in the fluorescence intensities of both peaks A- and C-regions of autochthonous fulvic acid (C-like) or in the overall absorbance properties of CDOM. Secondly, the fluorophores connected to the peak A-region of autochthonous fulvic acid (C-like) may undergo faster microbial decomposition compared to those

at peak C-region during the second phase (10–20 days). The result is a decrease in both the fluorescence intensities and the ratios of fluorescence intensities of peak A- and peak C-regions. Thirdly, microbial processes may slowly alter the fluorophores bound at both peak A- and C-regions during the third phase (20–70 days), and much more slowly during the fourth phase (80–180 days). The gradual increase in the fluorescence intensities of both peaks A and C suggest that a gradual conversion could be operational of autochthonous fulvic acid (C-like) into compounds highly recalcitrant or refractory to microbial degradation. These modifications are in agreement with earlier studies, which suggest that microbial processes induce rapid decomposition of the 'labile' fraction such as monosaccharides (e.g. glucose), amino acids and fatty acids, which are the monometric molecules that make up carbohydrates, proteins and lipids. In contrast, the 'refractory' fraction is decomposed more slowly (Zhang et al. 2009a; Hama 1991; Hama et al. 2004; Wakeham and Lee 1993; Wakeham et al. 1997; Harvey and Macko 1997; Hanamachi et al. 2008).

Microbial Degradation of FWAs (DAS1 and DSBP)

FWAs-like fluorescence (peak W) is often increased, by 6–14 % in rivers, by 8 % in drain samples, by 14 % for commercial detergents in Milli-Q water, and by 21 % in river waters plus commercial detergents after 6–10 days dark incubation (Table 4) (Mostofa et al. 2011). In rivers, commercial detergents or FWAs-like components typically undergo an increase in fluorescence after microbial degradation. Such a behavior is similar to that of fulvic acid under dark incubation in natural waters. Upon microbial processing, the fluorescence of standard DSBP does not change significantly upon 10 h of dark incubation (Table 4). Commercial detergent (component 2) that shows fluorescence peak at Ex/Em = 225–230/287–296 nm (peak T_{UV}-region), can be microbially decomposed by approximately 84 % in river plus detergent samples, 90 % in sewerage drain samples, and 15 % in commercial detergents samples dissolved in Milli-Q waters, within 10 days of dark incubation (Table 4) (Mostofa et al. 2010). These results suggest that highly polluted waters can rapidly decompose fluorophores at peak T_{UV}-region, i.e., partly the commercial detergents. In contrast, detergent components or FWAs (C-like) are unaltered microbially in natural waters. Microbes are primarily unable to decompose the FWAs (DSBP and DAS1) because of their complex molecular structure composed of a number of aromatic rings with several functional groups (Fig. 3y, a′) (Mostofa et al. 2010)).

Microbial Degradation of Aromatic Amino Acids

The fluorescence of tryptophan-like components under dark incubation is typically decreased, by approximately 13–24 % in unfiltered river waters, by 67 % in unfiltered sewerage drain samples, and by 11 % in filtered river samples (Table 4) (Mostofa et al. 2010). On the other hand, an increase in tryptophan-like fluorescence is often observed in filtered river waters (4–6 %), in lake water in the

molecular fractions <0.1 μm (68 % in surface water and 5 % in deep water) and <5 kDa (51 % in surface water and 28 % in deep water), and in estuaries (23–112 %) (Table 4). Upon microbial processing, the standard tryptophan fluorescence does not change significantly after 10 h incubation (Table 4). From these results it can be concluded that there are several characteristic phenomena concerning microbial degradation of tryptophan-like components in natural waters. First, tryptophan-like components are microbiologically labile but microbial degradation is a relatively slow process whilst photodegradation is rapid (Moran et al. 2000; Mostofa et al. 2007b; Baker and Inverarity 2004). Second, an increase in tryptophan-like fluorescence in filtered samples and a decrease in unfiltered samples can be rationalized considering that the filtration processes may deactivate or hinder the bacterial activity. Therefore, if the fluorescence intensity decrease in unfiltered samples may be due to the microbial degradation of tryptophan, the increase in filtered samples might be the result of the binding of tryptophan-like components to humic substances (Volk et al. 1997). Interestingly, an increase of fulvic acid-like FI is typically observed under dark incubation (Mostofa et al. 2007b) and in deep lake or seawaters (Hayase and Shinozuka 1995; Mostofa et al. 2005b). Finally, photo-bleached tryptophan-like DOM is resistant to microbial processes in natural waters. It has been shown that 70 % of the dissolved amino acids (DAA) and dissolved carbohydrates (DCHO) associated with the humic fraction are consumed by microbial degradation in natural waters (Rosenstock and Simon 2003).

3.3.1 Mechanism for Microbial Degradation of Fluorophores in FDOM

The microbial degradation of high molecular weight (HMW) DOM such as fulvic and humic acids (humic substances) of vascular plant origin and autochthonous fulvic acid of algal origin can increase the fluorescence intensities at both peak A- and C-regions. It is generally considered that the peak A-region is linked with aliphatic moieties and functional groups with less aromaticity, whilst the peak C-region is characterized by high aromaticity and functional groups with repeated structural units. Therefore, microbial degradation can effectively modify the aliphatic part of HMW DOM, which can enhance the fluorescence intensity mostly at peak A-region. The microbial increase of fluorescence intensity of HMW DOM is the result of changes in the molecular structure by several pathways.

Firstly, microbes can degrade aliphatic carbon (e.g. carbohydrates) or the functional groups of macromolecules such as fulvic and humic acids of vascular plant origin, as well as autochthonous fulvic acids of algal or phytoplankton origin, with subsequent release of a variety of end products such as CH_4, CO_2, DIC, PO_4^{3-}, NH_4^+, H_2O_2 and organic peroxides (see also chapters "Photoinduced and Microbial Generation of Hydrogen Peroxide and Organic Peroxides in Natural Waters", "Photoinduced and Microbial Degradation of Dissolved Organic Matter in Natural Waters" and "Impacts of Global Warming on Biogeochemical Cycles

in Natural Waters") (Ma and Green 2004; Mostofa and Sakugawa 2009; Palenik and Morel 1988; Conrad 1999; Lovley et al. 1996). Secondly, methanogenesis caused by microorganisms (methanogens and acetogens) is an important anaerobic process that can produce CH_4 and CO_2 by converting either acetate (and formate) or H_2/CO_2 in anaerobic environments (Conrad 1999; Lovley et al. 1996; Zinder 1993; Kotsyurbenko et al. 2001). It is presumably considered that the carbohydrate fraction or aliphatic carbon bound in macromolecules (allochthonous fulvic and humic acids) (Malcolm 1985; Peuravuori and Pihlaja 1999) may alter by the methanogenesis. This process can change the molecular structure either by modifying the existing functional groups in the macromolecules or by creating a new π-electron bonding system in the molecule.

3.3.2 Factors Affecting the Microbial Degradation of FDOM in Waters

An increase in fulvic acid-like or humic-like fluorescence at peak C- and A-regions as well as a decrease in fluorescence of aromatic amino acids either in deeper waters of lakes and ocean or in dark incubated water samples is an effect of the microbial degradation of organic matter and the related functional groups (Hayase and Shinozuka 1995; Coble 1996, 2007; Mostofa et al. 2010, 2007a, 2007b, 2011; Ma and Green 2004; Moran et al. 2000). Microbial degradation of DOM thus depends on several key factors that can be distinguished as: (1) Occurrence and nature of microbes in waters; (2) Sources of DOM and the quantity of their fermentation products; (3) Temperature; (4) pH; and (5) Sediment depths in pore waters.

3.4 Complex Formation of Trace Elements with FDOM

Trace elements can significantly affect the fluorescence properties of FDOM in natural waters (Mostofa et al. 2009a; Wu et al. 2004a, 2004b; Fu et al. 2007; Lu and Jaffé 2001). The trace elements or metals (M) can generally form complexes with the fluorophores or functional groups in fluorescent dissolved organic matter (FDOM), which are termed as M-DOM or M-FDOM. The relevant trace elements are transition metals such as Fe, V, Ce, Th, U, Mo, Cu, Mn, Ni, Co, Cr, Zn, Pb, Cd, Hg and UO_2(II), metal/metalloid such as Sb(III) and Al, as well as the alkaline earth elements (see also chapter "Complexation of Dissolved Organic Matter with Trace Metal Ions in Natural Waters") (Mostofa et al. 2009a, 2011; Wu et al. 2004a, 2004b, 2004c; Zhang et al. 2010; Yamashita and Jaffé 2008; Lu and Jaffé 2001). The relevant organic substances in M-DOM complexation are fulvic acid, humic acid, tryptophan, cysteine, selenoprotein P, extracellular polymeric substances (EPS), the Schiff base 2-[4-dimethylaminocinnamalamino]—benzoic acid, phenols and polyphenols (Mostofa et al. 2009a, 2011; Wu et al. 2004a, 2004b; Lu and Jaffé 2001). The fluorophores in FDOM or functional groups in DOM

are responsible for the formation of complex with trace elements. Therefore, the fluorescence intensity is either enhanced or quenched due to the complexation of FDOM fluorophores with trace elements (Wu et al. 2004a, 2004b; Fu et al. 2007; Lu and Jaffé 2001; Cabaniss and Shuman 1988; Cabaniss 1992).

The complexation of trace elements with fluorescent substances does not only affect the fluorescence intensity, but also the fluorescence peak position of the respective fluorophore (Wu et al. 2004c). Both excitation and emission wavelengths of the respective fluorophore peak in fulvic acid gradually increase with increasing reaction time (Wu et al. 2004c). It has been hypothesized that donation of electrons occurs from functional groups or fluorophores in DOM to empty *d*-orbitals in transition metals or in partially empty *p*-orbitals in metal/metalloid ($F: + M^{n+} \rightarrow F{:}M^{n+}$), thereby causing a strong π-electron bonding system between DOM and metals (Mostofa et al. 2009a, 2011). Donation of electrons from functional groups or fluorophores in DOM causes the *d*-orbitals to be either stabilized or destabilized in the complex compound, thereby causing the fluorescence to either decrease or increase, respectively, in the M-DOM complexes (Mostofa et al. 2009a, 2011).

3.5 Salinity

Salinity can significantly affect the fluorescence properties of FDOM in natural waters (Dorsch and Bidleman 1982; Hayase et al. 1987; Coble 1996; Determann et al. 1996; Parlanti et al. 2000; Nakajima 2006; Laane 1980; Willey and Atkinson 1982; Berger et al. 1984; Laane and Kramer 1990; de Souza Sierra et al. 1997; Boyd et al. 2010). The fluorescence intensity decreases linearly with salinity (Dorsch and Bidleman 1982; Hayase et al. 1987; Laane 1980; Willey and Atkinson 1982; Berger et al. 1984; Laane and Kramer 1990). It is shown that the fluorescence intensities of fulvic acid are quenched significantly with modest saline mixing (Boyd et al. 2010). Two types of result are detected during the mixing of freshwater and seawater (Determann et al. 1996; de Souza Sierra et al. 1997). First, a slow blue-shift of the fluorescence at peak C-region is detected for humic (fulvic)-like fluorophores during the initial mixing of freshwater to seawater between salinity 0 and 32 (de Souza Sierra et al. 1997). Secondly, for higher salinity (>32) a rapid wavelength shift is detected until the salinity reaches the maximum seawater value (de Souza Sierra et al. 1997).

On the other hand, salinity is presumably considered to shift the excitation–emission wavelengths of freshwater fulvic acid (peak C) from the shorter wavelengths found in freshwater rivers (325–340/450–475 nm) and lakes (310–350/410–464 nm) to longer wavelength regions (350–365/446–465 nm) in marine environments (Mostofa et al. 2009a, 2005a; Coble 1996; Parlanti et al. 2000; Yamashita and Tanoue 2003a; Nakajima 2006). The mixing of standard organic substances with Milli-Q and seawater shows that the excitation–emission wavelength maxima of SRFA, DAS1, tyrosine, benzoic acid, *p*-hydroxybenzoic acid,

p-hydroxybenzaldehyde and *p*-hydroxyacetophenone are significantly shifted from shorter to longer wavelength regions in seawater (Table 1) (Nakajima 2006). For example, the fluorescence peak C of SRFA dissolved in seawater is detected at Ex/Em = 345/452 nm, whilst the same peak in Milli-Q water is detected at Ex/Em = 325/442 nm. Peak A remains almost the same in both aqueous media (Table 1) (Nakajima 2006). The fluorescence peak C of autochthonous fulvic acid (C-like) of algal origin is detected at Ex/Em = 340/442–448 nm in Milli-Q water, and at Ex/Em = 340/454–455 nm in river waters during the photo- and microbial assimilations of algae (Table 2) (Mostofa KMG et al., unpublished data). In another study, the same fluorescence peak C of autochthonous fulvic acid (C-like) of algal origin has been detected at Ex/Em = 365/453 nm and 270/453 nm in an isotonic solution during the microbial assimilation of lake phytoplankton (0.5 ‰ salinity) (Table 2) (Zhang et al. 2009a). The autochthonous fulvic acid or marine humic-like of algal origin (peak M) at peak C-region has been found to shift from 290/400–410 nm in Milli-Q water to 300–310/400–410 nm in seawater (Table 2) (Parlanti et al. 2000)). Such a shift in excitation and emission wavelength maxima is presumably caused by the anions and cations present in sea water and is termed the red shift of fulvic acid-like fluorescence. The mechanism behind the red shift in sea water is attributed to complex formation between the functional groups (or flurophore at peak C- and A-regions) in fulvic acid and trace elements or ions. The complexation of trace elements with the functional groups (or fluorophores) bound at peak C or peak A in SRFA can significantly enhance the electron transfer from the ground state to the excited state by longer wavelength energy. This effect shifts the excitation–emission maxima of the peak C or peak A to longer wavelength regions. Such a shift in both excitation–emission wavelengths takes place during the initial complexation processes and increases with time (Wu et al. 2004a, 2004c). This is evidenced by the photoinduced formation of aqueous electrons (e_{aq}^-) from organic substances and by their high production in NaCl-mixed solutions compared to Milli-Q water (Gopinathan et al. 1972; Zepp et al. 1987; Fujiwara et al. 1993; Assel et al. 1998; Richard and Canonica 2005).

On the other hand, the mixing of some standard FDOM (e.g. DSBP, phenol, and tryptophan) with seawater shows that the fluorescence excitation–emission wavelength maxima (peak C-region and peak T-region) are shifted to shorter wavelengths compared to Milli-Q waters (Nakajima 2006). Such changes in fluorescence excitation–emission maxima are termed as blue-shift of the fluorophores in FDOM. In some cases the blue-shift of the fluorescence peaks could be caused by the loss of high molecular weight fluorescent components by physicochemical modifications such as flocculation, aggregation or precipitation during the initial mixing (de Souza Sierra et al. 1997; Sholkovitz 1976; Carlson and Mayer 1983; McCarthy et al. 1996; Van Heemst et al. 2000; Benner and Opsahl 2001). In the case of smaller molecules, the blue-shift phenomenon is presumably caused by complex formation between anions or cations and the fluorophores (or functional groups) of few fluorescent organic components. This may increase the excitation energy of the fluorophores bound to peak C or peak A-region and change the excitation–emission wavelengths from longer to shorter wavelength regions.

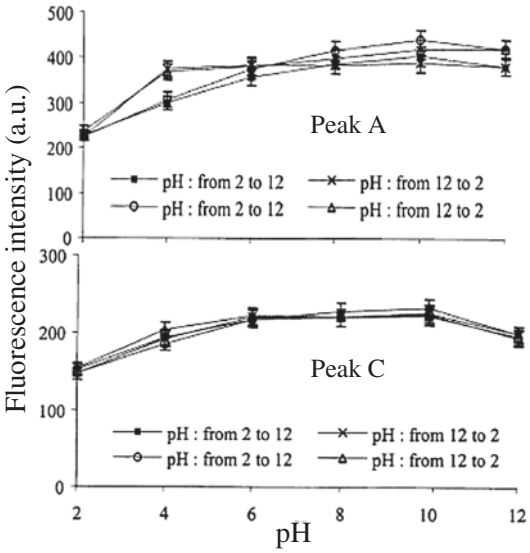

Fig. 7 Changes in the fluorescence intensities of the fluorophores regarding peak A- (**a**) and C-(**b**) regions with solution pH for bulk sample collected from Rio Solimoes in Amazon basin rivers. The *error bar* indicates their standard deviation. *Data source* Patel-Sorrentino et al. (2002)

3.6 pH

The fluorescence properties of various FDOM components are significantly changed by pH variations (2–12) in aqueous solution (Figs. 6, 7, 8) (Gosh and Schnitzer 1980; Henderson et al. 2009; Zhang et al. 2010; Laane 1982; Vodacek and Philpot 1987; Pullin and Cabaniss 1995; Mobed et al. 1996; Patel-Sorrentino et al. 2002; Baker et al. 2007; Spencer et al. 2007). The fluorescence intensities at peak C- and peak A-regions for fulvic acid in Amazon basin rivers are significantly increased up to pH 11, and then decrease in the pH interval 11–12 (Fig. 7) (Patel-Sorrentino et al. 2002). The ratios of fluorescence intensities of peak A and peak C are independent of the molecular fractions of particulate (>0.22 μm), colloidal and dissolved (<5 kDa) organic matter in natural waters (Patel-Sorrentino et al. 2002). The fluorescence intensity of peak C (Ex/Em = 320–340/410–430 nm, presumably caused by fulvic acid) is increased markedly between pH 2 and 6 and then decreases at pH 8–10. In contrast, the fluorescence of peak C (Ex/Em = 370–390/460–480 nm, possibly caused by humic acid) is unaltered at higher pH (Henderson et al. 2009; Spencer et al. 2007).

In the case of bulk lake DOM, the autochthonous fulvic acids (C-like and M-like, respectively, of algal origin) identified by PARAFAC modeling are detected at pH 8–10, but the C-like component is absent at pH 2–4 (Fig. 8) (Mostofa KMG et al., unpublished data). The fluorescence intensities of the M-like component are significantly influenced by pH in the peak A-region: compared to the initial lake-water pH (7.5), a 79 % increase is observed at pH 2, it decreases to 59 % at pH 4 and then gradually increases to 88 % at pH 10. The

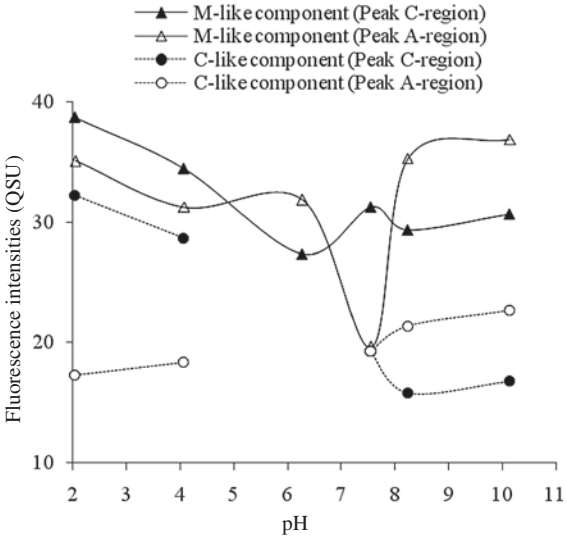

Fig. 8 Changes in the fluorescence intensities of algal-originated autochthonous fulvic acids (C-like and M-like component) identified in lake DOM (Lake Hongfeng, China) and its pH effect. The fluorescent components are identified using PARAFAC model on sample's EEM spectra. *Data source* Mostofa KMG et al. (unpublished data)

C-region is less affected by pH: there is a 24 % increase at pH 2, a decrease at pH 6 and a further increase up to pH 10. In contrast, the fluorescence intensity of the C-like component is significantly affected at the peak C-region: compared to the initial pH of 7.5 there is a 67 % increase at pH 2, then a gradual decrease up to the lowest intensity observed at pH 10. In the case of the peak A-region, one sees a 10 % decrease followed by a gradual increase up to a value that is 18 % higher compared to the initial one (Mostofa KMG et al., unpublished data). Therefore, the effect of pH on algal-originated autochthonous fulvic acids (M- and C-like) is quite different compared to allochthonous fulvic acids.

An increasing fluorescence intensity of humic substances has been detected as pH increases from 4 to 5.5, above which the increase is less important (Vodacek and Philpot 1987). In fulvic acid standards and wastewater treatment plant samples, when lowering the pH from 7 to 3 the decrease of the fluorescence intensity is 30–40 % at peaks C- and A-regions as well as over most of the EEM range, including the peak T- and T_{UV}-region (Westerhoff et al. 2001). For the fulvic acid-like component, the excitation–emission wavelengths for peak C undergo a red shift with increasing pH (Mostofa KMG et al., unpublished data; Westerhoff et al. 2001; Spencer et al. 2007). The pH effect on the complex formation of trace elements with DOM shows that, for DOM, the fluorescence index ($f_{450/500 \text{ at Ex370 nm}}$) has a decreasing trend with increasing pH. For DOM + Hg(II) complexation, one sees an increase of the fluorescence index till pH 8 followed by a decrease up to pH 10 (Fu et al. 2007). This suggests that the fluorescence properties of DOM might be affected by several factors such as pH, coexisting metal ions and other organic substances. In addition, the fluorescence properties of three fluorescent whitening agents (FWAs) are modified by pH in the 3–7 range, and the largest pH effect has been detected for the distyrylbiphenyl (DSBP) (Westerhoff et al. 2001).

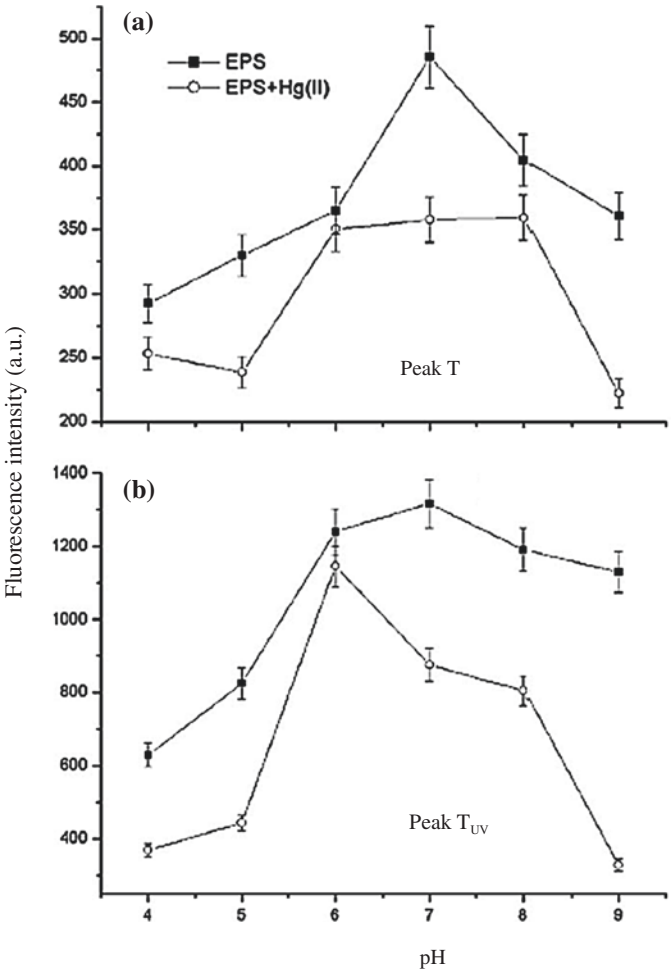

Fig. 9 Changes in the fluorescence intensities of peak T (**a**) and peak T_{UV} (**b**) for extracellular polymeric substances (EPS) with solution pH in the absence and presence of 3.0 mg L^{-1} Hg(II). The *error bar* indicates the standard deviation of three independent measurements. *Data source* Zhang et al. (2010)

In case of tryptophan-like substance or extracellular polymeric substances (EPS), the fluorescence intensities at peak T- and peak T_{UV}-regions are the highest at neutral pH (7.0) and often decrease when the solution pH increases (9.0) or decreases (4.0) (Fig. 9) (Zhang et al. 2010). The EPS is mostly composed of tryptophan-like substances that show a twice higher fluorescence intensity at peak T_{UV} than at peak T (Fig. 9). The pH effect on tryptophan-metal complexation has some characteristic features. The fluorescence intensity of peak T_{UV} is highest at pH 6 and peak T is similar at pH 6–8, differently from the trend of tryptophan fluorescence (Fig. 9) (Zhang et al. 2010). The fluorescence intensities of tryptophan

standards decrease by up to 15 % at pH <4.5, there is little effect at pH 5–8, and fluorescence is enhanced by up to 30 % at pH > 8. The peak B (tyrosine-like) is more sensitive to pH changes than the other peaks (Hudson et al. 2007; Reynolds 2003).

Therefore, the fluorescence properties of FDOM are significantly affected by pH, at a different extent for a variety of waters. The pH effect depends on several factors such as the sources and chemical nature of DOM, the occurrence of different functional groups, the presence of other organic substances and the contents of trace elements. Four possible mechanisms are proposed from earlier studies for the pH effect (Gosh and Schnitzer 1980; Henderson et al. 2009; Westerhoff et al. 2001; Laane 1982; Patel-Sorrentino et al. 2002; Myneni et al. 1999): (i) the alteration of the molecular orbitals of excitable electrons; (ii) physical changes in the molecular shape caused by changes in charge density (for instance, humic substances have a linear structure at high pH and coil when pH decreases); (iii) competition between H^+ and metal ions to form complexes with the fluorescent substances; and (iv) conformational changes in the molecules that can expose or hide their fluorescent parts. These mechanisms for the pH effect are not well understood. However, because changes in the fluorescence properties due to pH variation from pH 2 to 12 are reversible, it is excluded that irreversible structural changes may occur (Vodacek and Philpot 1987; Patel-Sorrentino et al. 2002).

Reversible pH-induced changes in the fluorescence properties may be caused by two phenomena. First, the H^+ or OH^- ions can alter the availability of electrons to be excited in a specific functional group or fluorophore in a fluorescent molecule, which can significantly modify the fluorescence intensity. Usually, the intensity is increased by an enhancement of electron excitation and decreased by an inhibition. For example, under neutral conditions the functional group ($–CH_2–(NH_3^+)–CH–COO^-$) bound to peak T-like flurophore in tryptophan can show a resonance configuration that favors electron excitation and results into the highest fluorescence intensity (Fig. 9). The availability of electrons to be excited, and the fluorescence intensity as a consequence, decreases both under acidic conditions ($–CH_2–(NH_2)–CH–COOH$) and under basic ones ($–CH_2–(NH_2)–CH–COO^-$). In addition, the availability of non-bonding electrons (:NH–) in another functional group of tryptophan ($C_8H_5(NH)–$) bound to the peak T_{UV}-like flurophore would be highest under neutral conditions, because there is no solvent effect on :NH–. In contrast, the non-bonding electrons of :NH– can react either with H^+ or with OH^-. In both cases the reaction can significantly reduce the availability of non-bonding electrons and, as a consequence, the fluorescence intensity in acidic and in basic solutions.

The main functional groups bound to fulvic and humic acids are –COOH, $–COOCH_3$, –OH, $–OCH_3$, –CH=O, –C=O, $–NH_2$, –NH–, –CH=CH–COOH, $–OCH_3$, S-, O- or N-containing aromatic compounds, although their parent molecular structures are unknown (Mostofa et al. 2009a; Senesi 1990a; Leenheer and Croué 2003; Malcolm 1985; Corin et al. 1996; Peña-Méndez et al. 2005; Seitzinger et al. 2005; Zhang et al. 2005). Such diverse functional groups have strong affinity for complex formation with metal ions. Therefore, the pH effect on fulvic and humic acids shows a different pattern compared to the tryptophan molecule.

3.7 Temperature

The fluorescence intensity of FDOM is inversely related to temperature because of an increased collisional quenching of fluorescence at higher temperatures (Wehry 1973; Vodacek and Philpot 1987). Within the range 10–45 °C, the fluorescence intensity can increase by approximately 1 % with a 1 °C decrease in temperature in the case of tryptophan-like, humic-like and fulvic-like substances, depending on colloid size and fluorophore (Henderson et al. 2009; Baker 2005; Vodacek and Philpot 1987; Elliott et al. 2006; Seredyńska-Sobecka et al. 2007). In contrast, the fluorescence intensities of tryptophan standards are almost unaffected by a temperature variation of ±8 °C (Reynolds 2003). The thermal quenching of fluorescence can be significant because of variation in water temperature between the summer and winter seasons as well as the high variation between boreal, tropical and Antarctic-Arctic regions. The effect of temperature on fluorescence quenching is linear and reversible, and it can be prevented in the laboratory by measuring the fluorescence of samples at a constant temperature (Vodacek and Philpot 1987). The thermal quenching effects can also be overcome by applying simple correction factors, but such factors may be different for fluorophores of different size fractions (Seredyńska-Sobecka et al. 2007). The mechanism of the temperature effect on fluorescence is that a rise in water temperature increases the likelihood that an excited electron will return to its ground state by radiationless decay, leading to reduced fluorescence intensity (Henderson et al. 2009). It is suggested that a variation of water temperature across a range of 20 °C or more between summer and winter would lead to a corresponding decrease by 20 % of the fluorescence intensity during summer (Henderson et al. 2009). Fluorescence changes caused by temperature may have no effect on the structure of the DOM. However, it has been shown that non-reversible changes may occur, possibly as a result of the application of a light-source that may cause photodegradation or thermal decomposition (Vodacek and Philpot 1987).

4 Kinetics of Photodegradation of the Fluorescence Intensity of Fulvic Acid and Tryptophan

Fulvic acid and tryptophan-like fluorescence intensity (FI) decreases monotonically with the number of absorbed UV photons or with integrated solar intensity, as a result of solar effects on water (Fig. 10) (Mostofa et al. 2007a). Photodegradation of fulvic acid often follows a two-step kinetics (Mostofa et al. 2007a; Ma and Green 2004), while tryptophan is photodegraded in a single step (Mostofa et al. 2007a). A decrease of FI can be best fit to a first-order kinetics as follows (Eq. 4.1):

$$\mathrm{Ln}\,(FI/FI_o) = -k_2 S \tag{4.1}$$

where k_2 is the reaction rate constant for photodegradation of FI in waters, FI is the fluorescence intensity obtained after illumination, FI_o is the initial fluorescence

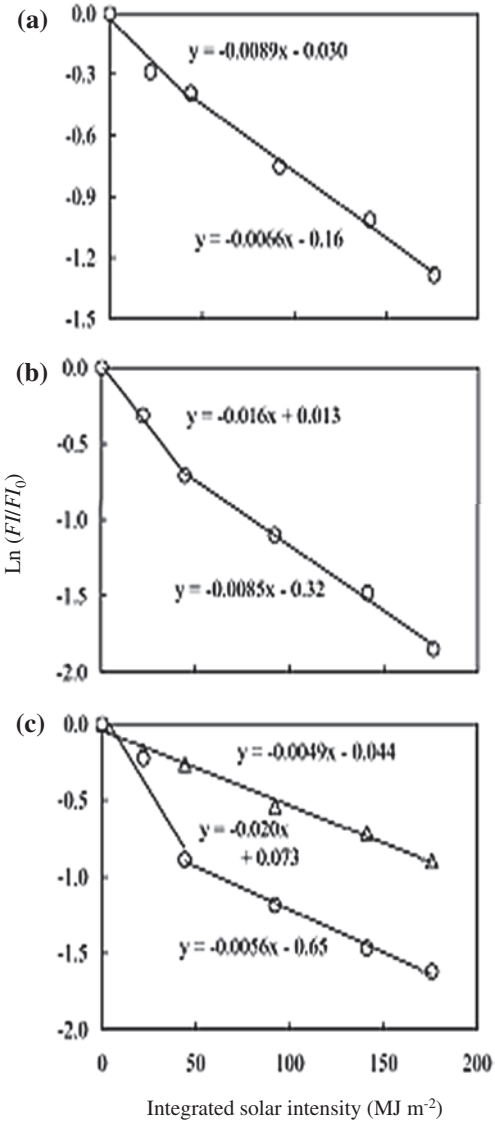

Fig. 10 Relationships between the Ln(FI/FI_0) and the integrated solar intensity and the integrated solar intensity for upstream waters (**a** and **b** Kago upstream and Nishi-Mataya upstream, respectively) and downstream waters (**c** Yasu River). *Open circle* indicates the changes in fulvic acid-like fluorescence intensity (FI) and *open triangle* in **c** shows the change in the protein-like FI under the irradiated condition. *Data source* Mostofa et al. (2007a)

intensity, and S is the integrated solar intensity (MJ m^{-2}). Photodegradation of FI can be clearly understood from the relationship between the S and Ln(FI/FI_o) (Mostofa et al. 2007a).

In river water, the reaction rate constant of fulvic acid-like FI is significantly higher in the first step of photodegradation (8.9–20 $\times$ 10^{-3} MJ^{-1} m^2) than in the second step (5.6–8.5 $\times$ 10^{-3} MJ^{-1} m^2) (Mostofa et al. 2007a). The photodegradation rate constant of protein-like FI often follows one-step kinetics with respect to integrated solar radiation. The photodegradation rate constant of tryptophan-like

FI (4.9×10^{-3} MJ^{-1} m^2) is quite similar to that observed in the second step of fulvic acid ($5.6–8.5 \times 10^{-3}$ MJ^{-1} m^2). From the results one can hypothesize several important photoinduced characteristics of fulvic acid and tryptophan components in waters. The fast first-step photodegradation of fulvic acid suggests the existence of highly sensitive fluorophores (and probably of a discrete class of them) that might undergo quick photoinduced decomposition (del Vecchio and Blough 2002). Schiff-base derivatives (–N=C–C=C–N–) are highly sensitive fluorophores that are commonly detected in DOM humic substances (fulvic and humic acids). They show a fluorescence peak at Ex/Em = 360–390/450–470 nm (Laane 1984) and could well be involved in the initial high losses of FI by fulvic acid in DOM in the aquatic environment. The almost linear reaction rate observed in the second step of fulvic acid photodegradation suggests the presence of homogeneous fluorophores which might be photolytically decomposed, although less quickly than the former ones. The linear photodegradation of tryptophan-like FI could be due to the presence of merely one type of fluorophore (–CH_2–$CH(NH_2)$–COOH), which would undergo gradual photoinduced decomposition. It is finally possible (unless it is a mere coincidence) that the similarity of the reaction rate constants of tryptophan-like FI and of fulvic acid in the second step are due to the presence of similar fluorophores (Mostofa et al. 2007a).

5 Ecological Significance of Photoinduced and Microbial Degradation of FDOM in Natural Waters

5.1 Ecological Significance of Photoinduced Degradation of FDOM

The decrease in fluorescence intensity of various FDOM samples reflects the sequential degradation and mineralization of the corresponding fluorophores or functional groups that are present in the chemical structure of FDOM (Corin et al. 1996; Mostofa et al. 2011; Amador et al. 1989; Bertilsson and Tranvik 1998). Photoinduced degradation modifies the fluorescence properties, and in particular the excitation–emission wavelengths (peaks A and C) of fulvic acid in the aquatic environments (Mostofa et al. 2007a, 2007b; Moran et al. 2000). From the photoinduced degradation of bog DOM and of International Humic Substances Society Nordic fulvic acid, it has been highlighted the losses of carbohydrates, secondary alcohols, protonated and substituted aromatic compounds, carboxyl, amide, ester, ketone and quinones, with no changes in aliphatic carbon (Osburn et al. 2001). Photoinduced changes in FDOM correspond to a decrease in the dissolved organic carbon (DOC) concentration (Brooks et al. 2007; Garcia et al. 2005; Moran et al. 2000; Osburn et al. 2009; Mostofa et al. 2007b; Vähätalo and Wetzel 2004) and to the generation of photoproducts. These processes can be summarized as: (i) Conversion of high-molecular weight into low-molecular weight DOM, which is generally observed in

experimental and field observations of natural waters (Corin et al. 1996; Yoshioka et al. 2007; Wu et al. 2005; Morris and Hargreaves 1997). (ii) Formation of microbiologically labile organic substances, which is commonly observed in the epilimnion of natural waters (Bertilsson and Tranvik 2000, 1998; Moran and Zepp 1997). (iii) Formation of CO, CO_2 and dissolved inorganic carbon (DIC, which is usually defined as the sum of dissolved CO_2, H_2CO_3, HCO_3^-, and CO_3^{2-}), which is generally observed upon photodegradation of DOM (Ma and Green 2004; Bertilsson and Tranvik 2000; Granéli et al. 1998; Valentine and Zepp 1993; Miller and Moran 1997). (iv) Formation of N-containing (NH_4^+ or NO_2^-) and P-containing inorganic compounds, which may typically be produced by degradation of dissolved organic nitrogen (DON) and dissolved organic phosphorus (DOP) in the epilimnion of natural waters (Bronk 2002; Zhang et al. 2004; Kim et al. 2006; Vähätalo and Järvinen 2007; Li et al. 2008). (v) Energy changes (±), such as supply (+) or consumption (−) of energy because of the photodegradation of DOM, with (+) representing the photoinduced formation of biologically labile compounds and (−) the abiotic mineralization of DOM (Wetzel 1992; Tranvik 1992; Hedges et al. 2000).

5.2 Ecological Significance of Microbial Degradation of FDOM

The major changes in FDOM components and organic matter by microbial degradation can be discriminated as (Mostofa et al. 2009b): (i) Microbial assimilation of organic matter (e.g. algae or phytoplankton) can produce autochthonous DOM or FDOM at different rates in lake waters, and it can simultaneously produce nutrients (PO_4^{3-}, NH_4^+), H_2O_2, organic peroxides, and DIC (Ma and Green 2004; Mostofa and Sakugawa 2009; Zhang et al. 2009a; Yamashita and Tanoue 2008; Palenik and Morel 1988; Weiss et al. 1991; Harvey et al. 1995; Lehmann et al. 2002). (ii) The fluorescence intensities of fulvic and humic acids are usually increased under dark incubation. It is suggested that these compounds are usually recalcitrant to microbial degradation, and microbial effects typically cause a change in the chemical compositions of aliphatic carbon, which may enhance the fluorescence intensity (Mostofa et al. 2009a; Ma and Green 2004; Moran et al. 2000). In contrast the fluorescence of tryptophan-like or protein-like components is often decreased under dark incubation, suggesting that tryptophan-like or protein-like components are labile to microbial degradation (Mostofa et al. 2010; Baker and Inverarity 2004). (iii) Changes in the FDOM components by microbial degradation under dark incubation induce the release of a variety of microbial products such as DIC, PO_4^{3-}, NH_4^+, H_2O_2, organic peroxides and so on (Ma and Green 2004; Moran et al. 2000; Mostofa and Sakugawa 2009; Palenik and Morel 1988). It is thus suggested that microbial processes can induce important changes in DOM composition in natural waters. (iv) Extracellular polymeric substances (EPSs), biologically produced by most bacteria, are composed of a mixture of polysaccharides, mucopolysaccharide and proteins. EPSs mostly show the Ex/

Em peak which is similar to those of protein-like or tryptophan-like fluorescence (Table 2) (Zhang et al. 2010). EPSs produced by anaerobic sludge under sulfate-reducing conditions are capable of biosorption of heavy metals to remove from the waste water treatment plant (Zhang et al. 2010).

6 FDOM Study: A Useful Indicator of DOM Dynamics in Natural Waters

The EEMS and its combination with PARAFAC modeling could be useful to identify the fluorescent organic substances, their sources and their physical, photoinduced and microbial alterations in water (Mostofa et al. 2009a; Hudson et al. 2007; Coble 2007). The main applications are as follows: (i) Identification of the allochthonous fulvic and humic acid of vascular plant origin and of their terrestrial sources (Mostofa et al. 2005a; Stedmon et al. 2003; Ohno and Bro 2006; Singh et al. 2010; Holbrook et al. 2006; Balcarczyk et al. 2009; Santín et al. 2009; Yamashita and Jaffé 2008); (ii) Identification of autochthonous fulvic acids (C-like and M-like) of algal origin and of their sources in water (Stedmon and Markager 2005a, 2005b; Stedmon et al. 2007a; Mostofa et al. 2005b; Zhang et al. 2009a; Kowalczuk et al. 2009; Balcarczyk et al. 2009; Santín et al. 2009; Murphy et al. 2008; Yamashita and Jaffé 2008; Cammack et al. 2004; Nieto-Cid et al. 2005; Boehme and Wells 2006); (iii) Identification of proteins, of aromatic amino acids (tryptophan-like, tyrosine-like and phenylalanine-like) and of their autochthonous sources in water (Yamashita and Tanoue 2003a; Stedmon and Markager 2005a, 2005b; Mostofa et al. 2010; Zhang et al. 2009a; Kowalczuk et al. 2009; Balcarczyk et al. 2009; Santín et al. 2009; Murphy et al. 2008; Yamashita and Jaffé 2008; Boehme and Wells 2006); (iv) Detection of fluorescent whitening agents, of components of detergents and of their anthropogenic sources (Mostofa et al. 2005a, 2010; Komaki and Yabe 1982; Westerhoff et al. 2001; Baker 2002, 2001); (v) Identification of various DOM components of terrestrial, algal and anthropogenic origin in sediment pore waters (Burdige et al. 2004; Fu et al. 2006; Li et al., Characteristics of sediment pore water dissolved organic matter in four Chinese lakes using EEM spectroscopy and PARAFAC modeling, unpublished data); (vi) Characterization of chemical properties of humic substances from soil and compost (Fuentes et al. 2006); (vii) Detection of photoinduced alterations in DOM and in its optical-chemical properties in water (Mostofa et al. 2005a, 2005b; Skoog et al. 1996; Moran et al. 2000; del Vecchio and Blough 2002; Zhang et al. 2009b; Wu et al. 2005), and (viii) Identification of changes in the redox state of fulvic acid (reduced and oxidized) caused by microbial processes in water (Fulton et al. 2004).

EEMS could be useful as a potential monitoring tool to control organic matter pollution (Mostofa et al. 2009a; Hudson et al. 2007; Henderson et al. 2009). It could be applied: (i) To analyze drinking water and sewerage-impacted wastewater (Mostofa et al. 2010; Chen et al. 2003; Baker et al. 2004; Holbrook et al. 2005; Hudson et al. 2008); (ii) To detect pollution levels of anthropogenic DOM

in freshwater (Mostofa et al. 2005a; Mostofa et al. 2010; Westerhoff et al. 2001; Baker 2002; Baker et al. 2004); (iii) To monitor the microbial decomposition of DOM (Hayase et al. 1988; Moran et al. 2000; Nieto-Cid et al. 2006); and (iv) to monitor the molecular weight distribution of DOM (Fu et al. 2006; Yoshioka et al. 2007; Wu et al. 2003a; Belzile and Guo 2006; Huguet et al. 2010) and changes in its composition at the watershed level (Mostofa et al. 2005b; Chen et al. 2003; Baker et al. 2004), or from coastal waters to open oceans (Yamashita and Tanoue 2003b).

Finally, the EEMS could be useful in technology development or fundamental research, in the field or at the level of molecular science (Mostofa et al. 2009a). The EEMS has already been applied: (i) In biomedicine or biotechnology to control fermentation in bioreactors (Li and Humphrey 1990) and to detect bacterial biofilms (Angell et al. 1993); (ii) In the detection of natural substances in water such as peroxides (hydrogen peroxide and organic peroxides), allochthonous fulvic and humic acids, proteins, amino acids and so on (Yamashita and Tanoue 2003a, 2003b; Nagao et al. 2003; Fujiwara et al. 1993; Wu et al. 2003a, 2003b); (iii) In the examination of the biological activity in cultures of marine bacteria, algae and coral extracts (Determann et al. 1998; Matthews et al. 1996; Cammack et al. 2004; Elliott et al. 2006); (iv) In the identification of the chemical properties at the molecular level, which arise by interaction between DOM and trace elements (Senesi 1990a, 1990b; Wu et al. 2004a, 2004b, 2007; Yamashita and Jaffé 2008), and (v) in the study of the interaction of DNA with fluorescent substances, e.g. in the framework of DNA–protein interaction (Taylor et al. 2000).

6.1 Are FDOM Studies Superior to CDOM?

The absorption spectra of chromophoric or colored dissolved organic matter (CDOM) usually do not show any specific identifiable peak for freshwater and marine CDOM. CDOM absorption and fluorescence (fulvic or humic acid-like) are significantly correlated with each other in a variety of waters (Ferrari et al. 1996a; del Vecchio and Blough 2004, 2002; Nieke et al. 1997; Vodacek et al. 1995; Ferrari et al. 1996b; Ferrari 2000; Green and Blough 1994; Seritti et al. 1998; Blough and del Vecchio 2002; Stabenau and Zika 2004). The absorbance of CDOM is useful for one to know the contents of the materials present as well as to identify changes in absorbance of total DOM due to physical, photoinduced and biological processes (del Vecchio and Blough 2004, 2002; Coble 2007; Vodacek et al. 1997; Vähätalo and Wetzel 2004; Vähätalo et al. 2000). The slope of the absorption spectrum is widely used in remote sensing in coastal and marine environments (Vodacek et al. 1995; Hoge et al. 1995). It has been reported that there are differences in levels and optical properties between freshwater and marine CDOM. Extreme enrichment in CDOM is usually observed in freshwater environments (Del Vecchio and Blough 2004, 2002; Conmy et al. 2004; Vähätalo and Wetzel 2004; Kowalczuk et al. 2003). Freshwater CDOM absorbs radiation at

wavelengths 450–800 nm (Kowalczuk et al. 2003), which is usually not observed in marine waters. This might be due to the large amount of humic substances in freshwater, which absorb radiation at >450 nm. The riverine input of chromophores contained in freshwater CDOM to the coastal marine environment usually meets photodegradation in the coastal areas, which significantly reduces the CDOM content of seawater (del Vecchio and Blough 2002; Vähätalo and Wetzel 2004; Vähätalo et al. 2000).

Excitation of electrons is a typical phenomenon in both CDOM chromophores and FDOM fluorophores (Senesi 1990a; Wu et al. 2005). Therefore, the DOM components contributing to CDOM and FDOM would be partially the same. On the other hand, the fluorescent components in DOM are identified and distinguished on the basis of specific excitation–emission (Ex/Em) wavelength maxima in EEM spectra, upon PARAFAC modeling (Coble 1996; Fulton et al. 2004; Cory and McKnight 2005; Hall et al. 2005; Stedmon and Markager 2005a, 2005b; Ohno and Bro 2006; Stedmon et al. 2007a, 2007b; Mostofa et al. 2010; Wu et al. 2003a). In contrast, it is not possible to identify and distinguish the specific CDOM components due to the absence of peaks in the CDOM absorption spectra (del Vecchio and Blough 2002; Vähätalo and Wetzel 2004; Vähätalo et al. 2000).

The fluorescent organic substances that are usually identified in natural waters using EEM spectra in combination with PARAFAC modeling are fulvic acid-like, humic acid-like, autochthonous fulvic acids (C-like and M-like), protein-like, tryptophan-like, tyrosine-like components, and fluorescent whitening agents (FWAs)-like (Tables 1, 2). On the other hand, absorption spectra at 350, 355 or 375 nm have been used to monitor the CDOM absorption properties (del Vecchio and Blough 2004, 2002; Kowalczuk et al. 2003, 2005), and the specific UV absorbance (SUVA) at 254 or 280 nm has been adopted to estimate the aromatic carbon contents and to understand the chemical characteristics of DOM (Chin et al. 1994; Croué et al. 2003; Weishaar et al. 2003; Świetlik and Sikorska 2004).

6.2 *How Do Fluorophores in FDOM Differ from Chromophores in CDOM?*

The fluorophores in FDOM are expected to be fundamentally similar to the chromophores in CDOM. For example, tryptophan amino acid ($C_8H_5(NH)$–$CH_2(NH_3^+)CHCOO^-$) has two fluorophores such as $–CH_2–(NH_3^+)–CH–COO^-$ (peak T) and $C_8H_5(NH)$– (peak T_{UV}). The two fluorophores absorb photons and are thus responsible for tryptophan absorption properties as well. In addition, macromolecules such as allochthonous fulvic acid or humic acid are composed of a number of fluorophores such as Schiff-base derivatives (–N=C–C=C–N–), –COOH, $–COOCH_3$, –OH, $–OCH_3$, –CH=O, –C=O, $–NH_2$, –NH–, –CH=CH–COOH, $–OCH_3$, S-, O- or N-containing aromatic compounds, and so on (Mostofa et al. 2009a; Senesi 1990a; Leenheer and Croué 2003; Malcolm 1985; Corin et al. 1996; Peña-Méndez et al. 2005; Seitzinger et al. 2005; Zhang et al. 2005). These

fluorophores need photon absorption for their initial excitation, thus they are fundamentally the chromophores in the respective organic molecule. The fluorophores present in allochthonous fulvic acid can have two fluorescence peaks at peak C-region and peak A-region, but allochthonous humic acid shows several peaks at peak C-region.

On the other hand, allochthonous fulvic acid generally exhibits monotonous absorption spectra whilst allochthonous humic acid has a shoulder at around 400 nm in aqueous media (Hayase and Tsubota 1985; Zepp and Scholtzhauer 1981; Ishiwatari 1973; Lawrence 1980). In addition, CDOM generally exhibits low absorbance at longer wavelengths and the absorbance increases with decreasing wavelength from 700 to 200 nm (Hayase and Tsubota 1985).

Allochthonous fulvic and humic acids, as well as autochthonous fulvic acids are part of the colored DOM (CDOM) and absorb radiation at 200–800 nm. Along with them, also FDOM, protein-like, tryptophan-like, tyrosine-like, FWAs-like and other fluorescent components absorb radiation at 200–800 nm. In addition, there is a vast number of allochthonous and autochthonous non-fluorescent organic substances. They do not display fluorescence properties, but absorb radiation at specific wavelength ranges. For example, acetaldehyde absorb light at 208–224 nm (Mopper et al. 1991; Kieber et al. 1990), acetate at 204–270 nm (Wetzel et al. 1995; Dahlén et al. 1996), formaldehyde at 207–250 nm (Mopper et al. 1991; Kieber et al. 1990), glyoxal at <240 nm (Mopper et al. 1991), malonate at 225–240 nm (Dahlén et al. 1996) and so on. All these organic molecules are termed as CDOM but they do not belong to FDOM because as they do not show fluorescence properties. Therefore 'all fluorescent DOM (FDOM) is colored or chromophoric DOM (CDOM), but not all CDOM is also FDOM'.

7 Scope of the Future Challenges

Autochthonous fulvic acids (C-like and M-like) of algal origin show fluorescence properties at peak C- and A- regions, for which they show a similar behavior as allochthonous fulvic and humic acids. Researchers did not distinguish between the photoinduced and microbial degradation of the autochthonous DOM (fulvic acids) nor its differentiation with terrestrial fulvic acid, and this should be a key focus for future research. Two types of autochthonous fulvic acids (C-like and M-like) can be distinguished based on the presence of fluorophores. This material is originated from algal biomass or phytoplankton biomass. Among these two fulvic acids, the C-like fulvic acid is produced photolytically and microbially and undergoes rapid photoinduced degradation, therefore it does not appear as a key component in natural waters. However, it is important to extract the autochthonous fulvic acids from water, to identify them using other spectroscopic methods and to make relationship with fluorescence properties. The extraction of autochthonous fulvic acids, which represent key DOM sources in lake and marine waters, and the

study of their photoinduced and biological changes would gain useful information by using EEM-PARAFAC.

A few studies have been conducted on the photoinduced and microbial changes of FDOM in natural waters. It should be important to conduct experiments in Asia, Africa and Latin America, because in these continents there are regions where freshwaters are highly contaminated with untreated sewerage and industrial effluents and few studies are presently available. Emerging contaminants such as pharmaceuticals, hormones, endocrine disrupting compounds and so on are widely detected in natural waters (Richardson 2007). The application of EEM-PARAFAC to identify emerging contaminants would constitute a new dimension to control and detect these harmful organic substances in aquatic environments. Finally, PARAFAC modeling of sample EEM spectra could be a useful parameter for the identification of DOM components and for the elucidation of photoinduced, biological and any other changes in the molecular properties of the fluorescent components. Some researchers use the Raman Unit fluorescence (nm^{-1}) EEM data for PARAFAC modeling, which causes significant changes in the component's fluorescence excitation–emission maxima and in the fluorescence intensity compared to QSU or a.u. calibration. It is strongly suggested to use either QSU or a.u. calibration, which allows a better comparison of the fluorescence properties and their application to DOM dynamics in natural waters.

8 Nomenclature

a.u.	Arbitrary unit
CDOM	Colored or chromophoric dissolved organic matter
DAS1	Diaminostilbene-type
DOC	Dissolved organic carbon
DOM	Dissolved organic matter
DSBP	Distyryl biphenyl
EEM	Excitation–emission matrix
EEMS	Excitation–emission matrix spectroscopy
FDOM	Fluorescent dissolved organic matter
FI	Fluorescence intensity
F_{index}	Fluorescence index
Fulvic acids	Two components are identified in standard SRFA
FWAs	Fluorescent whitening agents
Humic acids	Two components are identified in standard SRHA
NoHA	Nordic Reference-humic acid
NoFA	Nordic Reference-fulvic acid
PARAFAC	Parallel factor
QSU	Quinine sulfate unit
RU	Raman Unit

SRFA	Suwannee River Fulvic Acid
SRHA	Suwannee River Humic Acid

Problems

(1) Explain the principles of excitation–emission matrix spectroscopy.
(2) What is the fluorophore in a fluorescent molecule? What are the controlling factors that affect the fluorophores?
(3) Mention the key fluorescent substances detected in natural waters and explain how the fluorescence properties of allochthonous fulvic acids differ from those of humic acids.
(4) How is it possible to distinguish the fluorescence properties of fulvic acids of vascular plant origin from those of autochthonous fulvic acids of algal origin?
(5) What is PARAFAC modeling? Explain the importance of PARAFAC modeling in the separation and identification of the fluorescent components in EEM spectroscopy.
(6) Mention the key factors affecting the fluorescence properties of FDOM in natural waters, and explain how pH variation affects the fluorescence properties.
(7) Explain the effect of photoinduced degradation on the fluorescence properties of humic substances (fulvic and humic acids) in water, and provide the possible mechanism.
(8) What are the importance and impact of photoinduced degradation of FDOM in natural waters?
(9) Mention which FDOM components are significantly affected by microbial degradation in waters.
(10) Explain the changes of the fluorescent properties of various FDOM components due to microbial degradation in aqueous media.
(11) Mention the possible mechanisms for microbial degradation of fluorescent substances in aqueous media?
(12) What are the importance and impacts of microbial degradation of fluorescent substances in aqueous media?
(13) Explain the sentence ‘All fluorescent DOM (FDOM) is colored or chromophoric DOM (CDOM), but not all CDOM is also FDOM’.
(14) in what respect are FDOM studies superior to CDOM one?
(15) Explain how the fluorophores in FDOM differ from chromophores in CDOM.

Acknowledgments We thank Dr. Kazuhide Hayakawa of Lake Biwa Environmental Research Institute, Japan for his valuable comments; Dr. Jie Yuan and Dr. Ling Li of Institute of Geochemistry, Chinese Academy of Sciences for their generous help. This work was financially supported by the Institute of Geochemistry, the Chinese Academy of Sciences, Guiyang, China. This work was partly supported by Nanjing Institute of Geography and Limnology, Chinese Academy of Sciences, China; Kyoto University, Japan; University Turin, Italy; and Hiroshima University, Japan. This chapter acknowledges the reprinted from Senesi (1990a), Copyright (1990), with permission from Elsevier; reprinted from Zhang et al. (2010), Copyright (2010),

References

Abboudi M, Jeffrey W, Ghiglione JF, Pujo-Pay M, Oriol L, Sempéré R, Charrière B, Joux F (2008) Effects of photochemical transformations of dissolved organic matter on bacterial metabolism and diversity in three contrasting coastal sites in the Northwestern Mediterranean Sea during summer. Microb Ecol 55:344–357

Allard B, Borén H, Pattersson C, Zhang G (1994) Degradation of humic substances by UV irradiation. Environ Int 20:97–101

Almgren T, Josefsson B, Nyquist G (1975) A fluorescence method for studies of spent sulfite liquor and humic substances in sea water. Anal Chem Acta 78:411–422

Amador JA, Alexander M, Zika RG (1989) Sequential photochemical and microbial degradation of organic molecules bound to humic acid. App Environ Microb 55:2843–2849

Angell P, Arrage AA, Mittelman MW, White DC (1993) On line, non-destructive biomass determination of bacterial biofilms by fluorometry. J Microbiol Meth 18:317–327

Aoki S, Ohara S, Kimura K, Mizuguchi H, Fuse Y, Yamada E (2008) Characterization of fluorophores released from three kinds of lake phytoplankton using gel chromatography and fluorescence spectrophotometry. Anal Sci 24:1461–1467

Assel M, Laenen R, Laubereau A (1998) Ultrafast electron trapping in an aqueous NaCl-solution. Chem Phys Lett 289:267–274

Baek M, Nelson WH, Hargraves PE, Tanguay JF, Suib SL (1988) The steady state and decay characteristics of protein tryptophan fluorescence from algae. Appl Spectrosc 42:1405–1412

Baghoth SA, Sharma SK, Amy GL (2010) Tracking natural organic matter (NOM) in a drinking water treatment plant using fluorescence excitation emission matrices and PARAFAC. Water Res 45:797–809

Baker A (2001) Fluorescence excitation-emission matrix characterization of some sewage impacted rivers. Environ Sci Technol 35:948–953

Baker A (2002) Fluorescence excitation-emission matrix characterization of some farm wastes: Implications for water quality monitoring. Water Res 36:189–194

Baker A (2005) Thermal fluorescence quenching properties of dissolved organic matter. Water Res 39:4405–4412

Baker A, Curry M (2004) Fluorescence of leachates from three contrasting landfills. Water Res 38:2605–2613

Baker A, Inverarity R (2004) Protein-like fluorescence intensity as a possible tool for determining river water quality. Hydrol Process 18:2927–2945

Baker A, Ward D, Lieten SH, Periera R, Simpson EC, Slater M (2004) Measurement of protein-like fluorescence in river and waste water using a handheld spectrophotometer. Water Res 38:2934–2938

Baker A, Elliott S, Lead JR (2007) Effects of filtration and pH perturbation on freshwater organic matter fluorescence. Chemosphere 67:2035–2043

Balcarczyk KL, Jones Jr JB, Rudolf Jaffe' R, Maie N (2009) Stream dissolved organic matter bioavailability and composition in watersheds underlain with discontinuous permafrost. Biogeochemistry 94:255–270

Battin TJ (1998) Dissolved organic matter in a blackwater tributary of the upper Orinoco River, Venezuela. Org Geochem 28:561–569
Baunsgaard D, Munck L, Nørgaard L (2000) Evaluation of the quality of solid sugar samples by fluorescence spectroscopy and chemometrics. Appl Spectrosc 54:438–444
Baunsgaard D, Nørgaard L, Godshall MA (2001) Specific screening for color precursors and colorants in beet and cane sugar liquors in relation to model colorants using spectrofluorometry evaluated by HPLC and multiway data analysis. J Agric Food Chem 49:1687–1694
Belzile C, Guo L (2006) Optical properties of low molecular weight and colloidal organic matter: application of the ultrafiltration permeation model to DOM absorption and fluorescence. Mar Chem 98:183–196
Benner R, Opsahl S (2001) Molecular indicators of the sources and transformations of dissolved organic matter in the Mississippi river plume. Org Geochem 32:597–611
Berger P, Laane RPWM, IIahude AG, Ewald M, Courtot P (1984) Comparative study of dissolved fluorescent matter in four west-european estuaries. Oceanol Acta 7:309–313
Bertilsson S, Tranvik LJ (1998) Photochemically produced carboxylic acids as substrates for freshwater bacterioplankton. Limnol Oceanogr 43:885–895
Bertilsson S, Tranvik LJ (2000) Photochemical transformation of dissolved organic matter in lakes. Limnol Oceanogr 45:753–762
Bertilsson S, Carlsson P, Granéli W (2004) Influence of solar radiation on the availability of dissolved organic matter to bacteria in the Southern Ocean. Deep Sea Res II 51:2557–2568
Bianchi TS, Dawson R, Sawangwong P (1988) The effects of macrobenthic deposit-feeding on the degradation of chloropigments in sandy sediments. J Exp Mar Biol Ecol 122:243–255
Blough NV, Del Vecchio R (2002) Chromophoric DOM in the coastal environment. In: Hansell DA, Carlson CA (eds) Biogeochemistry of marine dissolved organic matter. Elsevier Science, New York, p 774
Boehme J, Wells M (2006) Fluorescence variability of marine and terrestrial colloids: examining size fractions of chromophoric dissolved organic matter in the Damariscotta River estuary. Mar Chem 101:95–103
Boehme J, Coble PG, Conmy RN, Stovall-Leonard A (2004) Examining CDOM fluorescence variability using principal component analysis: seasonal and regional modelling of three-dimensional fluorescence in the Gulf of Mexico. Mar Chem 89:3–14
Borisover M, Laor Y, Parparov A, Bukhanovsky N, Lado M (2009) Spatial and seasonal patterns of fluorescent organic matter in Lake Kinneret (Sea of Galilee) and its catchment basin. Water Res 43:3104–3116
Boyd TJ, Osburn CL (2004) Changes in CDOM fluorescence from allochthonous and autochthonous sources during tidal mixing and bacterial degradation in two coastal estuaries. Mar Chem 89:189–210
Boyd TJ, Barham BP, Hall GJ, Schumann BS, Paerl RW, Osburn CL (2010) Variation in ultrafiltered and LMW organic matter fluorescence properties under simulated estuarine mixing transects: 2 Mixing with photoexposure. J Geophys Res 115:G00F14. doi:101029/2009JG000994
Bro R (1997) PARAFAC tutorial and applications. Chemom Intell Lab Syst 38(2):149–171
Bro R (1998) Multi-way analysis in the food industry Models, algorithms, and applications. PhD thesis, University of Amsterdam, Netherlands
Bro R (1999) Exploratory study of sugar production using fluorescence spectroscopy and multiway analysis. Chemom Intell Lab Syst 46:133–147
Bronk DA (2002) Dynamics of DON. In: Carlson CA, Hansell DA (eds) Biogeochemistry of marine dissolved organic matter. Academic Press, San Diego, pp 153–249
Brooks ML, Meyer JS, McKnight DM (2007) Photooxidation of wetland and riverine dissolved organic matter: altered copper complexation and organic composition. Hydrobiologia 579:95–113
Brun GL, Milburn DLD (1977) Automated fluorescence determination of humic substances in natural water. Anal Lett 10:1209–1219

Burdige DJ, Kline SW, Chen W (2004) Fluorescent dissolved organic matter in marine sediment pore waters. Mar Chem 89:289–311
Cabaniss SE (1992) Synchronous fluorescence spectra of metal-fulvic acid complexes. Environ Sci Technol 26:1133–1139
Cabaniss SE, Shuman MS (1988) Fluorescence quenching measurements of copper–fulvic acid binding. Anal Chem 60:2418–2421
Cammack W, Kalff J, Prarie Y, Smith EM (2004) Fluorescent dissolved organic matter in lakes: relationship with heterotrophic metabolism. Limnol Oceanogr 49:2034–2045
Carlson DJ, Mayer LM (1983) Relative influence of riverine and macroalgal phenolic materials on UV absorbance in temperate coastal waters. Can J Fishering Aquatic Sci 40:1258–1263
Caroll JD, Chang J (1970) Analysis of individual differences in multidimensional scaling via an N-way generalisation of and Eckart–Young decomposition. Psychometrika 35:283
Chen RF, Bada JL (1989) Seawater and porewater fluorescence in the Santa Barbara Basin. Geophys Res Lett 16:687–690
Chen RF, Bada JL (1990) A laser-based fluorometry system for investigations of seawater and pore water fluorescence. Mar Chern 31:219–230
Chen RF, Bada JL (1992) The fluorescence of dissolved organic matter in seawater. Mar Chem 37:191–221
Chen W, Westerhoff P, Leenheer JA, Booksh K (2003) Fluorescence excitation-emission matrix regional integration to quantify spectra for dissolved organic matter. Environ Sci Tech 37:5701–5710
Chen M, Price RM, Yamashita Y, Jaffé R (2010) Comparative study of dissolved organic matter from groundwater and surface water in the Florida coastal Everglades using multi-dimensional spectrofluorometry combined with multivariate statistics. Appl Geochem 25:872–880
Chin YP, Aiken GR, ÖLoughlin E (1994) Molecular weight, polydispersity, and spectroscopic properties of aquatic humic substances. Environ Sci Technol 28:1853–1858
Christman RF, Ghassemi M (1966) Chemical nature of organic color in water. J Am Water Works Assoc 58:723–741
Christman RF, Minear RA (1967) Fluorometric detection of lignin sulfonates. Trend Eng 19:3–7 (University of Washington, Seattle, College of Engineering)
Clarke RH, Connors RE, Schaafsma TJ, Kleibeuker JF, Platenkamp RJ (1976) The triplet state of chlorophylls. J Am Chem Soc 98(12):3674–3677
Coble PG (1996) Characterization of marine and terrestrial DOM in sea water using excitation-emission matrix spectroscopy. Mar Chem 52:325–336
Coble PG (2007) Marine optical biogeochemistry: the chemistry of ocean color. Chem Rev 107:402–418
Coble PG, Green SA, Blough NV, Gagosian RB (1990) Characterization of dissolved organic matter in the Black Sea by fluorescence spectroscopy. Nature 348:432–435
Coble PG, Schultz CA, Mopper K (1993) Fluorescence contouring analysis of DOC inter calibration samples: a comparison of techniques. Mar Chem 41:173–178
Coble PG, Del Castillo CE, Avril B (1998) Distribution and optical properties of CDOM in the Arabian Sea during the 1995 Southwest Monsoon. Deep-Sea Res II 45:2195–2223
Conmy RN, Coble PG, Chen RF, Gardner GB (2004) Optical properties of colored dissolved organic matter in the Northern Gulf of Mexico. Mar Chem 89:127–144
Conrad R (1999) Contribution of hydrogen to methane production and control of hydrogen concentrations in methanogenic soils and sediments. FEMS Microbiol Ecol 28:193–202
Corin N, Backlund P, Kulovaara M (1996) Degradation products formed during UV-irradiation of humic waters. Chemosphere 33:245–255
Cory RM, McKnight DM (2005) Fluorescence spectroscopy reveals ubiquitous presence of oxidized and reduced quinines in dissolved organic matter. Environ Sci Technol 39:8142–8149
Cory RM, McKnight DM, Chin Y-P, Miller P, Jaros CL (2007) Chemical characteristics of fulvic acids from Arctic surface waters: microbial contributions and photochemical transformations. J Geophys Res 112:G04S51. doi:101029/2006JG000343

Croué JP, Benfdetti MF, Violleauand D, Leenheer JA (2003) Characterization and copper binding of humic and nonhumic organic matter isolated from the south platte river: evidence for the presence of nitrogenous binding site. Environ Sci Technol 37:328–336

da Silva JCGE, Leitao JMM, Costa FS, Ribeiro JLA (2002) Detection of verapamil drug by fluorescence and trilinear decomposition techniques. Anal Chim Acta 453:105–115

Dahlén J, Bertilsson S, Pettersson C (1996) Effects of UV-A irradiation on dissolved organic matter in humic surface waters. Environ Int 22:501–506

de Souza Sierra MM, Donard OFX, Lamotte M (1997) Spectral identification and behaviour of dissolved organic fluorescent materials during estuarine mixing processes. Mar Chem 58:51–58

de Souza-Sierra MM, Donard OFX, Lamotte M, Belin C, Ewald M (1994) Fluorescence spectroscopy of coastal and marine waters. Mar Chem 47:127–144

del Vecchio R, Blough NV (2002) Photobleaching of chromophoric dissolved organic matter in natural waters: kinetics and modeling. Mar Chem 78:231–253

del Vecchio R, Blough NV (2004) Spatial and seasonal distribution of chromophoric dissolved organic matter and dissolved organic carbon in the Middle Atlantic Bight. Mar Chem 89:169–187

Determann S, Reuter R, Wanger P, Willkomm R (1994) Fluorescence matter in the eastern Atlantic Ocean. Part 1: Method of measurement and near-surface distribution. Deep-Sea Res 41:659–675

Determann S, Reuter R, Willkomm R (1996) Fluorescence matter in the eastern Atlantic Ocean. Part 2: Vertical profiles and relation to water masses. Deep-Sea Res 43:345–360

Determann S, Lobbes JM, Reuter R, Rullkotter J (1998) Ultraviolet fluorescence excitation and emission spectroscopy of marine algae and bacteria. Mar Chem 62:137–156

Dorsch JE, Bidleman TF (1982) Natural organics as fluorescent tracers of river-sea mixing. Estuar Coast Shelf Sci 15:701–707

Dubnick A, Barker J, Sharp M, Wadham J, Lis G, Telling J, Fitzsimons S, Jackson M (2010) Characterization of dissolved organic matter (DOM) from glacial environments using total fluorescence spectroscopy and parallel factor analysis. Ann Glaciol 51:111–122

Duursma EK (1974) The fluorescence of dissolved organic matter in the sea. In: Jerlov NG, Nielsen ES (eds) Optical aspects of oceanography. Academic Press, New York, pp 237–256

Elliott S, Lead JR, Baker A (2006) Thermal quenching of fluorescence of freshwater, planktonic bacteria. Anal Chim Acta 564:219–225

Fellman JB, D'Amore DV, Hood E, Boone RD (2008) Fluorescence characteristics and biodegradability of dissolved organic matter in forest and wetland soils from coastal temperate watersheds in southeast Alaska. Biogeochemistry 88:169–184

Fellman JB, Hood E, D'Amore DV, Edwards RT, White D (2009) Seasonal changes in the chemical quality and biodegradability of dissolved organic matter exported from soils to streams in coastal temperate rainforest watersheds. Biogeochemistry 95:277–293. doi:10.1007/s10533-009-9336-6

Fellman JB, Spencer RGM, Hernes PJ, Edwards RT, D'Amore DV, Hood E (2010) The impact of glacier runoff on the biodegradability and biochemical composition of terrigenous dissolved organic matter in near-shore marine ecosystems. Mar Chem 121:112–122

Ferrari GM (2000) The relationship between chromophoric dissolved organic matter and dissolved organic carbon in the European Atlantic coastal area and in the West Mediterranean Sea (Gulf of Lions). Mar Chem 70:339–357

Ferrari GM, Dowell MD, Grossi S, Targa C (1996a) Relationship between the optical properties of chromophoric dissolved organic matter and total concentration of dissolved organic carbon in the southern Baltic Sea region. Mar Chem 55:299–316

Ferrari GM, Hoepffner N, Mingazzini M (1996b) Optical properties of the water in a deltaic environment: prospective tool to analyze satellite data in turbid waters. Remote Sens Environ 56:69–80

Fu P, Wu FC, Liu C, Wei Z, Bai Y, Liao H (2006) Spectroscopic characterization and molecular weight distribution of dissolved organic matter in sediment porewaters from Lake Erhai, Southwest China. Biogeochemistry 81:179–189

Fu PQ, Wu FC, Liu CQ, Wang F, Li W, Yue L, Guo QJ (2007) Fluorescence characterization of dissolved organic matter in an urban river and its complexation with Hg(II). Appl Geochem 22:1668–1679

Fu P, Mostofa KMG, Wu FC, Liu CQ, Li W, Liao H, Wang L, Wang J, Mei Y (2010) Excitation-emission matrix characterization of dissolved organic matter sources in two eutrophic lakes (Southwestern China Plateau). Geochem J 44:99–112

Fuentes M, González-Gaitano G, José M, García-Mina JM (2006) The usefulness of UV-vissible and fluorescence spectroscopies to study the chemical nature of humic substances from soils and composts. Org Geochem 37:1949–1959

Fujiwara K, Ushiroda T, Takeda K, Kumamoto Y, Tsubota H (1993) Diurnal and seasonal distribution of hydrogen peroxide in seawater of Seto Inland Sea. Geochem J 27:103–115

Fukushima M, Tatsumi K, Nagao S (2001) Degradation characteristics of humic acid during photo-fenton processes. Environ Sci Technol 35:3683–3690

Fulton JR, McKnight DM, Foreman CM, Cory RM, Stedmon C, Blunt E (2004) Changes in fulvic acid redox state through the oxycline of a permanently ice-covered Antarctic lake. Aquat Sci 66:27–46

Gao H, Zepp RG (1998) Factors influencing photoreactions of dissolved organic matter in a coastal river of the Southeastern United States. Environ Sci Technol 32:2940–2946

Gao L, Fan D, Li D, Cai J (2010) Fluorescence characteristics of chromophoric dissolved organic matter in shallow water along the Zhejiang coasts, Southeast China. Mar Environ Res 69:187–197

Garcia E, Amyot M, Ariya PA (2005) Relationship between DOC photochemistry and mercury redox transformations in temperate lakes and wetlands. Geochim Cosmochim Acta 69:1917–1924

Geller A (1986) Comparison of mechanisms enhancing biodegradability of refractory lake water constituents. Limnol Oceanogr 31:755–764

Ghassemi M, Christman RF (1968) Properties of the yellow organic acids of natural waters. Limnol Oceanogr 13:583–597

Gopinathan C, Damle PS, Hart EJ (1972) Gamma-ray irradiated sodium chloride as a source of hydrated electrons. J Phys Chem 76:3694–3698

Gosh K, Schnitzer M (1980) Fluorescence excitation spectra of humic substances. Can J Soil Sci 60:373–379

Grabowski ZR, Rotkiewicz K, Rettig W (2003) Structural changes accompanying intramolecular electron transfer: focus on twisted intramolecular charge-transfer states and structures. Chem Rev 103:3899–4032

Granéli W, Lindell M, Marcal De Farria B, De Assis Esteves F (1998) Photoproduction of dissolved inorganic carbon in temperate and tropical lakes-dependence on wavelength band and dissolved organic carbon concentration. Biogeochemistry 43:175–195

Green SA, Blough NV (1994) Optical absorption and fluorescence properties of chromophoric dissolved organic matter in natural waters. Limnol Oceanogr 39:1903–1916

Gron C, Wassenaar L, Krog M (1996) Origin and structures of groundwater humic substances from three Danish aquifers. Environ Int 22:519–534

Guglielmetti L (1975) Photochemical and biological degradation of water-soluble FWAs. In: Anliker R, Müller G (eds) Fluorescent whitening agents. Georg Thieme Publishers, Stuttgart, pp 180–190

Guilbault GG (1990) Practical fluorescence: theory, methods and techniques, 2nd edn. Dekker, New York

Guo W, Xu J, Wang J, Wen Y, Zhuo J, Yan Y (2010) Characterization of dissolved organic matter in urban sewage using excitation emission matrix fluorescence spectroscopy and parallel factor analysis. J Environ Sci 22:1728–1734

Hall KJ, Lee GF (1974) Molecular size and spectral characterization of organic matter in a meromictic lake. Water Res 8:239–251

Hall GJ, Clow KE, Kenny JE (2005) Estuarial fingerprinting thorough multidimensional fluorescence and multivariate analysis. Environ Sci Technol 39:7560–7567

Hama T (1991) Production and turnover rates of fatty acids in marine particulate matter through phytoplankton photosynthesis. Mar Chem 33:213–227

Hama T, Yanagi K, Hama J (2004) Decrease in molecular weight of photosynthetic products of marine phytoplankton during early diagenesis. Limnol Oceanogr 49:471–481
Hanamachi Y, Hama T, Yanai T (2008) Decomposition process of organic matter derived from freshwater phytoplankton. Limnology 9:57–69
Harshman RA (1970) Foundations of the PARAFAC procedure: model and conditions for an explanatory multi-mode factor analysis. UCLA Work Pap Phonetics 16:1–84
Harvey HR, Macko SA (1997) Kinetics of phytoplankton decay during simulated sedimentation: changes in lipids under oxic and anoxic conditions. Org Geochem 27:129–140
Harvey HR, Tuttle JH, Bell JT (1995) Kinetics of phytoplankton decay during simulated sedimentation: changes in biochemical composition and microbial activity under oxic and anoxic conditions. Geochim Cosmochim Acta 59:3367–3377
Hayakawa K, Sekino T, Yoshioka T, Maruo M, Kumagai M (2003) Dissolved organic carbon and fluorescence in Lake Hovsgol: factors reducing humic content of the lake water. Limnology 4:25–33
Hayase K, Shinozuka N (1995) Vertical distribution of fluorescent organic matter along with AOU and nutrients in the Equatorial Pacific. Mar Chem 48:282–290
Hayase K, Tsubota H (1983) Sedimentary humic acid and fulvic acid as surface active substances. Geochim Cosmochim Acta 47:947–952
Hayase K, Tsubota H (1985) Sedimentary humic and fulvic acids as fluorescent organic materials. Geochim Cosmochim Acta 49:159–163
Hayase K, Yamamoto M, Nakazawa I, Tsubota H (1987) Behavior of natural fluorescence in Sagami Bay and Tokyo Bay, Japan—vertical and lateral distributions. Mar Chem 20:265–276
Hayase K, Tsubota H, Sunada I, Goda S, Yamazaki H (1988) Vertical distribution of fluorescent organic matter in the North Pacific. Mar Chem 25:373–381
Hayashi Y, Managaki S, Takada H (2002) Fluorescent whitening agents in Tokyo Bay and adjacent rivers: their application as anthropogenic molecular markers in coastal environments. Environ Sci Technol 36:3556–3563
Hedges JI (1992) Global biogeochemical cycles: progress and problems. Mar Chem 39:67–93
Hedges JI, Eglinton G, Hatcher PG, Kirchman DL, Arnosti C, Dereenne S, Evershed RP, Kögel-Knabner I, de Leeuw JW, Littke R, Michaelis W, Rullkötter J (2000) The molecularly-uncharacterized component of nonliving organic matter in natural environments. Org Geochem 31:945–958
Helms JR, Stubbins A, Ritchie JD, Minor EC, Kieber DJ, Mopper K (2008) Absorption spectral slopes and slope ratios as indicators of molecular weight, source, and photobleaching of chromophoric dissolved organic matter. Limnol Oceanogr 53:955–969
Henderson RK, Baker A, Murphy KR, Hambly A, Stuetz RM, Khan SJ (2009) Fluorescence as a potential monitoring tool for recycled water systems: a review. Water Res 43:863–881
Hiriart-Baer VP, Smiith REH (2005) The effect of ultraviolet radiation on freshwater planktonic primary production: the role of recovery and mixing processes. Limnol Oceanogr 50:1352–1361
Hiriart-Baer VP, Diep N, Smith REH (2008) Dissolved organic matter in the great lakes: role and nature of allochthonous material. J Great Lakes Res 34:383–394
Hoge FE, Williams ME, Swift RN, Yungel JK, Vodacek A (1995) Satellite retrieval of the absorption coefficient of chromophoric dissolved organic matter in continental margins. J Geophy Res 100(24847):24854
Holbrook RD, Breidenich J, DeRose PC (2005) Impact of reclaimed water on select organic matter properties of a receiving stream-fluorescence and perylene sorption behavior. Environ Sci Technol 39:6453–6460
Holbrook RD, Yen JH, Grizzard TJ (2006) Characterizing natural organic material from the Occoquan Watershed (Northern Virginia, US) using fluorescence spectroscopy and PARAFAC. Sci Total Environ 361:249–266
Hua B, Dolan F, McGhee C, Clevenger TE, Deng B (2007) Water-source characterization with fluorescence EEM spectroscopy: PARAFAC analysis. Int J Environ Anal Chem 87:135–147
Hudson N, Baker A, Renolds D (2007) Fluorescence analysis of dissolved organic matter in natural, waste and polluted waters—a review. River Res Appl 23:631–649

Hudson N, Baker A, Ward D, Reynolds DM, Brunsdon C, Carliell-Marquet C, Browning S (2008) Can fluorescence spectrometry be used as a surrogate for the biochemical oxygen demand (BOD) test in water quality assessment? An example from South West England. Sci Total Environ 391:149–158

Huguet A, Vacher L, Relexans S, Saubusse S, Froidefond J-M, Parlanti E (2009) Properties of fluorescent dissolved organic matter in the Gironde Estuary. Org Geochem 40:706–719

Huguet A, Vacher L, Saubusse S, Etcheber H, Abril G, Relexans S, Ibalot F, Parlanti E (2010) New insights into the size distribution of fluorescent dissolved organic matter in estuarine waters. Org Geochem 41:595–610

Hulatt CJ, Thomas DN, Bowers DG, Norman L, Zhang C (2009) Exudation and decomposition of chromophoric dissolved organic matter (CDOM) from some temperate macroalgae. Estuar Coast Shelf Sci 84:147–153

Hunt JF, Ohno T, Fernandez IJ (2008) Influence of foliar phosphorus and nitrogen contents on chemical properties of water extractable organic matter derived from fresh and decomposed sugar maple leaves. Soil Biol Biochem 40:1931–1939

Ishiwatari R (1973) Chemical characterization of fractionated humic acids from lake and marine sediments. Chem Geol 12:113–126

Jaffé R, Boyer JN, Lu X, Maie N, Yange C, Scully NM, Mock S (2004) Source characterization of dissolved organic matter in a subtropical mangrovedominated estuary by fluorescence analysis. Mar Chem 84:195–210

Jiji RD, Cooper GA, Booksh KS (1999) Excitation–emission matrix fluorescence based determination of carbamate pesticides and polycyclic aromatic hydrocarbons. Anal Chim Acta 397:61–72

Johannessen SC, Peña MA, Quenneville ML (2007) Photochemical production of carbon dioxide during a coastal phytoplankton bloom. Estuar Coast Shelf Sci 73:236–242

Kalle K (1949) Fluoreszenz und Gelbstoff im Bottnischem und Finnishchen Meerbusen. Dtsch Hydrogr Z 2:9–124

Kalle K (1963) Uber das Verhalten und die Herkunft der in den Gewassern und in der Atmospheare vorhandenen himmelblauen Fluoreszenz. Dtsch Hydrogr Z 16:153–166

Kieber RJ, Zhou X, Mopper K (1990) Formation of carbonyl compounds from UV-induced photodegradation of humic substances in natural waters: fate of riverine carbon in the sea. Limnol Oceanogr 35:1503–1515

Kieber RJ, Hydro LH, Seaton PJ (1997) Photooxidation of triglycerides and fatty acids in seawater: implication toward the formation of marine humic substances. Limnol Oceanogr 42:1454–1462

Kim C, Nishimura Y, Nagata T (2006) Role of dissolved organic matter in hypolimnetic mineralization of carbon and nitrogen in a large, monomictic lake. Limnol Oceanogr 51:70–78

Klapper L, McKnight DM, Fulton JR, Blunt-Harris EL, Nevin KP, Lovley DR, Hatcher PG (2002) Fulvic acid oxidation state detection using fluorescence spectroscopy. Environ Sci Technol 36:3170–3175

Klein B, Gieskes WWC, Kraay GG (1986) Digestion of chlorophylls and carotenoids by the marine protozoan Oxyrrhis marina studied by h.p.l.c analysis of algal pigments. J Plankton Res 8:827–836

Komada T, Schofield OME, Reimers CE (2002) Fluorescence characteristics of organic matter released from coastal sediments during resuspension. Mar Chem 79:81–97

Komaki M, Yabe A (1982) Fluorometric analysis of fluorescent brightening agents in natural waters. Chem Soc J 5:859–867 (in Japanese)

Kotsyurbenko OR, Glagolev MV, Nozhevnikova AN, Conrad R (2001) Competition between homoacetogenic bacteria and methanogenic archaea for hydrogen at low temperature. FEMS Microbiol Ecol 38:153–159

Kowalczuk P, Cooper WJ, Whitehead RF, Durako MJ, Sheldon W (2003) Characterization of CDOM in an organic-rich river and surrounding coastal ocean in the South Atlantic Bight. Aquat Sci 65:384–401

Kowalczuk P, Stoń-Egiert J, Cooper WJ, Whitehead RF, Durako MJ (2005) Characterization of chromophoric dissolved organic matter (CDOM) in the Baltic Sea by excitation emission matrix fluorescence spectroscopy. Mar Chem 96:273–292

Kowalczuk P, Durako MJ, Young H, Kahn AE, Cooper WJ, Gonsior M (2009) Characterization of dissolved organic matter fluorescence in the South Atlantic Bight with use of PARAFAC model: Interannual variability. Mar Chem 113:182–196

Kramer JB, Canonica S, Hoigne J, Kaschig J (1996) Degradation of fluorescent whitening agents in sunlit natural waters. Environ Sci Technol 30:2227–2234

Kulovaara M, Corin N, Backlund P, Tervo J (1995) Impact of UV254-radiation on aquatic humic substances. Chemosphere 33:783–790

Kwan WP, Voelker BM (2002) Decomposition of hydrogen peroxide and organic compounds in the presence of dissolved iron and ferrihydrite. Environ Sci Technol 36:1467–1476

Laane RWPM (1980) Conservative behavior of dissolved organic carbon in the Ems-Dollart Estuary and the Western Sea. Neth J Sea Res 14:192–199

Laane RWPM (1982) Influence of pH on the fluorescence of dissolved organic matter. Mar Chem 11:395–401

Laane RWPM (1984) Comment on the structure of marine fulvic and humic acids. Mar Chem 15:85–87

Laane RWPM, Kramer KJM (1990) Natural fluorescence in the North Sea and its major estuaries. Neth J Sea Res 26:1–9

Lakowicz JR (1983) Principles of fluorescence spectroscopy. Plenum Press, New York

Lakowicz JR (1999) Principles of fluorescence spectroscopy, 2nd edn. Kluwer Academic, New York

Laurion I, Ventura M, Catalan J, Psenner R, Sommarruga R (2000) Attenuation of ultraviolet radiation in mountain lakes: factors controlling the among- and within-lake variability. Limnol Oceanogr 45:1274–1288

Lawrence J (1980) Semi-quantitative determination of fulvic acid, tannin and lignin in natural waters. Water Res 14:373–377

Leenheer JA, Croué JP (2003) Characterizing aquatic dissolved organic matter. Environ Sci Technol 37:18–26

Lehmann MF, Bernasconi SM, Peichert P, McKenzie JA (2002) Preservation of organic matter and alteration of its carbon and nitrogen isotope composition during simulated and in situ early sedimentary diagenesis. Geochim Cosmochim Acta 66:3573–3584

Lepane V, Persson T, Wedborg M (2003) Effects of UV-B radiation on molecular weight distribution and fluorescence from humic substances in riverine and low-salinity water. Estuar Coastal Shelf Sci 56:161–173

Levesque M (1972) Fluorescence and gel filtration of humic compounds. Soil Sci 113:346–353

Li K, Crittenden J (2009) Computerized pathway elucidation for hydroxyl radical-induced chain reaction mechanisms in aqueous phase advanced oxidation processes. Environ Sci Technol 43:2831–2837

Li JK, Humphrey AE (1990) Use of fluorometry for monitoring and control of a bioreactor. Biotechnol Bioeng 37:1043–1049

Li W, Wu FC, Liu CQ, Fu PQ, Wang J, Mei Y, Wang L, Guo J (2008) Temporal and spatial distributions of dissolved organic carbon and nitrogen in two small lakes on the Southwestern China Plateau. Limnology 9:163–171

Liu H, Fang HHP (2002) Characterization of electrostatic binding sites of extracellular polymers by linear programming analysis of titration data. Biotechnol Bioeng 80:806–811

Lochmuller CH, Saavedra SS (1986) Conformational changes in a soil fulvic acid measured by time dependent fluorescence depolarization. Anal Chem 38:1978–1981

Lovley DR, Coates JD, Blunt-Harris EL, Phillips EJP, Woodward JC (1996) Humic substances as electron acceptors for microbial respiration. Nature 382:445–448

Lu YF, Allen HE (2002) Characterization of copper complexation with natural dissolved organic matter (DOM)—link to acidic moieties of DOM and competition by Ca and Mg. Water Res 36:5083–5101

Lu XQ, Jaffé R (2001) Interaction between Hg(II) and natural dissolved organic matter: a fluorescence spectroscopy based study. Water Res 35:1793–1803
Lu F, Chang C-H, Lee D-J, He P-J, Shao L-M, Su A (2009) Dissolved organic matter with multipeak fluorophores in landfill leachate. Chemosphere 74:575–582
Luciani X, Mounier S, Paraquetti HHM, Redon R, Lucas Y, Bois A, Lacerda LD, Raynaud M, Ripert M (2008) Tracing of dissolved organic matter from the SEPETIBA Bay (Brazil) by PARAFAC analysis of total luminescence matrices. Mar Environ Res 65:148–157
Ma XD, Ali N (2009) Detection of a DNA-like materials in Suwannee River Fulvic Acid. In: Wu FC, Xing B (eds) Natural organic matter and its significance in the environment. Science Press, Beijing, pp 66–89
Ma X, Green SA (2004) Photochemical transformation of dissolved organic carbon in Lake Superior—an in situ experiment. J Great Lakes Res 30(suppl 1):97–112
Mack J, Bolton JR (1999) Photochemistry of nitrite and nitrate in aqueous solution: a review. J Photochem Photobiol A Chem 128:1–13
Malcolm RL (1985) Geochemistry of stream fulvic and humic substances. In: Aiken GR, McKnight DM, Wershaw RL, MacCarthy P (eds) Humic substances in soil, sediment, and water: geochemistry, isolation and characterization. Wiley, New York, pp 181–209
Malcolm RL (1990) The uniqueness of humic substances in each of soil, stream and marine environments. Anal Chim Acta 232:19–30
Managaki S, Takada H (2005) Fluorescent whitening agents in Tokyo Bay sediments: molecular evidence of lateral transport of land-derived particulate matter. Mar Chem 95:113–127
Manciulea A, Baker A, Lead JR (2009) A fluorescence quenching study of the interaction of Suwannee River fulvic acid with iron oxide nanoparticles. Chemosphere 76:1023–1027
Marmé N, Knemeyer J-P, Sauer M, Wolfrum J (2003) Inter- and intramolecular fluorescence quenching of organic dyes by tryptophan. Bioconjugate Chem 14:1133–1139
Matthews BJH, Jones AC, Theodorou NK, Tudhope AW (1996) Excitation-emission matrix fluorescence spectroscopy applied to humic acid in coral reefs. Mar Chem 55:312–317
Mayer LM, Schick LL, Loder TC (1999) Dissolved protein fluorescence in two Maine estuaries. Mar Chem 64:171–179
McCarthy MD, Hedges JI, Benner R (1996) Major biochemical composition of dissolved high molecular weight organic matter in seawater. Mar Chem 55:281–297
McCreary JJ, Snoeyink VL (1980) Characterization and activated carbon adsorption of several humic substances. Water Res 14:151–160
McCullen WL (1996) Polymers for detergents: current technology and future trends. In: Coffey RT (ed) New horizons: an AOCS/CSMA detergent industry conference. The American Oil Chemists Society—Science, Washington, DC, pp 42–55
McKnight DM, Boyer EW, Westerhoff PK, Doran PT, Kulbe T, Andersen DT (2001) Spectrofluorometric characterization of dissolved organic matter for indication of precursor organic material and aromaticity. Limnol Oceanogr 46:38–48
Miles CJ, Brezonik L (1981) Oxygen consumption in humic-colored waters by a photochemical ferrous-ferric catalytic cycle. Environ Sci Technol 15:1089–1095
Miller WL, Moran MA (1997) Interaction of photochemical and microbial processes in the degradation of refractory dissolved organic matter from a coastal marine environment. Limnol Oceanogr 42:1317–1324
Miller WL, Moran MA, Sheldon WM, Zepp RG, Opsahl S (2002) Determination of apparent quantum yield spectra for the formation of biologically labile photoproducts. Limnol Oceanogr 47:343–352
Miller MP, McKnight DM, Chapra SC (2009) Production of microbially-derived fulvic acid from photolysis of quinone-containing extracellular products of phytoplankton. Aquat Sci 71:170–178
Minakata D, Li K, Westerhoff P, Crittenden J (2009) Development of a group contribution method to predict aqueous phase hydroxyl radical (HO•) reaction rate constants. Environ Sci Technol 43:6220–6227

Mobed JJ, Hemmingsen SL, Autry JL, McGown LB (1996) Fluorescence characterization of IHSS humic substances: total luminescence spectra with absorbance correction. Environ Sci Technol 30:3061–3065

Moberg L, Robertsson G, Karlberg B (2001) Spectrofluorimetric determination of chlorophylls and pheopigments using parallel factor analysis. Talanta 54:161–170

Momzikoff A, Dallot S, Pizay M-D (1992) Blue and yellow fluorescence of filtered seawater in a frontal zone (Ligurian Sea, northwest Mediterranean Sea). Deep-Sea Res 39:1481–1498

Mopper K, Schultz CA (1993) Fluorescence as a possible tool for studying the nature and water column distribution of DOC components. Mar Chem 41:229–238

Mopper K, Zhou X, Kieber RJ, Kieber DJ, Sikorski RJ, Jones RD (1991) Photochemical degradation of dissolved organic carbon and its impact on the oceanic carbon cycle. Nature 353:60–62

Moran MA, Zepp RG (1997) Role of photoreactions in the formation of biologically labile compounds from dissolved organic matter. Limnol Oceanogr 42:1307–1316

Moran MA Jr, Sheldon WM, Zepp RG (2000) Carbon loss and optical property changes during long-term photochemical and biological degradation of estuarine dissolved organic matter. Limnol Oceanogr 45:1254–1264

Morris DP, Hargreaves BR (1997) The role of photochemical degradation of dissolved organic carbon in regulating the UV transparency of three lakes on the Pocono Plateau. Limnol Oceanogr 42:239–249

Mostofa KMG (2005) Dynamics, characteristics and photochemical processes of fluorescent dissolved organic matter and peroxides in river water. Ph D Thesis, Sept 2005, Hiroshima University, Japan

Mostofa KMG, Sakugawa H (2009) Spatial and temporal variations and factors controlling the concentrations of hydrogen peroxide and organic peroxides in rivers. Environ Chem 6:524–534

Mostofa KMG, Honda Y, Sakugawa H (2005a) Dynamics and optical nature of fluorescent dissolved organic matter in river waters in Hiroshima prefecture, Japan. Geochem J 39:257–271

Mostofa KMG, Yoshioka T, Konohira E, Tanoue E, Hayakawa K, Takahashi M (2005b) Three-dimensional fluorescence as a tool for investigating the dynamics of dissolved organic matter in the Lake Biwa watershed. Limnology 6:101–115

Mostofa KMG, Yoshioka T, Konohira E, Tanoue E (2007a) Photodegradation of fluorescent dissolved organic matters in river waters. Geochem J 41:323–331

Mostofa KMG, Yoshioka T, Konohira E, Tanoue E (2007b) Dynamics and characteristics of fluorescent dissolved organic matter in the groundwater, river and lake water. Water Air Soil Pollut 184:157–176

Mostofa KMG, Wu FC, Yoshioka T, Sakugawa H, Tanoue E (2009a) Dissolved organic matter in the aquatic environments. In: Wu FC, Xing B (eds) Natural organic matter and its significance in the environment. Science Press, Beijing, pp 3–65

Mostofa KMG, Liu CQ, Wu FC, Fu PQ, Ying WL, Yuan J (2009b) Overview of key biogeochemical functions in lake ecosystem: impacts of organic matter pollution and global warming. Proceedings of 13th World Lake Conference, Wuhan, China, 1–5 Nov 2009, Keynote Speech, pp 59–60

Mostofa KMG, Wu FC, Liu CQ, Fang WL, Yuan J, Ying WL, Wen L, Yi M (2010) Characterization of Nanming River (Southwestern China) impacted by sewerage pollution using excitation-emission matrix and PARAFAC. Limnology 11:217–231. doi:101007/s10201-009-0306-4

Mostofa KMG, Wu FC, Liu CQ, Yoshioka T, Sakugawa H, Tanoue E (2011) Photochemical, microbial and metal complexation behavior of fluorescent dissolved organic matter in the aquatic environments. Invited review. Geochem J 45:235–254

Mounier S, Zhao H, Garnier C, Redon R (2011) Copper complexing properties of dissolved organic matter: PARAFAC treatment of fluorescence quenching. Biogeochemistry. doi:10.1007/s10533-010-9486-6

Muller-Karger FE, Hu C, Andrefouet S, Varela R, Thunell R (2005) The color of the coastal ocean and applications in the solution of research and management problems. Springer, Dordrecht

Münster U (1991) Extracellular enzyme activity in eutrophic and polyhumic lakes. In: Chrost RJ (ed) Microbial enzymes in aquatic environments. Springer, New York, pp 96–122

Murphy KR, Stedmon CA, Waite TD, Ruiz GM (2008) Distinguishing between terrestrial and autochthonous organic matter sources in marine environments using fluorescence spectroscopy. Mar Chem 108:40–58

Myneni SCB, Brown JT, Martinez GA, Meyer-Ilse W (1999) Imaging of humic substance macromolecular structures in water and soils. Science 286:1335–1337

Nagao S, Matsunaga T, Suzuki Y, Ueno T, Amano H (2003) Characteristics of humic substances in the Kuji River as determined by high-performance size exclusion chromatography with fluorescence detection. Water Res 37:4159–4170

Nakajima H (2006) Studies on photochemical degradation processes of dissolved organic matter in seawater. MS Thesis, Hiroshima University, pp 1–173

Nieke B, Reuter R, Heuermann R, Wang H, Babin M, Therriault JC (1997) Light absorption and fluorescence properties of chromophoric dissolved organic matter (CDOM), in the St Lawrence estuary (Case 2 waters). Cont Shelf Res 17:235–252

Nieto-Cid M, Álvarez-Salgado A, Gago J, Pérez FF (2005) DOM fluorescence, a tracer for biogeochemical processes in a coastal upwelling system (NW Iberian Peninsula). Mar Ecol Prog Ser 297:33–50

Nieto-Cid M, Álvarez-Salgado A, Pérez FF (2006) Microbial and photochemical reactivity of fluorescent dissolved organic matter in a coastal upwelling system. Limnol Oceanogr 51:1391–1400

Obernosterer I, Herndl GJ (2000) Differences in the optical and biological reactivity of the humic and nonhumic dissolved organic carbon component in two contrasting coastal marine environments. Limonl Oceanogr 45:1120–1129

Obernosterer I, Ruardij P, Herndl GJ (2001) Spatial and diurnal dynamics of dissolved organic matter (DOM) fluorescence and H2O2 and the photochemical oxygen demand of surface water DOM across the subtropical Atlantic Ocean. Limnol Oceanogr 46:632–643

Oheim M, Michael DJ, Geisbauer M, Madsen D, Chow RH (2006) Principles of two-photon excitation fluorescence microscopy and other nonlinear imaging approaches. Adv Drug Deliv Rev 58:788–808

Ohno T, Bro R (2006) Dissolved organic matter characterization using multiway spectral decomposition of fluorescence landscapes. Soil Sci Soc Am J 70:2028–2037

Ohno T, Amirbahman A, Bro R (2007) Parallel factor analysis of excitation–emission matrix fluorescence spectra of water soluble soil organic matter as basis for the determination of conditional metal binding parameters. Environ Sci Technol 42:186–192

Ohno T, Hunt JF, Gray KA (2009) Multi-dimensional fluorescence spectroscopy and PARAFAC for dissolved organic matter characterization In: Wu FC, Xing B (Ed), Natural Organic Matter and its Significance in the Environment, Science Press, Beijing, pp 90-104

Osburn CL, Morris DP, Thorn KA, Moeller RE (2001) Chemical and optical changes in freshwater dissolved organic matter exposed to solar radiation. Biogeochemistry 54:251–278

Osburn CL, O'Sullivan DW, Boyd TJ (2009) Increases in the longwave photobleaching of chromophoric dissolved organic matter in coastal waters. Limnol Oceanogr 54:145–159

Otto L (1967) Investigations on optical properties and water-masses of the Southern North Sea. Neth J Sea Res 3:532–552

Palenik B, Morel FMM (1988) Dark production of H2O2 in the Sargasso Sea. Limnol Oceanogr 33:1606–1611

Parlanti P, Worz K, Geoffroy L, Lamotte M (2000) Dissolved organic matter fluorescence spectroscopy as a tool of estimate biological activity in a coastal zone submitted to anthropogenic inputs. Org Geochem 31:1765–1781

Patel-Sorrentino N, Mounier S, Benaim JY (2002) Excitation- emission fluorescence matrix to study pH influence on organic matter fluorescence in the Amazon basin rivers. Water Res 36(10):2571–2581

Patel-Sorrentino N, Mounier S, Lucas Y, Benaim JY (2004) Effects of UV-visible irradiation on natural organic matter from the Amazon basin. Sci Total Environ 321:231–239
Peña-Méndez EM, Havel J, Patočka J (2005) Humic substances-compounds of still unknown structure: applications in agriculture, industry, environment, and biomedicine. J Appl Biomed (Rev) 3:13–24
Persson T, Wedborg M (2001) Multivariate evaluation of the fluorescence of aquatic organic matter. Anal Chim Acta 434:179–192
Petersen HT (1989) Determination of an Isochrysis galbana algal bloom by L-tryptophan fluorescence. Mar Pollut Bull 20:447–451
Peuravuori J, Pihlaja K (1999) Structural characterization of humic substances. In: Keskitalo J, Eloranta P (eds) Limnology of humic waters. Backhuy Publishers, Leiden, pp 22–39
Poiger T, Field JA, Field TM, Giger W (1996) Occurrence of fluorescent whitening agents in sewage and river water determined by solid-phase extraction and high-performance liquid chromatography. Environ Sci Technol 30:2220–2226
Poiger T, Kari FG, Giger W (1999) Fate of fluorescent whitening agents in the River Glatt. Environ Sci Technol 33:533–539
Provenzano MR, Orazio VD, Jerzykiewicz M, Senesi N (2004) Fluorescence behaviour of Zn and Ni complexes of humic acids from different sources. Chemosphere 55:885–892
Pullin MJ, Cabaniss SE (1995) Rank analysis of the pH dependent synchronous fluorescence spectra of six standard humic substances. Environ Sci Technol 29:1460–1467
Qian J, Mopper K, Kieber DJ (2001) Photochemical production of the hydroxyl radical in Antarctic waters. Deep-Sea Res I 48:741–759
Randall CE, Harvey VL, Manney GL, Orsolini Y, Codrescu M, Sioris C, Brohede S, Haley CS, Gordley LL, Zawdony JM, Russell JM (2005) Stratospheric effects of energetic particle precipitation in 2003–2004. Geophys Res Lett:LO5082. doi:101029/2004GL022003
Reche I, Pace ML, Cole JJ (1999) Relationship of trophic and chemical conditions to photobleaching of dissolved organic matter in lake ecosystems. Biogeochemistry 44:259–280
Reynolds DM (2003) Rapid and direct determination of tryptophan in water using synchronous fluorescence spectroscopy. Water Res 37:3055–3060
Richard C, Canonica S (2005) Aquatic phototransformation of organic contaminants induced by coloured dissolved natural organic matter. Hdb Env Chem 2(Part M):299–323
Richardson SD (2007) Water analysis: emerging contaminants and current issue. Anal Chem 79:4295–4324
Rochelle-Newall EJ, Fisher TR (2002) Production of chromophoric dissolved organic matter fluorescence in marine and estuarine environments: an investigation into the role of phytoplankton. Mar Chem 77:7–21
Rochelle-Newall EJ, Fisher TR, Fan C, Glibert PM (1999) Dynamics of chromophoric dissolved organic matter and dissolved organic carbon in experimental mesocosms. Int J Remote Sens 20:627–641
Rosenstock B, Simon M (2003) Consumption of dissolved amino acids and carbohydtares by limnetic bacterioplankton according to molecular weight fractions and proportions bound to humic matter. Microb Ecol 45:433–443
Rosenstock B, Zwisler W, Simon M (2005) Bacterial consumption of humic and non-humic low and high molecular weight DOM and the effect of solar irradiation on the turnover of labile DOM in the Southern Ocean. Microb Ecol 50:90–101
Ross RT, Lee C, Davis CM, Ezzeddine BM, Fayyad EA, Leurgans SE (1991) Resolution of the fluorescence spectra of plant pigment complexes using trilinear models. Biochim Biophys Acta 1056:317–320
Santín C, Yamashita Y, Otero XL, Álvarez MÁ, Jaffé R (2009) Characterizing humic substances from estuarine soils and sediments by excitation-emission matrix spectroscopy and parallel factor analysis. Biogeochemistry 96:131–147
Schwede-Thomas SB, Chin Y, Dria KJ, Hatcher P, Kaiser E, Sulzberger B (2005) Characterizing the properties of dissolved organic matter isolated by XAD and C-18 solid phase extraction and ultrafiltration. Aquat Sci 67:61–71

Seitzinger SP, Hartnett H, Lauck R, Mazurek M, Minegishi T, Spyres G, Styles R (2005) Molecular-level chemical characterization and bioavalability of dissolved organic matter in stream water using electrospray-ionization mass spectrometry. Limnol Oceanogr 50:1–12

Senesi N (1990a) Molecular and quantitative aspects of the chemistry of fulvic acid and its interactions with metal ions and organic chemicals. Part II: The fluorescence spectroscopy approach. Anal Chim Acta 232:77–106

Senesi N (1990b) Molecular and quantitative aspects of the chemistry of fulvic acid and its interactions with metal ions and organic chemicals. Part I: The electron spin resonance approach. Anal Chim Acta 232:51–75

Seredyńska-Sobecka B, Baker A, Lead JR (2007) Characterisation of colloidal and particulate organic carbon in freshwaters by thermal fluorescence quenching. Water Res 41:3069–3076

Seritti A, Russo D, Nannicini L, del Vecchio R (1998) DOC, absorption and fluorescence properties of estuarine and coastal waters of the northern Tyrrhenian Sea. Chem Speciat Bioavailab 10:95–105

Shank GC, Zepp RG, Vähätalo A, Lee R, Bartels E (2010) Photobleaching kinetics of chromophoric dissolved organic matter derived from mangrove leaf litter and floating Sargassum colonies. Mar Chem 119:162–171

Sholkovitz ER (1976) Flocculation of dissolved organic and inorganic matter during the mixing of river water and seawater. Geochim Cosmochim Acta 40:831–845

Shriner RL, Horne WH, Cox RFB (1943) p-Nitrophenyl Isocyanate. Org Synth Coll 2:453–455

Singh S, D'Sa EJ, Swenson EM (2010) Chromophoric dissolved organic matter (CDOM) variability in Barataria Basin using excitation-emission matrix (EEM) fluorescence and parallel factor analysis (PARAFAC). Sci Total Environ 408:3211–3222

Skoog A, Wedborg M, Fogelqvist E (1996) Photobleaching of fluorescence and the organic carbon concentration in a coastal environment. Mar Chem 55:333–345

Smith DS, Kramer JR (1999) Fluorescence analysis for multisite aluminium binding to natural organic matter. Environ Int 25:307–314

Southworth BA, Voelker BM (2003) Hydroxyl radical production via the photo-Fenton reaction in the presence of fulvic acid. Environ Sci Technol 37:1130–1136

Spencer RGM, Bolton L, Baker A (2007) Freeze/thaw and pH effects on freshwater dissolved organic matter fluorescence and absorbance properties from a number of UK locations. Water Res 41:2941–2950

Stabenau ER, Zika RG (2004) Correlation of the absorption coefficient with a reduction in mean mass for dissolved organic matter in southwest Florida river plumes. Mar Chem 89:55–67

Stedmon CA, Markager S (2005a) Tracing the production and degradation of autochthonous fractions of dissolved organic matter by fluorescence analysis. Limnol Oceanogr 50:1415–1426

Stedmon CA, Markager S (2005b) Resolving the variability in dissolved organic matter fluorescence in a temperate estuary and its catchment using PARAFAC analysis. Limnol Oceanogr 50:686–697

Stedmon CA, Markager S, Bro R (2003) Tracing dissolved organic matter in aquatic environments using a new approach to fluorescence spectroscopy. Mar Chem 82(3–4):239–254

Stedmon CA, Markager S, Tranvik L, Kronberg L, Slätis T, Martinsen W (2007a) Photochemical production of ammonium and transformation of dissolved organic matter in the Baltic Sea. Mar Chem 104:227–240

Stedmon CA, Thomas DN, Granskog M, Kaartokallio H, Papaditriou S, Kuosa H (2007b) Characteristics of dissolved organic matter in Baltic coastal sea ice: allochthonous or autochthonous origins? Environ Sci Technol 41:7273–7279

Steelink C (2002) Investigating humic acids in soils. Anal Chem 74:328A–333A

Stewart AJ, Wetzel RG (1980) Fluorescence: absorbance ratios-a molecular-weight tracer of dissolved organic matter. Limnol Oceanogr 25:559–564

Stoll J-MA, Giger W (1998) Mass balance for detergent-derived fluorescent whitening agents in surface waters of Switzerland. Water Res 32:2041–2050

Stoll J-MA, Ulrich MM, Giger W (1998) Dynamic behavior of fluorescent whitening agents in Greifensee: field measurements combined with mathematical modeling of sedimentation and photolysis. Environ Sci Technol 32:1875–1881

Sugiyama Y, Anegawa A, Inokuchi H, Kumagai T (2005) Distribution of dissolved organic carbon and dissolved fulvic acid in mesotrophic Lake Biwa, Japan. Limnology 6:161–168

Sun M, Lee C, Aller RC (1993) Anoxic and oxic degradation of 14C-labeled chloropigments and a 14C-labeled diatom in Long Island Sound sediments. Limnol Oceanogr 38:1438–1451

Sun Q, Lu R, Yu A (2012) Structural heterogeneity in the collision complex between organic dyes and tryptophan in aqueous solution. J Phys Chem B 116:660–666

Suzuki Y, Nagao S, Nakaguchi Y, Matsunaga T, Muraoka S, Hiraki K (1997) Spectroscopic properties of fluorescent substances in natural waters. Geochemistry 31:171–180 (in Japanese)

Świetlik J, Sikorska E (2004) Application of fluorescence spectroscopy in the studies of natural organic matter fractions reactivity with chlorine dioxide and ozone. Water Res 38:3791–3799

Tadrous PJ (2000) Methods for imaging the structure and function of living tissues and cells: 2. Fluorescence lifetime imaging. J Pathol 191:229–234

Taylor JR, Fang MM, Nie S (2000) Probing specific sequences on single DNA molecules with bioconjugated fluorescent nanoparticles. Ana Chem 72:1979–1986

Thomas DN, Lara RJ (1995) Photodegradation of algal derived dissolved organic carbon. Mar Ecol Prog Ser 116:309–310

Thurman EM (1985) Humic substances in groundwater. In: Aiken GR, McKnight DM, Wershaw RL, MacCarthy P (eds) Humic substances in soil, sediment, and water: geochemistry, isolation, and characterization, Wiley, New York, pp 87–103

Tranvik LJ (1992) Allochthonous disolved organic matter as an energy source for pelagic bacteria and the concept of the microbial loop. Hydrobiologia 229:107–114

Uyguner CS, Bekbolet M (2005) Evaluation of humic acid photocatalytic degradation by UV-vis and fluorescence spectroscopy. Catal Today 101:267–274

Vacher L (2004) Etude par fluorescence des propriétés de la matière organique dissoute dans les systèmes estuariens. Cas des estuaires de la Gironde et de la Seine, PhD thesis, Université Bordeaux 1, pp 255. http://archives.disvu.ubordeaux1.fr/proprietes.html?numero_ordre=2923

Vähätalo AV, Järvinen M (2007) Photochemically produced bioavailable nitrogen from biologically recalcitrant dissolved organic matter stimulates production of a nitrogen-limited microbial food web in the Baltic Sea. Limnol Oceanogr 52:132–143

Vähätalo AV, Wetzel RG (2004) Photochemical and microbial decomposition of chromophoric dissolved organic matter during long (months-years) exposures. Mar Chem 89:313–326

Vähätalo AV, Salkinoja-Saonen M, Taalas P, Salnen K (2000) Spectrum of the quantum yield for photochemical mineralization of dissolved organic carbon in a humic lake. Limnol Oceanogr 45:664–676

Valentine RL, Zepp RG (1993) Formation of carbon monoxide from the photodegradation of terrestrial dissolved organic carbon in natural waters. Environ Sci Technol 27:409–412

Van Heemst JDH, Megens L, Hatcher PG, de Leeuw JW (2000) Nature, origin and average age of estuarine ultrafiltered dissolved organic matter as determined by molecular and carbon isotope characterization. Org Geochem 31:847–857

Vione D, Lauri V, Minero C, Maurino V, Malandrino M, Carlotti ME, Olariu RI, Arsene C (2009) Photostability and photolability of dissolved organic matter upon irradiation of natural water samples under simulated sunlight. Aquat Sci 71:34–45

Visser SA (1984) Fluorescence phenomena of humic matter of aquatic origin and microbial cultures. In: Christman RF, Gjessing ET (eds) Aquatic and Terrestrial Humic materials. Ann Arbor Science, Ann Arbor, pp 183–202

Vodacek A, Philpot WD (1987) Environmental effects on laser induced fluorescence spectra of natural waters. Remote Sens Environ 21:83–95

Vodacek A, Hoge F, Swift RN, Yungel JK, Peltzer ET, Blough NV (1995) The use of in situ and airborne fluorescence measurements to determine UV absorption coefficients and DOC concentrations in surface waters. Limnol Oceanogr 40:411–415

Vodacek A, Blough NV, DeGrandpre D, Peltzer ET, Nelson RK (1997) Seasonal variation of CDOM and DOC in the Middle Atlantic Bight: terrestrial input and photooxidation. Limnol Oceanogr 42:674–686

Volk CJ, Volk CB, Kaplan LA (1997) Chemical composition of biodegradable dissolved organic matter in streamwater. Limnol Oceanogr 42:39–44

Waiser MJ, Robarts RD (2004) Photodegradation of DOC in a shallow prairie wetland: evidence from seasonal changes in DOC optical properties and chemical characteristics. Biogeochemistry 69:263–284

Wakeham SG, Lee C (1993) Production, transport, and alteration of particulate organic matter in the marine water column. In: Engel MH, Macko SA (eds) Org Geochem. Plenum Press, New York, pp 145–169

Wakeham SG, Lee C, Hedges JI, Hernes PJ, Peterson ML (1997) Molecular indicators of diagenetic status in marine organic matter. Geochim Cosmochim Acta 61:5363–5369

Wang GS, Liao CH, Wu FJ (2001) Photodegradation of humic acids in the presence of hydrogen peroxide. Chemosphere 42:379–387

Wang Z-G, Liu W-Q, Zhao N-J, Li H-B, Zhang Y-J, Si-Ma W-C, Liu J-G (2007) Composition analysis of colored dissolved organic matter in Taihu Lake based on three dimension excitation-emission fluorescence matrix and PARAFAC model, and the potential application in water quality monitoring. J Environ Sci 19:787–791

Wedborg M, Persson T, Larsson T (2007) On the distribution of UV-blue fluorescent organic matter in the Southern Ocean. Deep-Sea Res I 54:1957–1971

Wehry EL (1973) Effects of molecular structure and molecular environment on fluorescence. In: Guilbault GG (ed) Practical fluorescence: theory, methods, and techniques. Marcel Dekker, New York, pp 79–136

Weishaar JL, Aiken GR, Bergamaschi BA, Fram MS, Fujii R, Mopper K (2003) Evaluation of specific ultraviolet absorbance as an indicator of the chemical composition and reactivity of dissolved organic carbon. Environ Sci Technol 37:4702–4708

Weiss RF, Carmack EC, Koropalov VM (1991) Deep-water renewal and biological production in Lake Baikal. Nature 349:665–669

Westerhoff P, Chen W, Esparza M (2001) Fluorescence analysis of a standard fulvic acid and tertiary treated wastewater. J Environ Qual 30:2037–2046

Wetzel RG (1992) Gradient-dominated ecosystems: Sources and regulatory functions of dissolved organic matter in freshwater ecosystems. Hydrobiologia 229:181–198

Wetzel RG, Hatcher PG, Bianchi TS (1995) Natural photolysis by ultraviolet irradiance of recalcitrant dissolved organic matter to simple substrates for rapid bacterial metabolism. Limnol Oceanogr 40:1369–1380

White EM, Vaughan PP, Zepp RG (2003) Role of the photo-Fenton reaction in the production of hydroxyl radicals and photobleaching of colored dissolved organic matter in a coastal river of the southeastern United States. Aquat Sci 65:402–414

Willey JD (1984) The effect of seawater magnesium on natural fluorescence during estuarine mixing, and implications for tracer applications. Mar Chem 15:19–45

Willey JD, Atkinson LP (1982) Natural fluorescence as a tracer for distinguishing between Piedmont and coastal plain river waters in the nearshore waters of Georgia and North Carolina. Estuarine Coastal Shelf Sci 14:49–59

Winter AR, Fish TAE, Playle RC, Smith DS, Curtis PJ (2007) Photodegradation of natural organic matter from diverse freshwater sources. Aquat Toxicol 84:215–222

Wolfbeis OS (1985) The fluorescence of organic natural products In: Schulman SG (ed) Molecular luminescence spectroscopy, methods and applications V 77: Part I. Wiley, New York, pp 167–370

Wu FC, Tanoue E (2001a) Molecular mass distribution and fluorescence characteristics of dissolved organic ligands for copper (II) in Lake Biwa, Japan. Org Geochem 32:11–20

Wu FC, Tanoue E (2001b) Geochemical characterization of organic ligands for copper (II) in different molecular size fractions in Lake Biwa, Japan. Org Geochem 32:1311–1318

Wu FC, Midorikawa T, Tanoue E (2001) Fluorescence properties of organic ligands for copper(II) in Lake Biwa and its rivers. Geochem J 35:333–346

Wu FC, Evans RD, Dillon PJ (2002) Fractionation and characterization of fulvic acid by immobilized metal ion affinity chromatography. Anal Chim Acta 452:85–93
Wu FC, Tanoue E, Liu CQ (2003a) Fluorescence and amino acid characteristics of molecular size fractions of DOM in the waters of Lake Biwa. Biogeochem 65:245–257
Wu FC, Evans RD, Dillon PJ (2003b) High-performance liquid chromatographic fractionation and characterization of fulvic acid. Anal Chim Acta 464:47–55
Wu FC, Cai YR, Evans RD, Dillon PJ (2004a) Complexation between Hg(II) and dissolved organic matter in stream waters: an application of fluorescence spectroscopy. Biogeochemistry 71:339–351
Wu FC, Evans RD, Dillon PJ, Schiff S (2004b) Molecular size distribution characteristics of the metal-DOM complexes in stream waters by high-performance size-exclusion chromatography and high-resolution inductively coupled plasma mass spectrometry. J Anal Atomic Spectrom 19:979–983
Wu FC, Mills RB, Evans RD, Dillon PJ (2004c) Kinetics of metal-fulvic acid complexation using a stopped-flow technique and three-dimensional excitation emission fluorescence spectrometer. Anal Chem 76:110–113
Wu FC, Mills RB, Evans RD, Dillon PJ (2005) Photodegradation-induced changes in dissolved organic matter in acidic waters. Can J Fish Aqua Sci 62:1019–1027
Wu FC, Liu CQ, Wang FY, Xing BS, Fu PQ, Mostofa KMG (2007) Natural organic matter and its role in the environment water-rock interaction. In: Bullen TD, Wang Y (eds) Proceedings of the 12th international symposium on water-rock interaction WRI-12, Kunming, China, 31 July–5 August 2007, vol 1. Taylor & Francis Group, London, pp 37–40
Wu J, Zhang H, He P-J, Shao L-M (2011) Insight into the heavy metal binding potential of dissolved organic matter in MSW leachate using EEM quenching combined with PARAFAC analysis. Water Res 45:1711–1719
Xie HX, Zafiriou OC, Cai WJ, Zepp RG, Wang YC (2004) Photooxidation and its effects on the carboxyl content of dissolved organic matter in two coastal rivers in the Southeastern United States. Environ Sci Technol 38:4113–4119
Yamaji N, Hayakawa K, Takada H (2010) Role of photodegradation in the fate of fluorescent whitening agents (FWAs) in lacustrine environments. Environ Sci Technol 44:8791
Yamashita Y, Jaffé R (2008) Characterizing the interactions between trace metals and dissolved organic matter using excitation-emission matrix and parallel factor analysis. Environ Sci Technol 42:7374–7379
Yamashita Y, Tanoue E (2003a) Chemical characterization of protein-like fluorophores in DOM in relation to aromatic amino acids. Mar Chem 82:255–271
Yamashita Y, Tanoue E (2003b) Distribution and alteration of amino acids in bulk DOM along a transect from bay to oceanic waters. Mar Chem 82:145–160
Yamashita Y, Tanoue E (2004) In situ production of chromophoric dissolved organic matter in coastal environments. Geophys Res Lett 31:L14302. doi:101029/2004GL019734
Yamashita Y, Tanoue E (2008) Production of bio-refractory fluorescent dissolved organic matter in the ocean interior. Nature Geosci:579–582. doi:101038/ngeo279
Yamashita Y, Tsukasaki A, Nishida T, Tanoue E (2007) Vertical and horizontal distribution of fluorescent dissolved organic matter in the Southern Ocean. Mar Chem 106:498–509
Yamashita Y, Jaffé R, Maie N, Tanoue E (2008) Assessing the dynamics of dissolved organic matter (DOM) in coastal environments by excitation emission matrix fluorescence and parallel factor analysis (EEM-PARAFAC). Limnol Oceanogr 53:1900–1908
Yamashita Y, Cory RM, Nishioka J, Kuma K, Tanoue E, Jaffe R (2010) Fluorescence characteristics of dissolved organic matter in the deep waters of the Okhotsk Sea and the northwestern North Pacific Ocean. Deep-Sea Res II 57:1478–1485
Yamashita Y, Panton A, Mahaffey C, Jaffé R (2011) Assessing the spatial and temporal variability of dissolved organic matter in Liverpool Bay using excitation–emission matrix fluorescence and parallel factor analysis. Ocean Dyn 61:569–579. doi:10.1007/s10236-010-0365-4
Ying GG (2006) Fate, behavior and effects of surfactants and their degradation products in the environment. Environ Int 32:417–431

Yoshioka T, Mostofa KMG, Konohira E, Tanoue E, Hayakawa K, Takahashi M, Ueda S, Katsuyama M, Khodzher T, Bashenkhaeva N, Korovyakova I, Sorokovikova L, Gorbunova L (2007) Distribution and characteristics of molecular size fractions of freshwater dissolved organic matter in watershed environments: its implication to degradation. Limnology 8:29–44

Yu G-H, Luo Y-H, Wu M-J, Tang Z, Liu D-Y, Yang X-M, Shen Q-R (2010) PARAFAC modeling of fluorescence excitation–emission spectra for rapid assessment of compost maturity. Bioresour Technol 101:8244–8251

Yue L, Wu FC, Liu C, Li W, Fu P, Bai Y, Wang L, Yin Z, Lü Z (2006) Relationship between fluorescence characteristics and molecular weight distribution of natural dissolved organic matter in Lake Hongfeng and Lake Baihua, China. Chin Sci Bull 51:89–96

Zanardi-Lamardo E, Moore C, Zika RG (2004) Seasonal variation in molecular mass and optical properties of chromophoric dissolved organic material in coastal waters of southwest Florida. Mar Chem 89:37–54

Zepp RG, Scholtzhauer PF (1981) Comparisson of photochemical behavior of various humic substances in water: III Spectroscopic properties of humic substances. Chemosphere 10:479–486

Zepp RG, Braun AM, Hoigne J, Leenheer JA (1987) Photoproduction of hydrated electrons from natural organic solutes in aquatic environments. Environ Sci Technol 21:485–490

Zepp RG, Faust BC, Hoigné J (1992) Hydroxyl radical formation in aqueous reactions (pH 3–8) of iron(II) with hydrogen peroxide: the Photo-Fenton reaction. Environ Sci Technol 26:313–319

Zhang Y, Zhu L, Zeng X, Lin Y (2004) The biogeochemical cycling of phosphorus in the upper ocean of the East China Sea. Est Coast Shelf Sci 60:369–379

Zhang X, Minear RA, Barrett SE (2005) Characterization of high molecular weight disinfection byproducts from chlorination of humic substances with/without coagulation pretreatment using UF-SEC-ESI-MS/MS. Environ Sci Technol 39:963–972

Zhang Y, van Dijk MA, Liu M, Zhu G, Qin B (2009a) The contribution of phytoplankton degradation to chromophoric dissolved organic matter (CDOM) in eutrophic shallow lakes: field and experimental evidence. Water Res 43:4685–4697

Zhang Y, Liu M, Qin B, Feng S (2009b) Photochemical degradation of chromophoric-dissolved organic matter exposed to simulated UV-B and natural solar radiation. Hydrobiologia 627:159–168

Zhang DY, Pan XL, Mostofa KMG, Chen X, Mu G, Wu FC, Liu J, Song WJ, Yang JY, Liu Y, Fu QL (2010) Complexation between Hg(II) and biofilm extracellular polymeric substances: an application of fluorescence spectroscopy. J Hazard Matter 175(1–3):359–365

Zhao WH, Wang JT, Cui X, Ji NY (2006) Research on fluorescence excitation and emission matrix spectra of dissolved organic matter in phytoplankton growth process. Chin High Technol Lett 16:425–430 (in Chinese with English abstract)

Zhao W, Wang J, Chen M (2009) Three-dimensional fluorescence characteristics of dissolved organic matter produced by Prorocentrum donghaiense Lu. Chin J Oceanol Limnol 27:564–569. doi:10.1007/s00343-009-9141-z

Zimmerman JTF, Rommets JW (1974) Natural fluorescence as a tracer in the Dutch Wadden Sea and the adjacent North Sea. Neth J Sea Res 8:117–125

Zinder SH (1993) Physiological ecology of methanogens. In: Ferry JG (ed) Methanogenesis: ecology, physiology, biochemistry and genetics. Chapman and Hall, New York, pp 128–206

Zsolnay A, Baigar E, Jimenez M, Steinweg B, Saccomandi F (1999) Differentiating with fluorescence spectroscopy the sources of dissolved organic matter in soils subjected to drying. Chemosphere 38:45–50